6-2007

Effect of Prior Aging on Fatigue Behavior of IM7/BMI 5250-4 Composite at 191°C

Christine G. Ladrido

EFFECT OF PRIOR AGING ON FATIGUE BEHAVIOR OF IM7/BMI 5250-4 COMPOSITE AT 191°C

THESIS

Christine G. Ladrido, Captain, USAF

AFIT/GAE/ENY/07-J10

DEPARTMENT OF THE AIR FORCE
AIR UNIVERSITY

AIR FORCE INSTITUTE OF TECHNOLOGY

Wright-Patterson Air Force Base, Ohio

The views expressed in this thesis are those of the author and do not reflect the official policy or position of the United States Air Force, Department of Defense, or the U.S. Government.

AFIT/GAE/ENY/07-J10

EFFECT OF PRIOR AGING ON FATIGUE BEHAVIOR OF IM7/BMI 5250-4 COMPOSITE AT 191°C

THESIS

Presented to the Faculty

Department of Aeronautics and Astronautics

Graduate School of Engineering and Management

Air Force Institute of Technology

Air University

Air Education and Training Command

In Partial Fulfillment of the Requirements for the

Degree of Master of Science in Aeronautical Engineering

Christine G. Ladrido, BS

Captain, USAF

June 2007

AFIT/GAE/ENY/07-J10

EFFECT OF PRIOR AGING ON FATIGUE BEHAVIOR OF IM7/BMI 5250-4 COMPOSITE AT 191°C

Christine G. Ladrido, BS

Captain, USAF

Approved:

Dr. Marina Ruggles-Wrenn (Chairman)	Date
Dr. Richard B. Hall (Member)	Date
Dr. Greg A. Schoeppner (Member)	Date

Acknowledgments

I would like to thank my sponsors, Dr. Greg Schoeppner (AFRL/MLBCM), Dr. Charles Y-C Lee (AFOSR/NE), and Dr. Richard Hall (AFRL/MLBCM) for supporting my research effort. I would also like to express my sincere appreciation to my thesis advisor, Dr. Marina Ruggles-Wrenn, for her patience and guidance throughout the entire process. She is a great representative and mentor for women in the engineering field.

In addition, I would like to thank all of the lab technicians and AFRL personnel, especially Barry Paige, John Hixenbaugh, and Jay Anderson, for all their help with providing adequate tools and maintenance required to conduct the tests and Bill Ragland and Ron Trejo for their help with fabrication and aging of the specimens.

Finally, I would like to thank my family and friends for their constant support.

Christine G. Ladrido

Table of Contents

Page

List of Figures

Page

List of Tables

Page

Abstract

The effect of prior aging on the mechanical response of IM7/BMI 5250-4 graphite/bismaleimide composite with $[\pm 45]_{4s}$ and $[0/90]_{4s}$ fiber orientation was analyzed using fatigue and tensile to failure testing at 191°C. Ultimate tensile strengths (UTS) were obtained from the tension to failure tests prior to fatigue testing. Tension-tension fatigue testing was performed on the unaged specimens at 80%, 70%, 60%, and 40% of the UTS. If a specimen did not fail, it was said to have reached run-out and a tension to failure test was then performed on the specimen to discover how much strength and stiffness was retained. Test pieces from both fiber orientations were also aged for a series of 10, 50, 100, 250, and 1000 hours. The mechanical responses of these aged specimens were examined with a tension-tension fatigue loading procedure using 70% of the UTS. As with the unaged specimen, those that survived cyclic fatigue loading were also tested for retained strength. It was found that the [±45] laminates were weaker after aging, but the fiber dominated [0/90] laminates retained much of their strength even after aging.

EFFECT OF PRIOR AGING ON FATIGUE BEHAVIOR OF IM7/BMI 5250-4 COMPOSITE AT 191°C

I. Introduction

Background

High-temperature polymer matrix composites (HTPMCs) in aerospace applications, such as turbine engines and high-speed aircraft skin, must operate in extreme hygro-thermal environments. Failure of composites in these aggressive environments has a direct impact on operational cost and fleet readiness. To assure long-term durability and structural integrity of HTPMC components, reliable experimentally-based life-prediction methods must be developed. Thorough understanding of aging and degradation mechanisms and their synergistic effects on mechanical behavior of HTPMCs is critical to development of predictive models and methodologies. Key technical issues are the degrading effects that long-term exposure to elevated temperature, moisture, and oxidizing environment, as well as cyclic loadings, can have on the dimensional stability, strength, and stiffness of HTPMC aerospace structures. Over the years, the successful use of these composites in aerospace engines ranging from the outer nacelle to core bearing housing structures [20], have motivated research that will incorporate them on supersonic transports (SST) (Figure 1) as well as over and under the exhaust nozzle and skin of Unmanned Combat Aircraft Vehicles (UCAVs) such as the X-45A [21]. The high performance of carbon fiber/polymer matrix composites, such as IM7/BMI 5250-4 in hygro-thermal environments have also made them excellent

candidates for application in launch vehicle cryogenic tanks and liquid rocket motor propellant ducts [5].

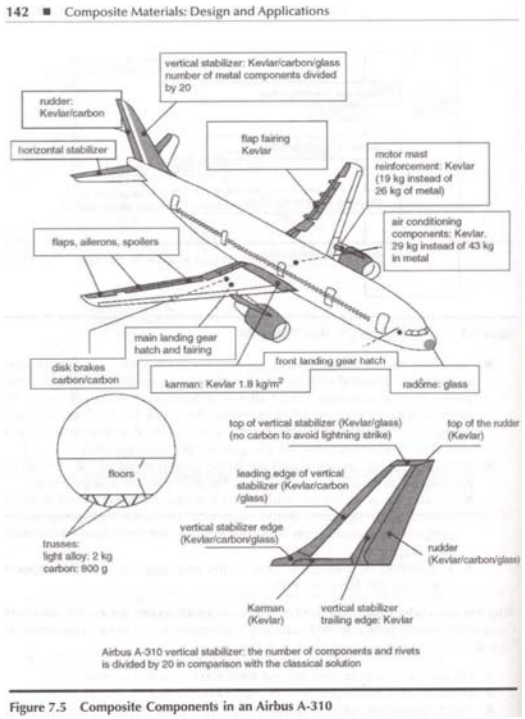

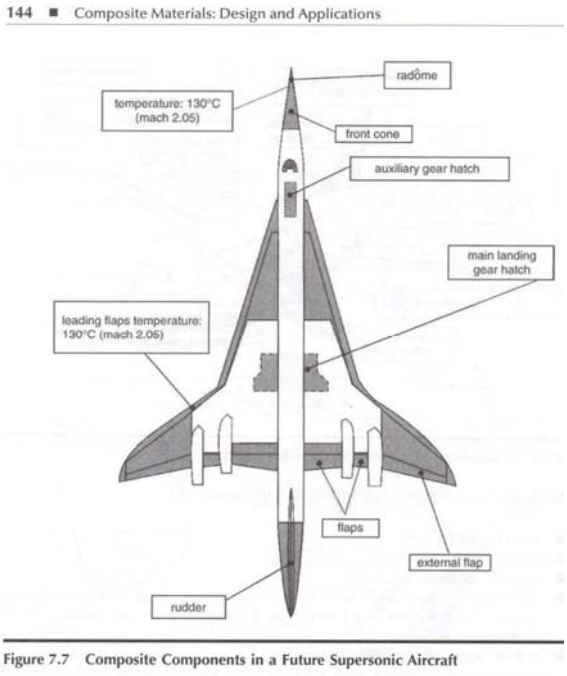

Figure 1. Examples of the use of composites in aerospace applications today and for the future [10]

Problem Statement

With the advancement of technology in the aerospace field such as in propulsion, communication/navigation, as well as computer software, it is imperative that the materials that house or even make up these systems can support the advanced capabilities during operation. New types of materials can be designed or even fully fabricated, but their uses cannot be determined until they have undergone extensive testing of their limits and capabilities. Models to predict the general behavior of materials can be utilized, but

with the introduction of more and more engineered materials, the need for actual experimental tests on these materials serve to provide more realistic data.

Scope

This particular study focuses on one specific HTPMC. IM7/BMI 5250-4 is a type of polymer matrix composite made up of carbon fibers and a bismaleimide resin matrix. This study will test specimens as received from fabrication, as well as the durability of specimens after aging. Tension and fatigue testing will be used to determine the mechanical behavior of this composite material. Both types of tests will be conducted in air at a temperature of 191°C (376°F).

Related Research

Several investigations have been accomplished on the fatigue of various polymer matrix composites, more specifically, BMI 5250-4 neat resin and IM7/BMI 5250-4.

For BMI neat resin, the studies have led to the creation of different chemical compositions and curing processes in order to improve it. It has been in production by many companies, like Hexcel and Cytec Engineered Materials Inc. Creep experiments performed by a graduate student from the Air Force Institute of Technology (AFIT), Capt John Balaconis in 2006 which investigated the ability to apply existing models to the resin after many creep and tensile tests were performed [3]. Other areas of testing BMI have involved elevated temperatures and hot/wet service applications (up to 232°C/450°F). From these, variations in the chemical makeup as well as curing processes of the bismaleimide resin are developed. Over the years, different commercial

material suppliers like Hexcel and Cytec Inc, have modified their processing techniques in order to create a stronger, cheaper, and even less hazardous BMI resin [6, 22].

A number of experiments have been done on variations of IM7/BMI 5250-4. The variation in these previous experiments exists in the orientation of the fibers, number of plies, as well as ply thicknesses. Pagano *et al*. [26] examined the initiation and propagation of ply-level matrix cracks for cross-ply and unidirectional laminates of IM7/BMI 5250-4. Bechel *et al*. studied the mechanical properties of the composite in reference to its individual constituents [4] in an 8-ply unidirectional laminate and the effects of stacking sequence on cryogenically cycled laminates in varying multidirectional and cross-ply laminates up to 9-plies [5].

Methodology

The following sections will thoroughly describe all the procedures taken to perform the study. In order to fully understand the motivation behind this study, a discussion will be given on the significance behind the temperature as well as fatigue. In addition, a sub-section will be dedicated to explaining what a composite is. Afterwards, a full description of the test setup will be given. Then the results of all the tests will be analyzed and presented. Finally, everything will be summarized in the Conclusions section. In addition, suggestions for future studies will be presented.

II. Background

Chapter Overview

The purpose of this chapter is to explain all the relevant information in order to completely understand the study. A brief overview of the significance of the temperature value, fatigue testing, as well as the type of material studied will be presented.

Composites

Composites are essentially two or more types of materials (phases) combined together to form a new material (composite) that can perform far more superior than either of the materials that make it up could ever perform independently of each other. Figure 2 shows the different phases of what make up a composite. In IM7/BMI 5250-4, the carbon fibers serve as the reinforcement portion, while the bismaleimide plays the role of the matrix. The carbon fibers are stronger than BMI, but without the BMI resin, the carbon fibers would not be able to stay together to form a sturdy material that could be fabricated to form things such as beams or skins of an aircraft (Figure 3). The matrix (BMI) can also contribute to the overall strength and stiffness of the composite material in addition to aiding in thermal, oxidative, and moisture resistance [36].

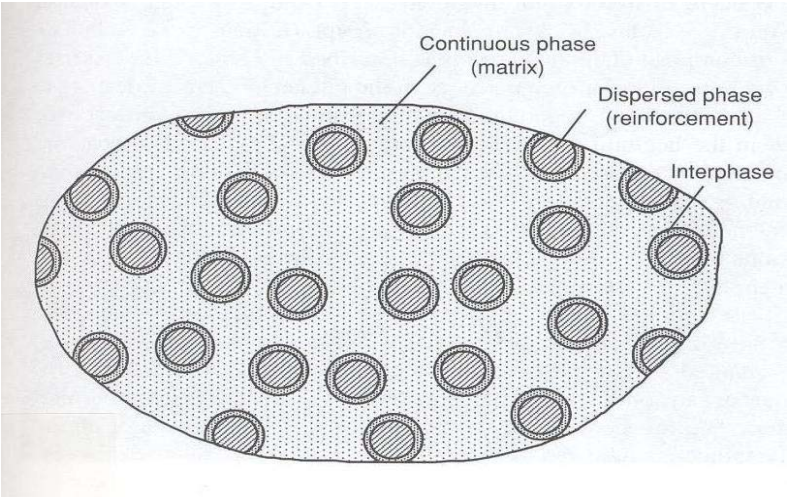

Figure 2. Phases of a composite material [10]

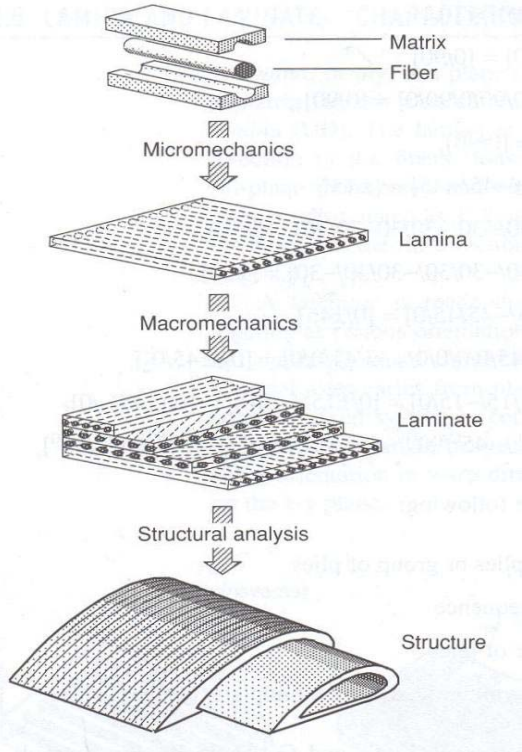

Figure 3. Different levels of analysis of composite materials [10]

Taking a closer look at the three phases that make up the composite in this study will provide an important basis from which the performance of this material can be analyzed.

Carbon Fiber

The reinforcement of carbon fiber provides huge benefits to the strength of this composite. There are actually variations of carbon fibers manufactured and used. These include AS4, T300, T-400H, IM-6, IM-7 [10]. Each of these has their own tensile strengths and stiffness properties which range from 3700 MPa to 5520 MPa and 235 GPa to 290 GPa respectively. The chemical makeup of these fibers depends on the manufacturer. For IM7 carbon fiber, the tensile strength is about 5520 MPa with a modulus of about 276 GPa [10]. Like most fibers in a composite material, this provides much of the tensile strength of the IM7/5250-4 composite. This is evident in the [0/90] fiber orientation laminates.

Bismaleimide

The job of the matrix in PMCs is to support the sensitive fibers as well as provide stress transfer from one fiber to another. Unfortunately, a big issue with bismaleimide, like most materials used in as a matrix, is brittleness.

The development of thermoset polymers, such as BMI, began back in the 1970s at NASA. The materials are produced by dissolving an aromatic diamine, a dialkyl ester of tetraxarboxylic acid and a monofunctional nadic ester endcapping agent in a solvent, such as alcohol [6]. Polymerization of monomer reactants (PMR-15) is a widely known polyimide that is also a close relative (chemically) to BMI [6]. BMI is actually a separate material entity than polyimide, but hold such close chemical relations, they often get grouped together. Typical strength and stiffness ranges for these types of materials are 70 to 120 MPa and 3.1 to 4.9 GPa respectively. Tests conducted at room temperature by

the manufacturer of the resin (Cytec Inc) concluded that the Ultimate Tensile Strength was 103 MPa and that the modulus of elasticity was 4.6 GPa. This is 98% less than the strength of the carbon fibers tested at room temperature.

Other types of thermosets like BMI and polyimide are epoxies, phenolics, and cyanate esters (CEs). Each of these comprises a separate category depending on chemical properties.

Most thermosets are limited to low temperature resistance uses. Thermoset polyimides like PMR-15 and BMI 5250-4, on the other hand, can be used in higher temperature applications up to 300°C. Thermosets, unlike thermoplastics (such as polypropelene, polyphenelyne sulfide [10]), do not soften or melt upon reheating. These types of resins decompose thermally because they undergo polymerization and cross-linking during curing with the aid of a hardening agent and heating [10].

Interphase

The fiber/matrix interphase serves an important role in the transfer of stresses between the fiber reinforcement and the resin matrix. If things like oxidation or aging cause the interphase to weaken in some way the integrity of the entire material or part could be compromised [36].

Fatigue Testing

Fatigue by definition is the tendency of a material to break under repeated loading [23]. One of the earliest studies of cyclic stress controlled loading effects on fatigue life was conducted by German engineer, August Wöhler in 1840 [12]. His study on fatigue initiated from a series of failures of railroad wheel axles. From these first studies, fatigue

was observed to be a three-stage process (Figure 4). Defects in fabrication or design caused the initiation stage to be shortened or nonexistent leading to shorter cycle life [12].

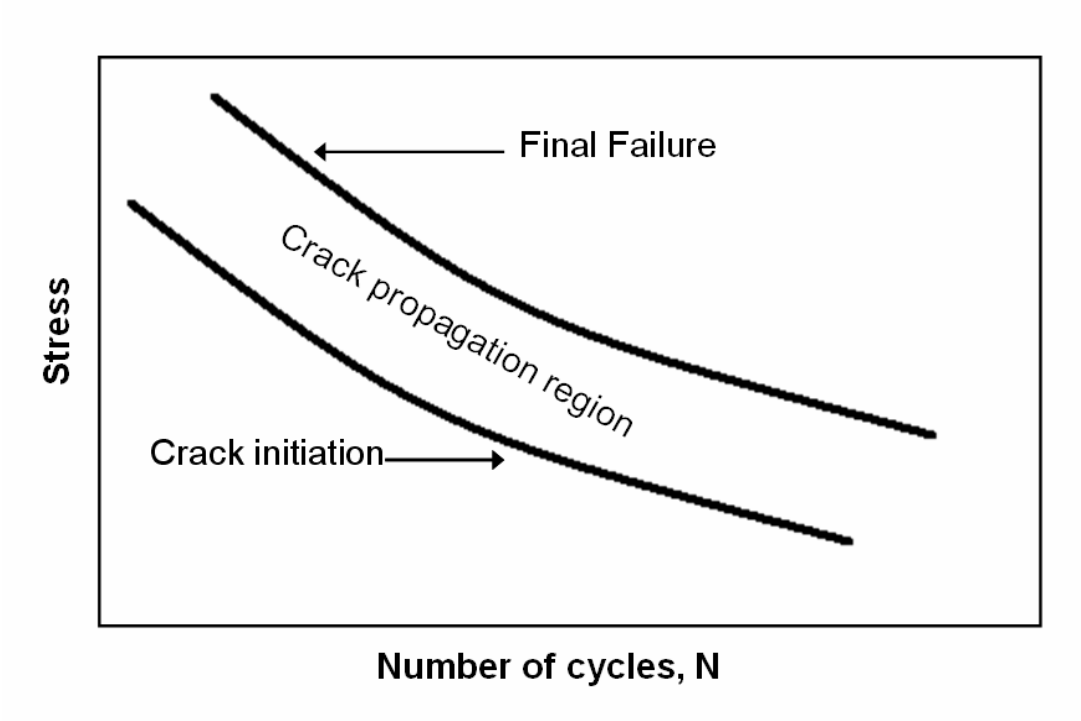

Figure 4. Three stages of fatigue life cycle for general material

Fatigue testing has been performed on virtually all materials since it was found to be a main culprit in a series of failures back in 1840. Like humans, many materials can break down due to fatigue after different lengths of time. Coincidently, this breaking point can be different for other materials, depending on the amount and type of loads, strains, or temperatures any given material can handle. The models, including the plot in Figure 4, developed to predict fatigue life, primarily applied to metals. Metals usually exhibit crack nucleation under fatigue loading. This means that when a crack is initiated, bands of cracks propagate around this initial crack origin forming a pattern that looks like

the rings in a tree stump. Previous studies have concluded that composites do not react like metals in that there is a single point of failure initiation leading to the rupture of the entire material. Composites can suffer multiple failure modes such as matrix cracking, interfacial debonding, and delamination of adjacent plies.

Unlike creep tests which are time-dependent, fatigue tests are cycle-dependent [8]. This means that accelerated testing by simply increasing the loads or temperatures during the cycles may decrease the testing time of the material, but it will not provide results that are realistic to the actual service environment of the material. Therefore, it is necessary to maintain as much of the actual or expected service loads, temperatures, and strains during fatigue testing in order to get reliable and accurate data.

Different types of fatigue tests exist and which one is applied to a specific material usually depends on its intended application. For materials that have not yet been put into service, all of these types of tests serve to be important and could essentially show what the material is capable of and could be used for. Fatigue tests can be conducted under a range of different conditions such as constant load or moment, constant deflection or strain, or constant stress intensity factor [15]. Figure 5 illustrates some typical cyclic stress controlled fatigue, which was the focus of this study. One type of loading not shown is compression-compression.

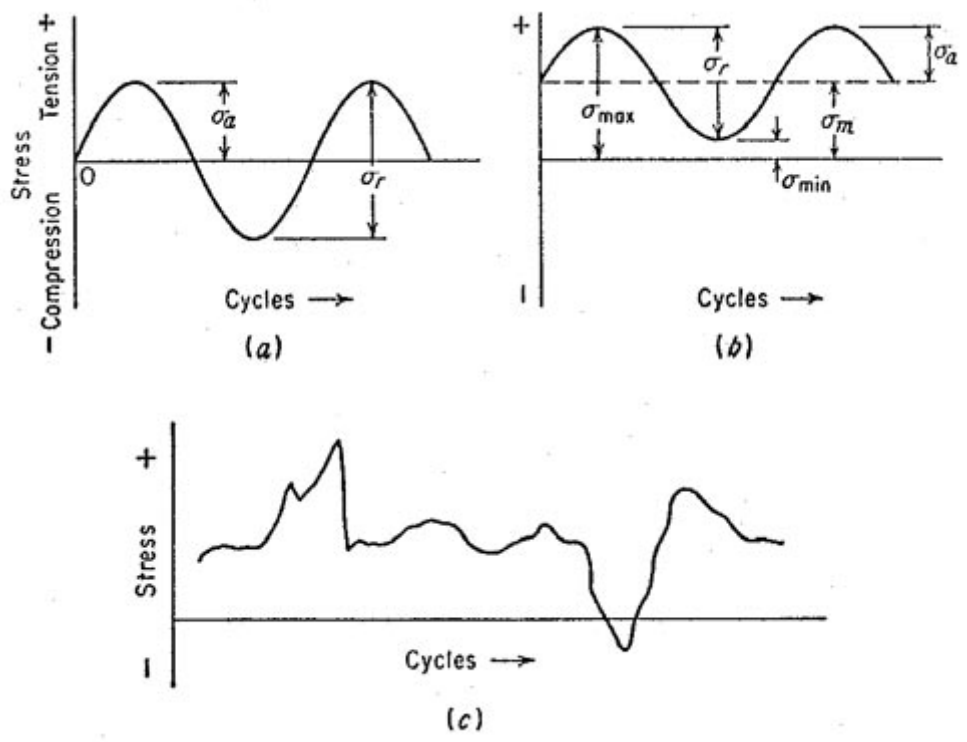

Figure 5. Typical fatigue stress cycles. (a) Reversed stress; (b) repeated stress; (c) irregular or random stress cycle. [11]

Summary

IM7/BMI 5250-4 is a composite made up of carbon fiber reinforcement, a bismaleimide resin matrix, and a strong interphase. There are many types of fatigue testing that can be accomplished to test a material. The type of test that is conducted on a material usually depends on the desired application when put into operation. However, for testing of material that is not yet in service, testing in all these areas of fatigue are important. Fatigue testing aids in predicting the service life of a material so that no catastrophic failures occur while the material is in operation.

III. Experimental Setup and Test Procedures

Chapter Overview

The purpose of this chapter is to describe the equipment and assembly used to perform the experimental tests. A description of the type of machine used, its components, and how the specimens were prepared and loaded for testing will be presented. A thorough explanation of the specimen from creation is provided. Detailed explanations of the process of temperature calibration, the aging process, tension to failure testing, tuning, and the tension-tension fatigue testing procedure used will be provided in this chapter.

Machine Setup

A vertically configured 810 Material Test System (MTS) machine was used to perform the mechanical testing on the specimen (Figure 6). Figure 7 shows the setup as it was used in the Structures and Materials Testing Laboratory in the Air Force Institute of Technology (AFIT).

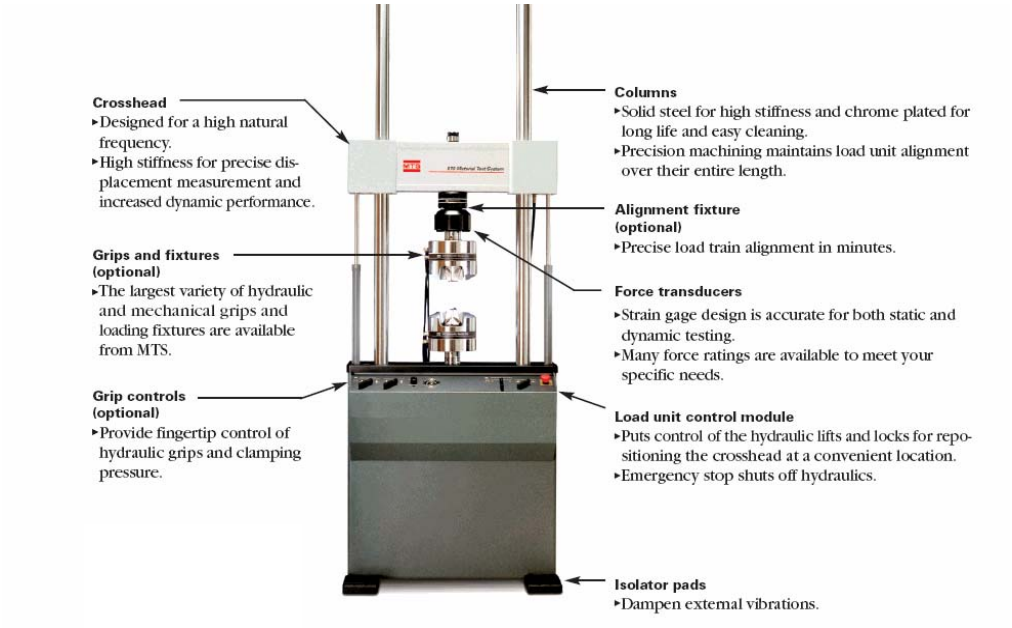

Figure 6. 810 Material Test System [23]

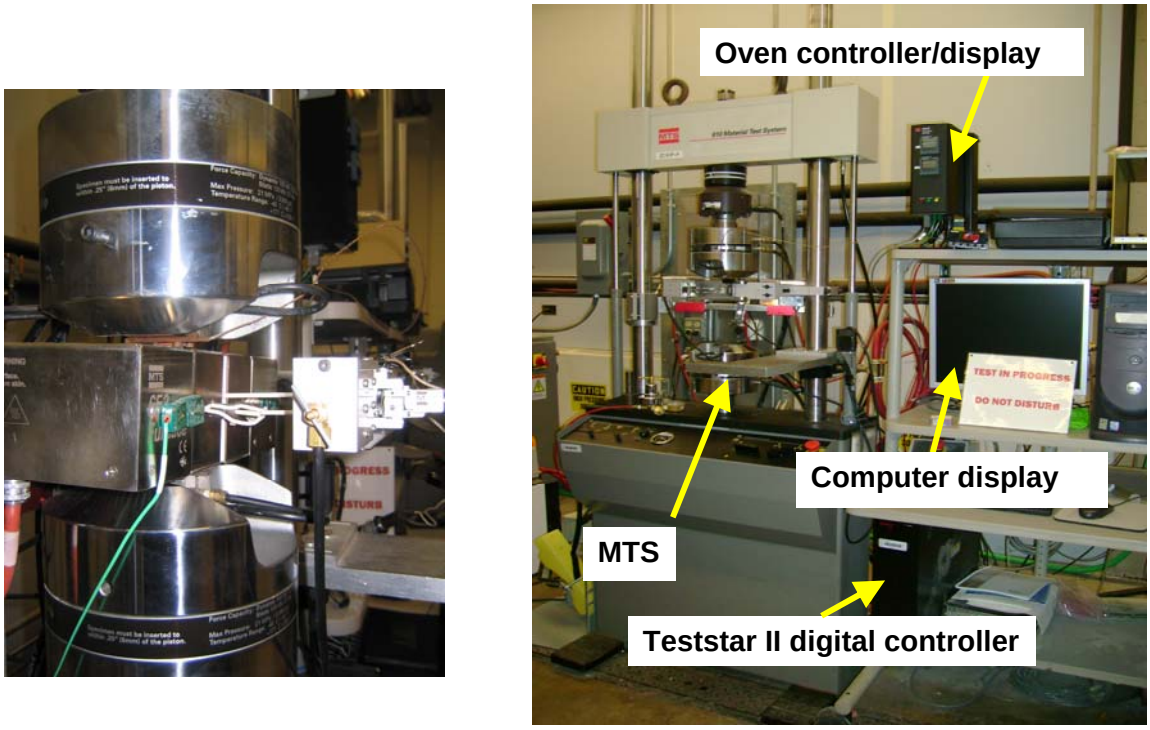

Figure 7. MTS Machine setup (a) loaded specimen with extensometer and closed furnace (b) shows locations of some key components that were utilized

The MTS machine used for the study was capable of forces ranging between ±20 kips. The system was equipped with a TestStar II digital controller that allowed the use of graphical interfaces to intuitively and easily develop the procedures as well as run the tests. The software associated with the digital controller, called MTS Multi-Purpose Testware (MPT) was used to develop the procedures, monitor its progress, as well as display the time, strain, stress, and force being applied to the material. Upon completion of the test procedure, all the data requested (time, left oven temperature, right oven temperature, strain, displacement, displacement command (tensile testing under displacement control), load, load command (fatigue testing under load control)) was collected and transferred to Microsoft Excel spreadsheets. The machine was equipped with a dual controller oven. This is discussed in more detail later in this section.

In addition to the basic MTS machine, the use of a MTS 632.53E-14 low contact force high-temperature extensometer was used to track the strain (in mm/mm) on the specimen during testing. Figure 8b shows a general diagram of how the extensometers would rest on the specimen. The extensometer was made up of two alumina (white) rods about 3.5 mm in diameter that came to a cone-shaped point which would rest in "dimples" applied to the side of the specimen using a hammer and small dimpling tool provided by MTS. The dimples were placed in the straight center portion (gage section) of the specimen and were measured using a ruler to be 12.7 mm (0.5 in) (length **A** in Figure 8b) apart in order to correspond to the gage length of the extensometer. The extensometer mount served to hold the extensometer in front of the specimen as well as shielded the mechanism part of the extensometer away from the heat of the ovens. The

use of this type of extensometer can introduced some noise/error on the strain results since the rods simply rested inside the manually placed dimples with low force. This low contact force was important so that there would be no additional damage introduced onto the specimen as with a high contact force extensometer. Since the specimens were composite materials, the specimen would undergo a series of "failures". The first failure occurred by the cracking of the matrix. The fibers, however, still maintained some strength in them. The first fracture usually resulted in a highly audible pop or loud crack. This was the point for some of [0/90] specimens that the extensometer usually popped out of the dimples and strain measurements were harder to quantify. For the [±45] specimen the extensometer remained in place inside the dimples throughout testing. For the [0/90] specimen, it proved difficult to capture a good measure of the strains since after the first failure the extensometer would detach, even though much of the 0° fibers (along the load path) were still holding the piece to maintain much of the specimen's strength.

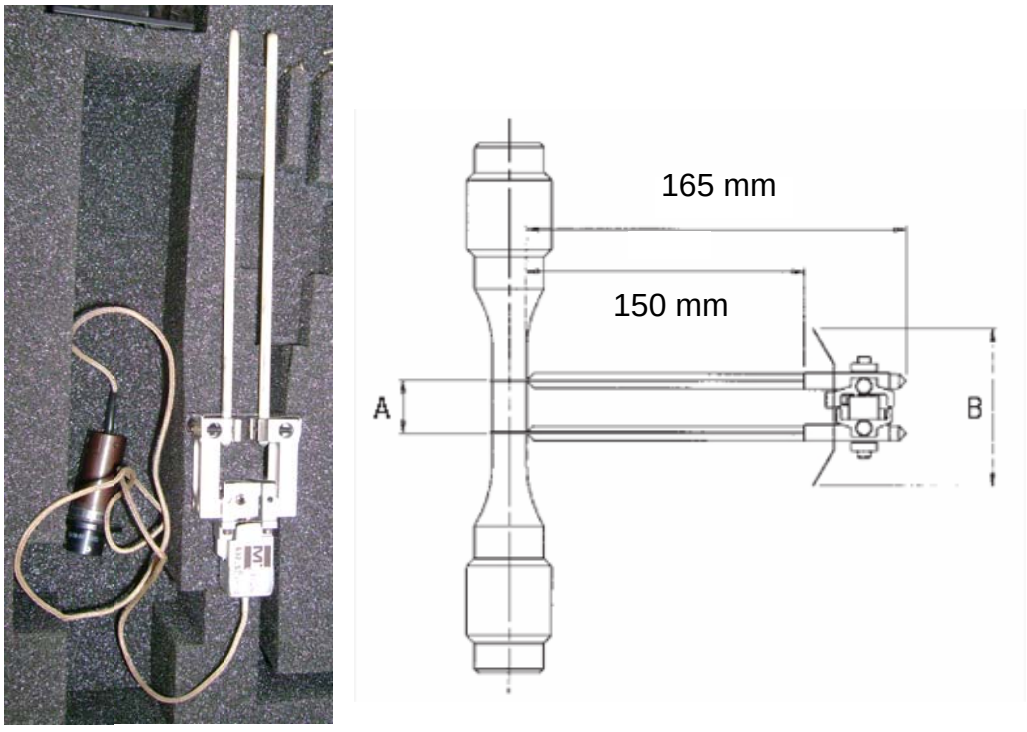

(a) **(b)**

Figure 8. Extensometer (a) not mounted (b) schematic of mounting with specimen

To heat the specimens to the desired testing temperature of 191°C, an MTS model 652 furnace was used. This type of oven had two separate MTS model 409.83 temperature controllers (Figure 9). This caused temperature calibration on the specimen to be more difficult that just using a furnace with a single controller. The fact that this furnace (also called oven) used two controllers required having to set two different temperatures (for each side of the oven), in addition to ensuring that both sides of the specimen were also reaching the desired test temperature of 191°C.

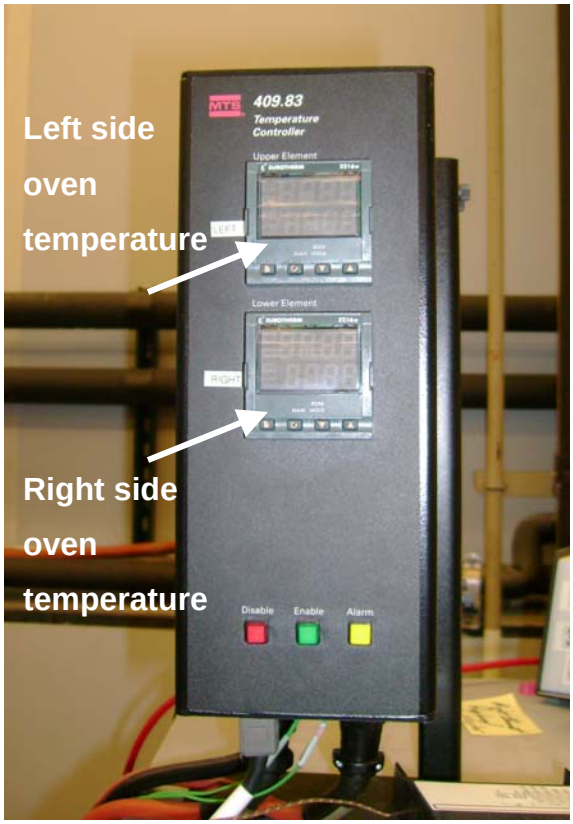

Figure 9. MTS Temperature Controller

The following steps were repeated prior to the initiation of every test. First the machine was put through a sine wave shaped cyclic displacement (from 1.5 inches to 0.5 inches) to warm up the hydraulic shafts. This ensured that they would move smoothly during testing because the warming up process lubricated and warmed up the movement of the shaft that the grip fixtures were connected to. To load the specimen, the top grip was closed onto the specimen first. Using the offset menu on the MPT software, the force was zeroed out to ensure that the weight of the specimen was not taken into account for how much force was being applied during testing, and then the bottom grips were closed. The extensometer was then attached to the specimen. To ensure that the extensometer could accomplish the task of measuring the full spectrum of the strain to be

applied, upon placing in the dimples created, it was important to make sure that the strain reading prior to testing was less than ±1%. This made sure that the extensometer rods were placed as close to 0.5 in (gage length) as possible. If the extensometer rods were at this distance, the strain offset was zeroed out prior to test run. Finally, the ovens were closed around the specimen with care not to affect the position of the extensometer rods on the specimen.

Test Specimen

The material used for the study was IM7/BMI 5250-4 graphite/bismaleimide composite. It was made up of 16 plies of unidirectional lamina. One laminate was composed of +45° and -45° angled fibers and the other was composed of 0° and 90° angled fibers. The process of creating the specimens began with CYCOM® 5250-4 composite prepreg tapes from Cytec Engineering Materials Inc. This prepreg tape consisted of a layer of parallel fibers preimpregnated with resin and partially cured. These prepregs contained 60% fiber volume fraction [9]. Cytec Inc. sometimes produces these prepreg tapes with a combination of glass and carbon fibers, but the IM7 signifies the use of only high-strain carbon fibers and the term BMI 5250-4 states the use of the bismaleimide resin. The prepregs were shipped to the Air Force Research Laboratory (AFRL) at Wright-Patterson Air Force Base (WPAFB) in 4 foot rolls at 25 to 100 lbs each (depending on the order). Each ply (lamina) is then cut from the 4 ft roll in the orientation of the fiber desired. The composite backing paper was removed from the sheet of the composite prior to stacking. The prepregs were laid on top of each other at alternating fiber orientations (Figure 10). Since the backing paper was removed, the plies

actually stuck together like tape so it was important to keep track of which direction the fibers were angled while stacking.

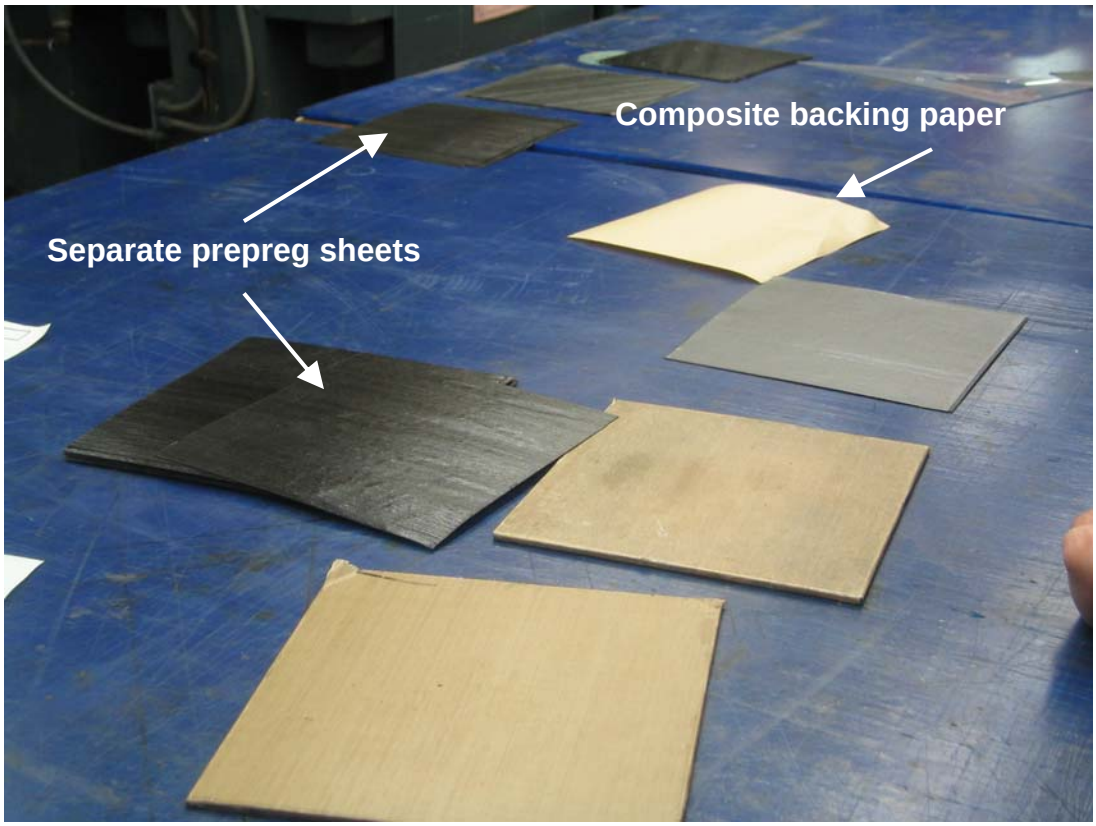

Figure 10. Prepreg tapes of IM7/BMI 5250-4 laid out ready to be stacked

A total of 8 plies from each fiber orientation were used to create a laminate of 16 plies. These stacked sheets of lamina were then placed in an autoclave which is pictured in Figure 11. Figure 12 shows an example of how the material is setup while inside the autoclave. The autoclave molding process is used for fabrication of high-performance advanced composites for military, aerospace, transportation, marine, and infrastructure applications. The bleeders (also called breathers) consist of dry glass fibers or mat. These are used to absorb the excess resin and allow for the escape of volatiles during the curing process. The entire assembly of prepreg layup and auxiliary materials is sealed

with a vacuum bag onto a tool plate (Aluminum plate) [10]. The curing process is essentially, the manufacturer prescribed temperature-pressure-vacuum-time cycle inside the autoclave chamber. Four laminate plates of IM7/BMI 5250-4 were created using the manufacturer suggested curing temperature and time of 375°F (191°C) for 6 hours and a 6 hour post-cure at 440°F (Figure 13).

Figure 11. Autoclave setup which was used to fabricate the laminates (at AFRL facility)

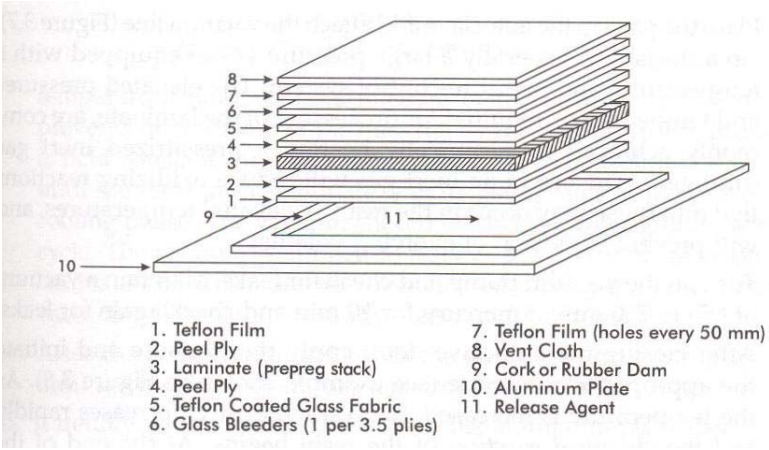

Figure 12. Vacuum bag preparation for autoclave cure of thermoset composite [10]

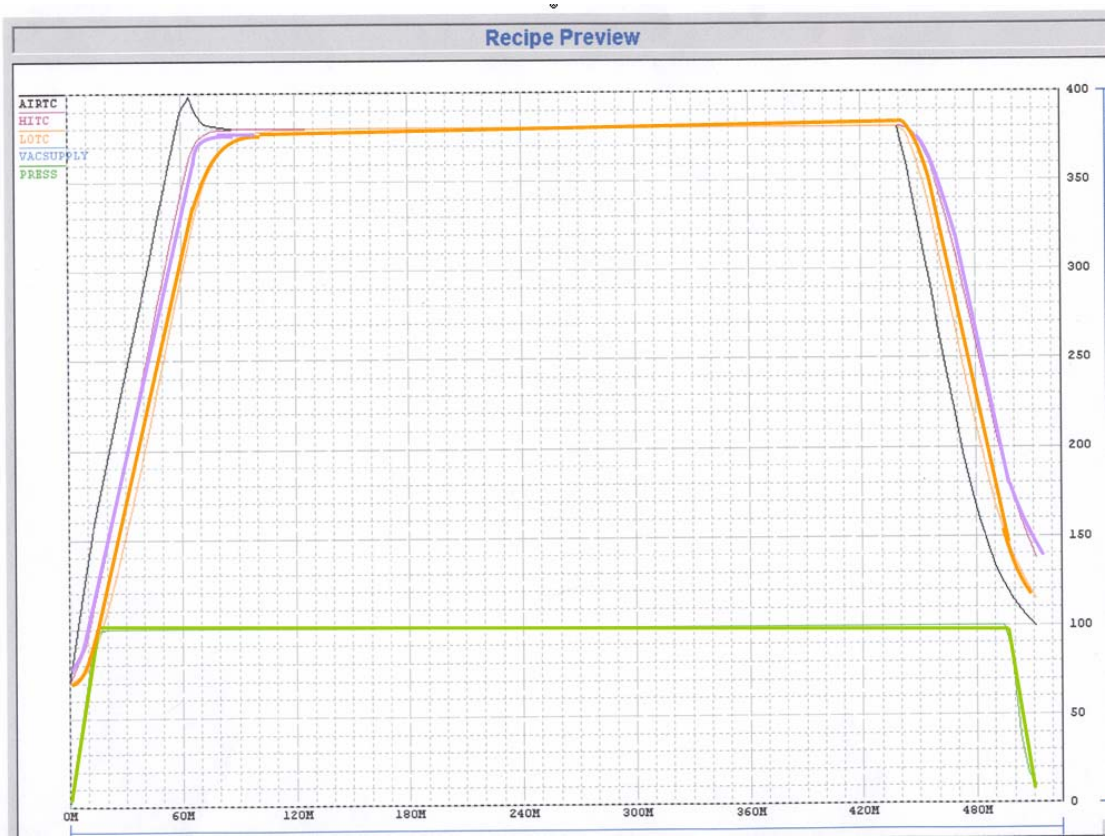

Figure 13. Plot of manufacturer's suggested curing cycle for the IM7/BMI 5250-4 prepreg in the autoclave

Two panels were fabricated in the $[\pm 45]_{4s}$ fiber orientation and the other two were cross-ply laminates with a $[0/90]_{4s}$ fiber orientation. The 4s subscript signifies the fact that there are 4 plies of +45 plies and -45 plies each on one side of the reference plane which adds up to 8 plies. These are symmetric ("s") about the center (reference plane) of the specimen, totaling in 16 plies for each multidirectional laminate. This is more easily seen in Figure 14. Since the lamina contain unidirectional fibers, it was necessary to alternate the fiber orientations so that it would create the [± 45] and the [0/90] effect. The highlighted line is the line about which the specimen is symmetric and is called the reference plane. Each prepreg tape is considered a separate ply. The [0/90]

specimen are created similarly except for the fiber orientations of the woven carbon fiber fabric are 0 and 90. These are alternately stacked in the same fashion and are also symmetric about the center.

The dog bone shaped coupon specimens were cut from the four fabricated panels using a diamond-impregnated saw to create a total of 40 coupons for each fiber orientation. Water jet cutting was considered, but in past experiences would cause damage to the edge of the specimen so it was not used. The area of the tested specimen was determined by measuring the immediate straight center portion of the dog bone test piece. This is called the gage section and is the actual test area. The thickness and width at this point of the specimen was measured and annotated prior to any loading onto the MTS machine and on average were about 2.2 mm and 7.7 mm respectively. The aged specimen were measured prior to aging as well as immediately prior to loading but showed little to no difference in the dimensions (about 0.02 mm on average). The length, thickness, and width measurements were taken using a digital micrometer with 0.000001 mm accuracy.

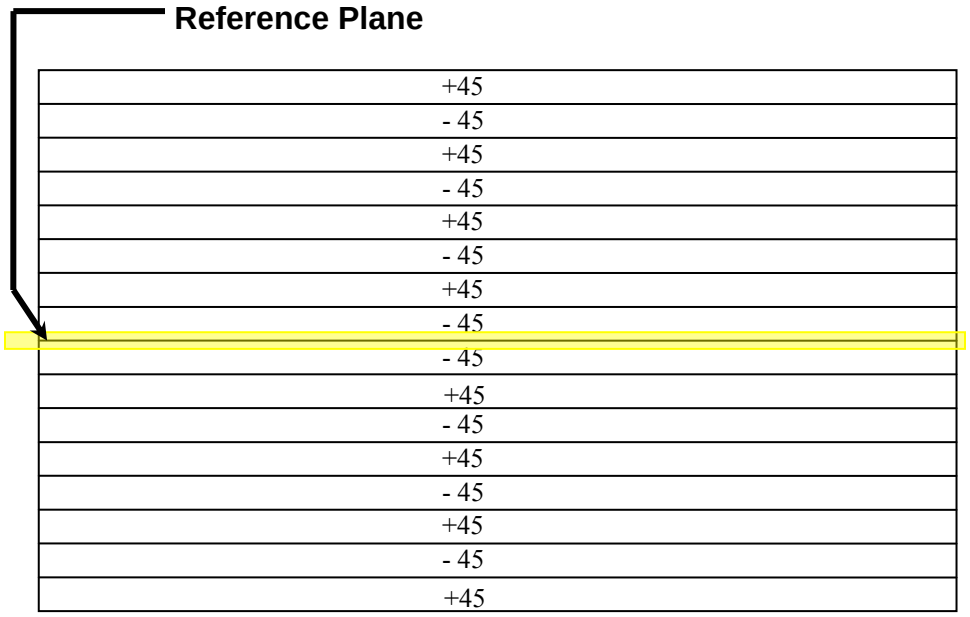

Figure 14. Schematic of the 16 plies that make up the [±45] laminate

The first step in preparing the specimen for testing required that the specimen be tabbed on both the top and the bottom portions of the dog bone (Figure 15). This was done to protect the specimen's integrity during testing. When the grips applied pressure to the specimen, it was important that no damage would be applied to the actual specimen so that during testing, the failure would occur in the gage section (center of the specimen) only and not have any affect from the portion of the specimen in the grips. This would provide more accurate results of the behavior of the specimen.

Temperature Calibration

In order to guarantee that the specimen was being tested at the desired temperature of 191°C, a temperature calibration was performed by securing a thermocouple to both sides of the specimen using Kapton adhesive tape and thin

aluminum wires (Figure 15) paying careful attention not to place the wires in direct contact with the ends of the thermocouple.

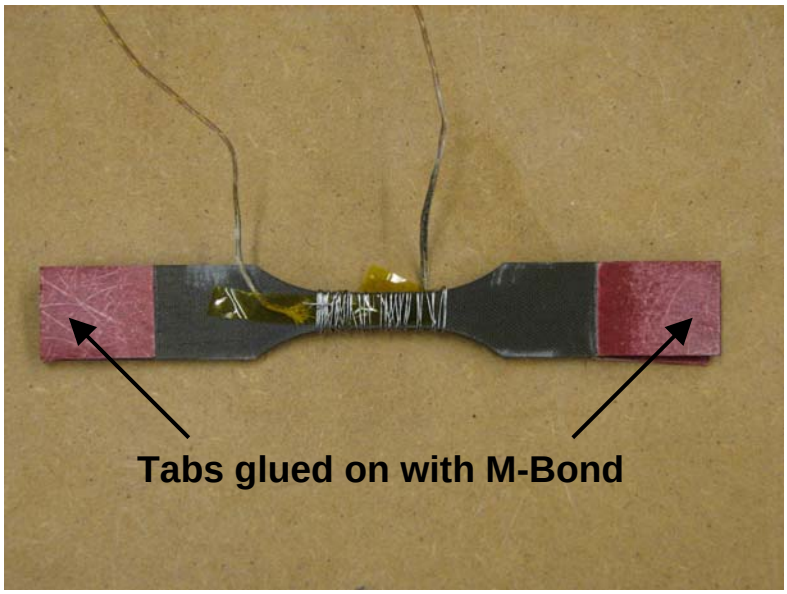

Figure 15. Thermocouples attached to a test specimen for temperature calibration

This temperature calibration was carried out on both the $[\pm 45]_{4s}$ and $[0/90]_{4s}$ just in case the fiber orientation would affect how the material heated. The reason for using two separate thermocouples (one on each side) was because the oven used (Figure 16) had two separate temperature controls. Due to the fact that the oven had different controllers it was very likely, that the sides of the specimen were not heating up at the same rate or to the same temperature. This could also occur with a single controller oven, but more significant for one that has dual controls. The process used to determine the oven temperature settings were performed by manually increasing the temperature one or two degrees at a time using the MPT software interface TestStar II controller to control the ovens. Due to the programming of the machine by MTS, immediately setting the temperature to a high level such as 100°C from room temperature commanded the oven

to overshoot this temperature and then bring itself back down. This was not desired since the integrity of the specimen was important in obtaining reliable data. Allowing it to experience temperatures greater than that of the desired test temperature could alter the chemical properties of the material or cause more degradation to the matrix which would lead to less reliable results for this test. Therefore, starting at room temperature (approximately 23°C), the oven temperature was increased to 75°C at a rate of 2°C/min. At this temperature, a dwell period of about 30 minutes was given to allow the specimen to equalize in temperature. If the specimen temperature reading on the Omega meter still had not reached the desired temperature, the oven temperatures were then increased at a rate of about 1 to 2°C/ min until the specimen temperature had reached about 191°C on both sides. Figure 17 shows the setup used for temperature calibration with the specimen mounted on the MTS machine with the ovens surrounding it and thermocouples attached, leading to the Omega meter which displayed the actual temperature of the specimen.

In the end it was determined that in order to have both sides of the specimen reach the desired testing temperature of approximately 191°C, the left furnace had to be set to 186°C and the right was set to 178°C for both fiber orientations. The reasoning behind the similarity is due to the fact that both laminates used the same type of resin as a matrix.

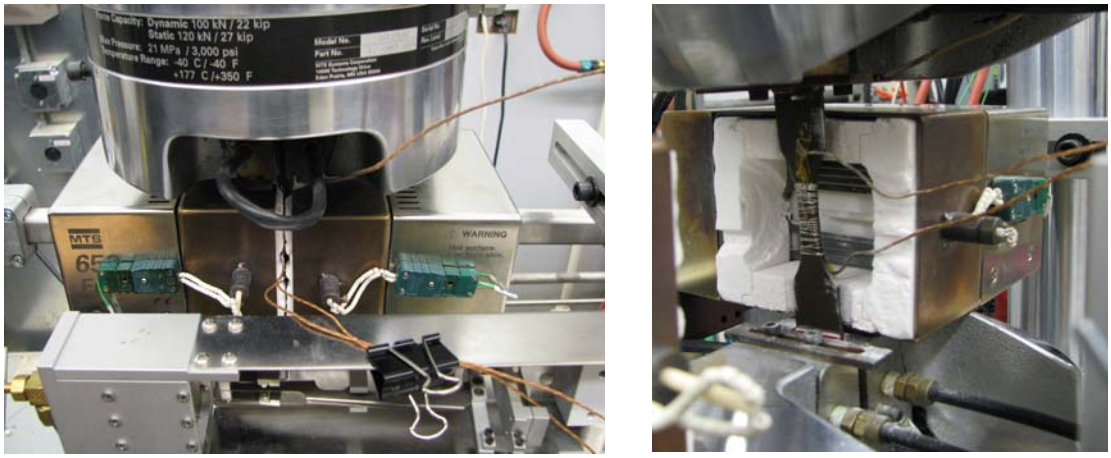

(a) **(b)**

Figure 16. Thermocouple setup: (a) Inserted through oven (b) attached to loaded specimen (inside of right oven showing)

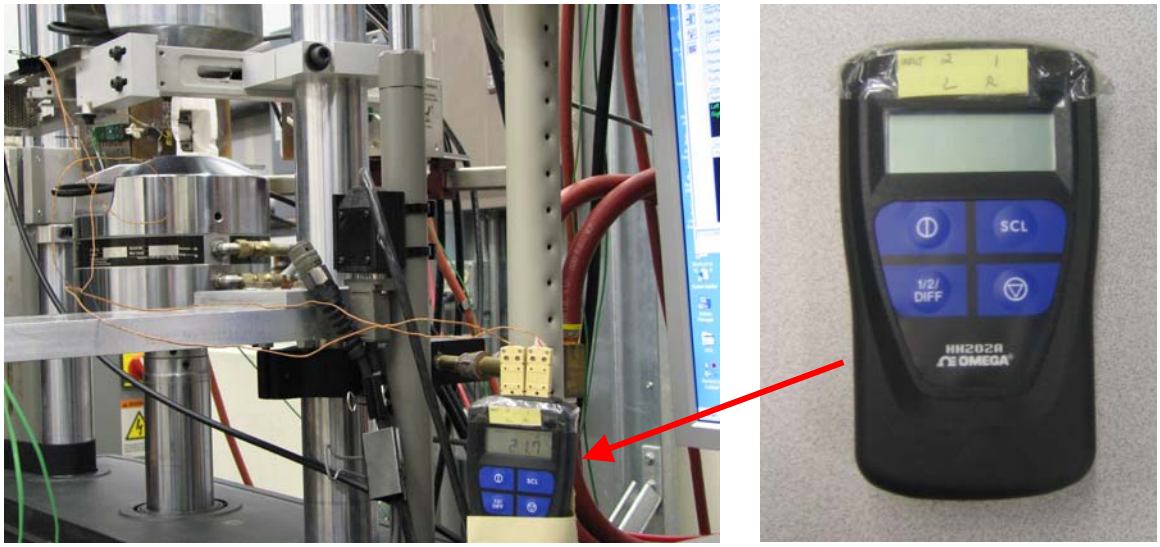

Figure 17. Omega thermocouple reader setup

Aging Process

Twenty (half of the total) specimens from each fiber orientation were aged in air at 191°C (375°F) to test the effects of aging on the overall tensile strength of the material. Prior to aging the excess moisture was removed using a Blue M brand vacuum oven set at

70°C for 48 hours. The specimens were then removed from the vacuum oven and placed into a desiccator for about 24 to 48 hours. The specimens were aged in a staggered scheduled to ensure that the AFRL facility would be open when the specimen end aging time was reached. The desired times of aging were: 10, 50, 100, 250, 500, and 1000 hours. The staggered aging schedule was useful because the oven was not big enough to hold all the specimens at one time and it also ensured that the aging times were not being cut short or exceeded by more than two hours. The specimens were placed in a desiccator while waiting to be placed into the Blue M brand aging oven which was set at 375°F (191°C). The aging of the specimen simulates the aging of a part during operation in an accelerated form to determine its mechanical behavior after many hours of service.

Due to the fact that there was a limit on how many test specimens were available, the number of specimens for each aging time was carefully decided. Table 1 shows the breakdown of how many test pieces were chosen for each aging time.

Table 1. Table of how 40 samples were allotted for aging

Aging Time (hours)	**$[\pm 45]_{4s}$ # of specimen**	**$[0/90]_{4s}$ # of specimen**
10	3	3
50	3	3
100	3	3
250	3	3
500	4	4
1000	4	4

More specimens were chosen for the 500 and 1000 hour aging times because these were predicted to show the most significant difference as compared to the unaged specimen.

For the first week, all of the 1000 hour aged specimens were measured everyday to analyze the amount of weight fluctuation due to aging using a Mettler Toledo AT200 brand balance with 0.0001 grams of accuracy. After the first week they were weighed only once every week because it has been found that these types of specimen tend to undergo less weight change after the first week. Tests performed on PMR-15 with fibers, determined that the removal of the test specimen from the aging oven for short periods of time in order to weigh the specimen is not significantly different from if the specimen were kept in the oven for the full duration. Sparse intermittent cooling and reheating of the specimens has a negligible effect on the material response [32].

Tension to Failure Test

One tension to failure test was completed on each set of specimens. This was used to create a baseline for the modulus of elasticity (also called the modulus) and Ultimate Tensile Strength (UTS). One unaged (as received) test specimen from each fiber orientation was tested. Then one specimen from each of the six aging times for each fiber orientation (total of 12) was tested.

The procedure to run these tests lasted only an average of about 2.5 hours and was automatically run using the MPT software. The oven temperatures were increased to the desired setting which were determined through the temperature calibration at a rate of 2^{o}C/min and then allowed to dwell for 30 minutes prior to any loading to allow the specimen to normalize at the target temperature. The test was conducted under displacement control. The displacement was increased at a rate of 0.025 mm/sec up to 38.1 mm (1.5 inches). The data collected from these tests were the time, temperatures

(for both controllers), strain (mm/mm), force (Newtons), displacement (mm), and displacement command (mm). Using the area measurement (thickness * width) taken prior to loading onto the machine, the stress and strain were calculated. The stress was calculated by dividing force experienced over the area. The maximum stress reached was found by looking at the highest number in the stress column (Excel file). This maximum stress was considered the Ultimate Tensile Strength. The modulus was determined by selecting a range in the linear portion of the stress-strain curve (10 to 40 MPa range). Using Microsoft Excel, a trend line was placed for this range of data and the slope of this line was taken as the modulus of the specimen.

Tuning

Tuning played a significant role in the successful execution of this study. Since the experiment was conducted under load control, it was imperative that the loads the machine was being set to were also being applied to the specimen. This would allow a more accurate test. Figure 18 is a print screen of a test that was conducted prior to tuning the machine effectively. Tuning on the MTS machine is a delicate process. If it is accomplished by an untrained individual, it could leave permanent damage to the components of the machine.

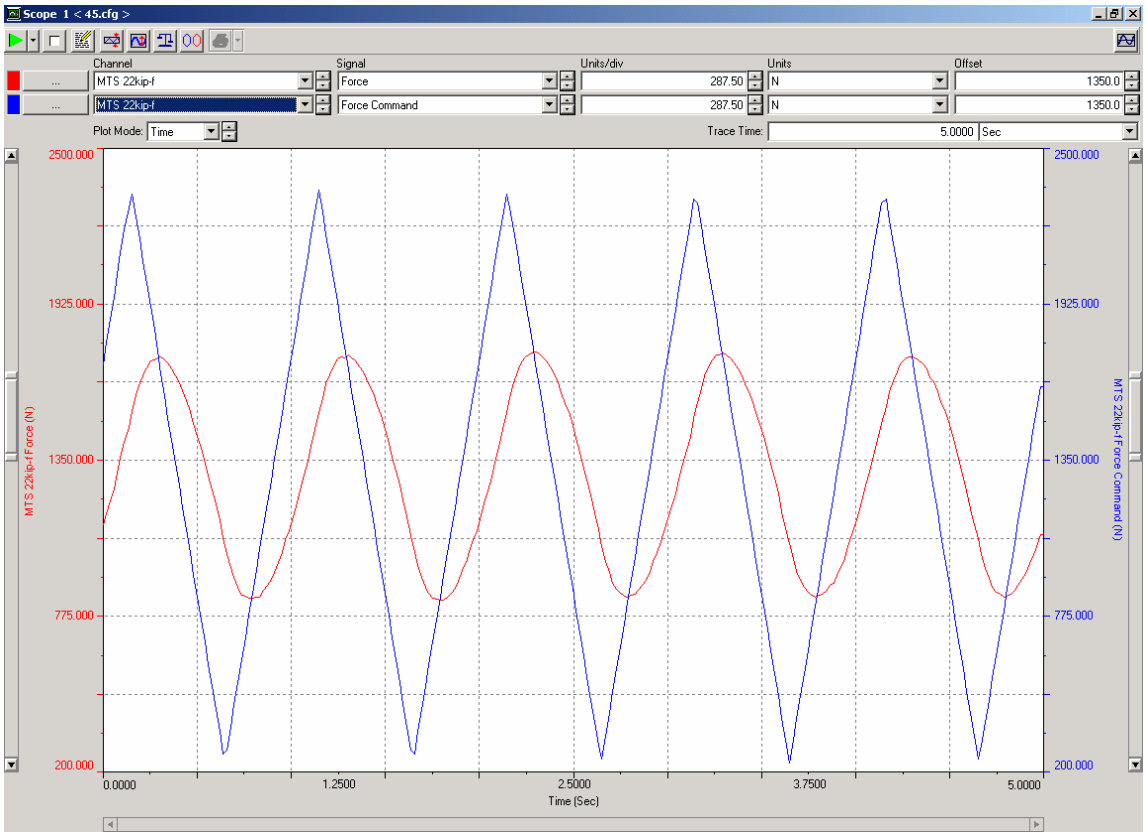

Figure 18. Graph of cyclic fatigue loading without proper tuning.

As seen from Figure 18, the triangular-wave is the command wave, whereas the smoother sine-wave is the actual force experienced by the specimen. During this test, the loads that were desired to be placed on the specimen were not being attained. Fatigue testing was conducted under load control. The tuning process was set to load command. To tune the machine successfully it was important to tune for the control type that would be used as well as for each fiber orientation. Two tuning exercises were completed, one for each of the fiber orientation since it was assumed that both fiber orientations would not behave the same. To tune the MTS machine, one specimen was loaded onto the machine. The MTS machine was set to load control and a frequency of 1 Hz was used. A square-wave was chosen for tuning since it was known to be the most difficult wave to

calibrate to. The loads were set to less than 80% of the known UTS of the specimen so that it would not break during the tuning process. The MTS machine was equipped with five available tuning controls: proportional gain (P-Gain), integral gain (I-Gain), derivative gain (D-Gain), feed forward gain (F-Gain), and forward loop filter (FL Filter). For this test, only the P-Gain and I-Gain were adjusted. The function of the P-Gain is to increase the system response and the function of the I-Gain is to increase system accuracy during static or low-frequency operation and maintains the mean level at high frequency operation [23]. The P-Gain value at the beginning of tuning was initially set really low. After examination of the waves, the P-Gain is increased in increments of about 0.05 until the square wave that coincides with the actual force being applied to the specimen is coincident with that of the MTS force command. It is pertinent to point out that any alteration to either *P* or *I*, it is necessary to allow a few oscillations to pass in order to quench any transient effects and allow the new value of the parameter to fully manifest itself [15]. In addition, it is advised that the I-Gain be initially set at only 10% during tuning. Tab1e 2 gives the tuned parameter values for each fiber orientation. Figure 19, shows a graph of the force waves during one fatigue test. This figure shows that both lines are fairly coincident with each other which means that the loads being commanded by the MTS machine are being transferred to the specimen. There is a slight delay on the load being applied to the specimen after the load command, but this is negligible since it was a matter of seconds and the loads desired were still attained. Upon retuning the machine, the command wave was changed to a sinusoidal shape so that the actual load applications on the specimen were also being applied to the specimen. As seen from

Figure 18, the specimen exhibits the sinusoidal wave form even prior to retuning. This was taken into consideration for actual fatigue testing.

Table 2. Tuning parameters for each fiber orientation

Gain	$[\pm 45]_{4s}$	$[0/90]_{4s}$
P	0.85	3.5
I	0.110	0.110
D	0.0	0.0
F	0.0	0.0

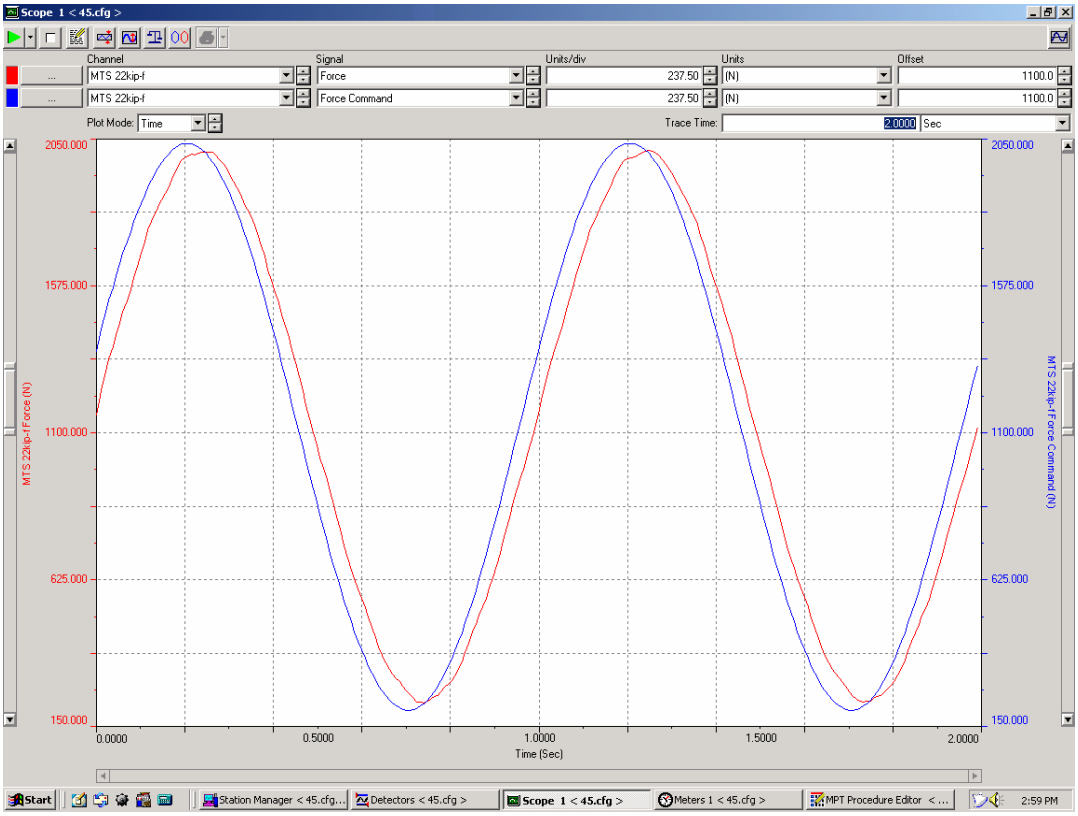

Figure 19. Proper tuning shows that both waves are coincident with each other.

Tension-Tension Fatigue

Fatigue tests were conducted at 191°C in load control and used the UTS and modulus values from the tension to failure tests. First, the unaged (as received) specimens were investigated. Starting with the [± 45] fiber orientation, a series of fatigue

tests were done to discover at what percent of the UTS the specimen would either reach failure or remain in tact after a series of cyclic loading (survive to run-out). First, the specimen was tested at 80% UTS, then, at 70%, 60%, and finally 40%. The specimen failed at 80% UTS, but did reached run-out at 70% UTS or less. For comparison, the aged [±45] specimen were all tested at the 70% UTS level to determine if run-out would be achieved as well. Following these tests, one [0/90] was tested at 80% UTS. Unlike the [± 45] specimen, the [0/90] reached run-out at 80% UTS. Therefore, the 1000 hour aged specimen was tested at this level. This was performed first due to time constraints as well as under the assumption that the 1000 hour specimen would show the most drastic difference because the [0/90] specimen were dominated by the fiber strength as opposed to the matrix. Figure 20 shows the general fatigue procedure as entered into the MTS program.

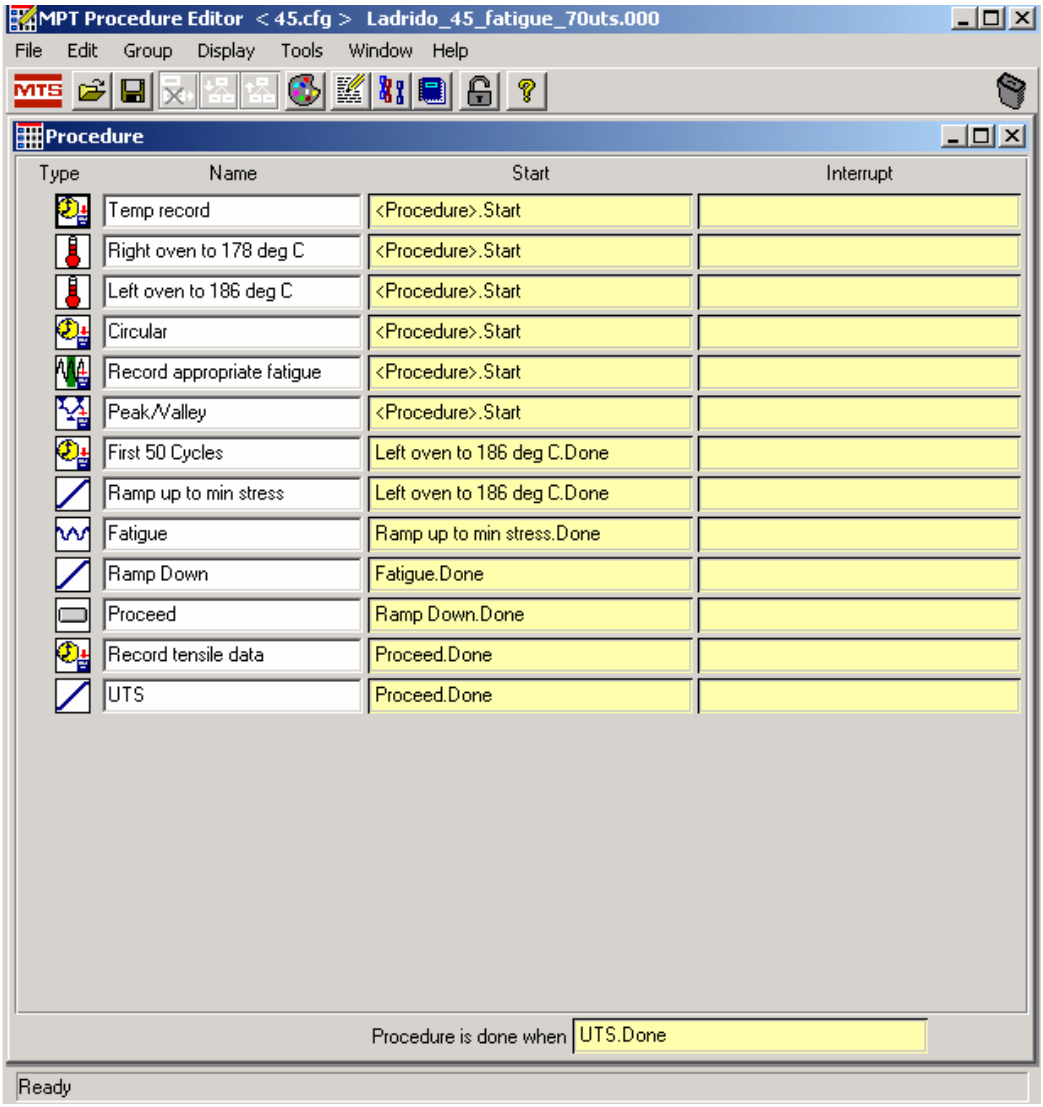

Figure 20. MTS Tension-Tension Fatigue Procedure

Time, oven temperatures, strain, displacement, and force data were collected during the temperature increase of the ovens to the target temperature. The temperature of the ovens was increased at a rate of 2°C/min until the target temperature was reached and was held at that point for 30 minutes to allow the specimen to normalize. Figure 21 shows a diagram of how the loads/stresses were applied for the

tension-tension cyclic fatigue test. The *Circular* data collection was set to record the same data listed above, in addition to force command and segment (segment = 2 x cycle) about every 0.05 seconds. It was found that during practice tests on aluminum, this provided a sufficient amount of data to be collected and analyzed. The *Circular* data collection command allowed for constant data collection in case of a malfunction of either the procedure or the machine and provided a backup that could aid in ensuring data was being collected throughout the entire procedure. *Record appropriate fatigue* data collection recorded all of the same data as the *Circular* but only up to maximum of 100050 cycles and were specifically set to record at the specified cycles. *Peak/Valley* recorded the information at the maximum and minimum loads only, and the *First 50 Cycles* recorded all the data through the first 50 cycles only. After the data collection parameters were set for the fatigue portion of the procedure the first step required the load on the specimen to be increased to the minimum level in 20 seconds so that no creep like forces were introduced due to a slow tensile load. Immediately following, the specimen was put through 10^5 cycles of loading from minimum to maximum loads which were set at different values depending on the area of the gage length of each specimen. The cyclic loading followed a sine-wave shape. Initially, a saw tooth shape was used, but due to the limitations of the machine, the forces were not reaching close to the desired (commanded) loads even after extensive tuning.

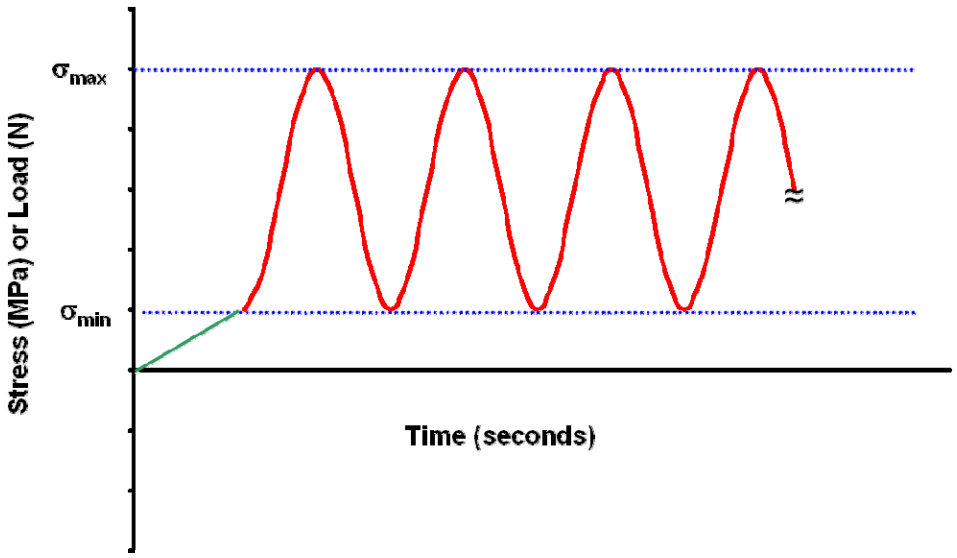

Figure 21. Tension-Tension Fatigue Test Diagram

If the specimen failed before the procedure was complete, the procedure would stop. If it remained in tact (reached run-out) for the entire duration of the 10^5 cycles, the load would be brought from the minimum setting to zero in 10 seconds. A segment command parameter was placed after this had occurred. It required the operator to be present for the final portion of the procedure. Upon selecting the "Proceed" button, a tension to failure test as the one described in the previous section (under displacement control) was conducted to determine how much strength and stiffness the specimen had retained after undergoing cyclic fatigue loading. A more detailed version of this MPT procedure is located in Appendix A.

Summary

The IM7/BMI 5250-4 graphite/bismaleimide composite went through extensive temperature calibration in order to determine the final proper temperature settings for the left and right furnaces used in this experiment which were determined to be 186°C and 178°C respectively. The MTS machine used was also carefully tuned so that the forces commanded by the controller were actually being applied to the specimens during the load controlled tension-tension cyclic load fatigue tests. Fatigue load levels were established using the data collected from the tension to failure tests.

IV. Analysis and Results

Chapter Overview

The purpose of this chapter is to present and interpret the results obtained from the tension to failure tests, aging, and fatigue testing. The results for both the [±45] and [0/90] fiber orientations will be presented together to show a comparison of how both behaved. In some cases where there is a significant difference, the data for each will be presented separately.

Tension to Failure Test Results

For the specimen tested as it was received, it is evident that the [0/90] fiber orientations exhibit more elastic deformation and little to no plastic deformation. The [±45] specimens exhibited more plastic deformation, and had higher amount of strains. Figure 22 shows a plot of the results of the tensile to failure tests at 191°C comparing both of the fiber orientations, without prior cyclic fatigue loading or aging.

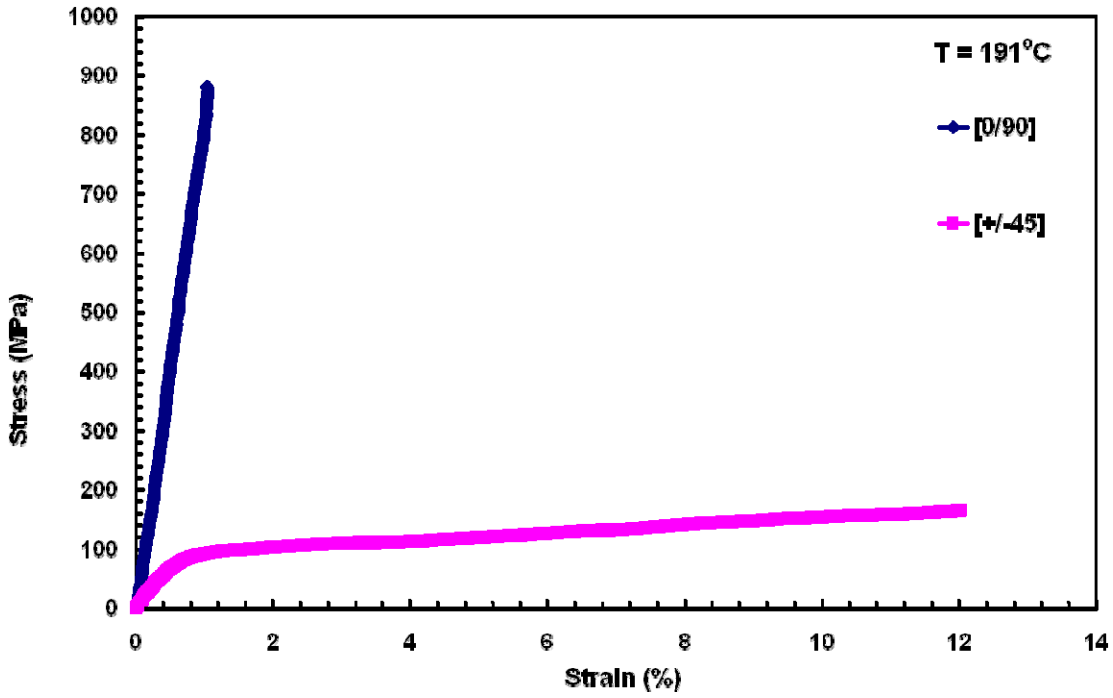

Figure 22. Plot of ±45 and 0/90 stress-strain after tensile loading for as received specimen

For the as received (virgin) specimen, the numerical data collected on these specimens is summarized in Table 3. The UTS for the [0/90] fiber orientation ranged from 800 to 900 MPa, modulus ranged from about 60 to 90 GPa, and the strain at failure fell in a range of 0.6 to 1%.

Table 3. Experimental material properties of both fiber orientations

Property	**$[\pm 45]_{4s}$**	**$[0/90]_{4s}$**
Tensile Strength (MPa)	165	780
Young's Modulus (GPa)	16	75
Strain (%)	12 %	1%

In addition to the as received (virgin) specimen, tensile to failure tests were also conducted on the aged material. Figure 23 shows a plot of the [±45] aged specimens compared to that of the unaged virgin specimen.

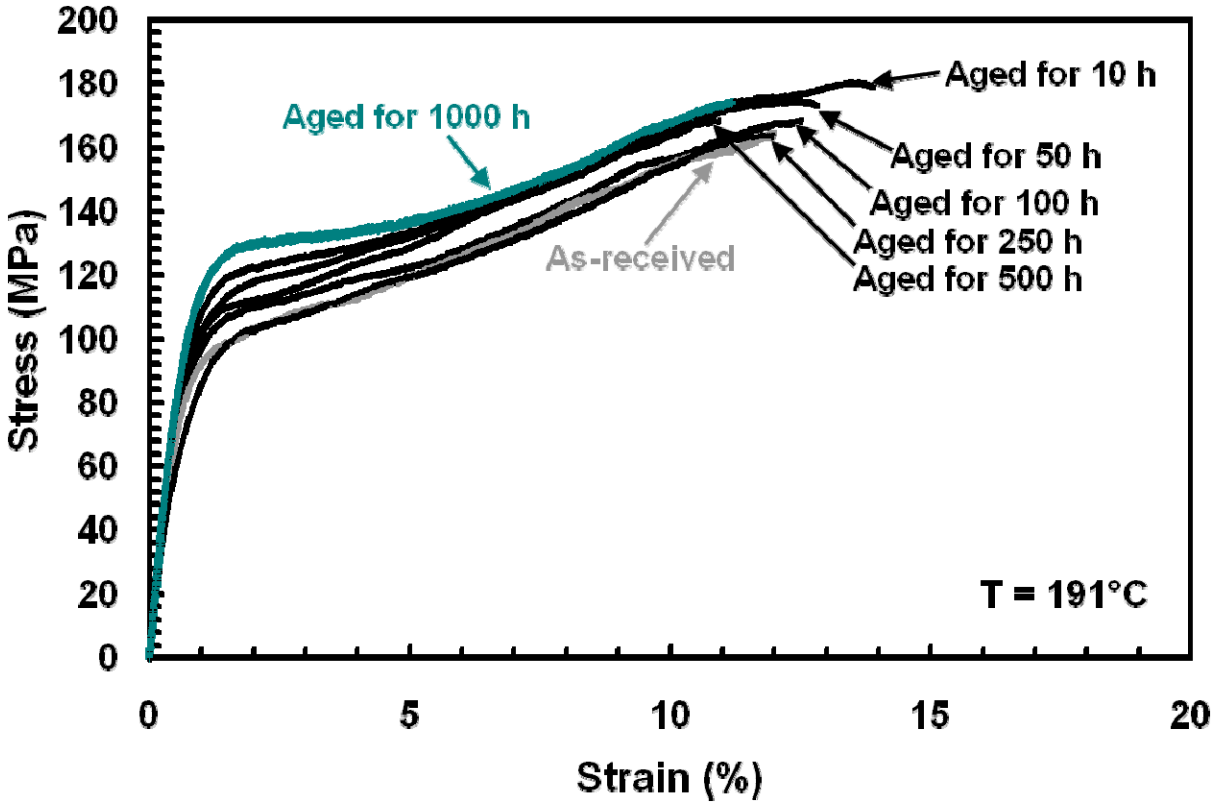

Figure 23. Stress-strain curve of all the [±45] specimens after tensile to failure test

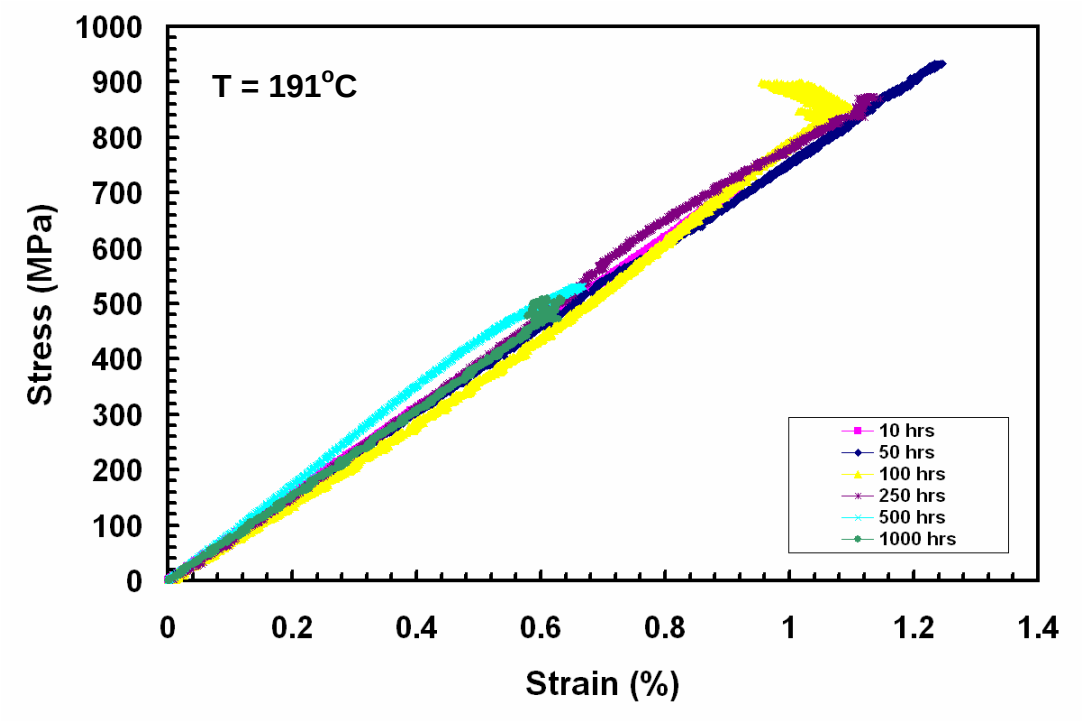

Figure 24. Stress-Strain curve of all the [0/90] specimens after tensile to failure

Table 4. Properties of the [0/90] aged specimen from tensile to failure

Aging Time h	E GPa	UTS MPa	ε_{fail} %
10	75.0971	907.0725466	0.921170718
50	59.0595	932.8793812	1.24613179
100	63.9148	898.4986188	0.95474109
250	54.355	875.111852	1.12997836
500	76.6153	629.9808021	0.66872162
1000	82.9155	683.5454696	0.732505262

Table 4 shows the values for all of the aged [0/90] tests. As with the unaged virgin specimen, the strain at failure reached 0.7 to 1%, the UTS decreased but still remained within the range of the unaged virgin specimen, and the modulus stayed close to the initial values as well.

Figure 25 and 26 are micrograph photos taken using a Zeiss Axiocam HRc digital imaging microscope. Both of these figures show that from tensile loading, a "scissoring" effect was exhibited by the specimens. This "scissoring" is essentially the detaching of the fibers from the edge of the specimen and realigning in the longitudinal direction of the force applied. This fiber "scissoring" was evident through all testing procedures.

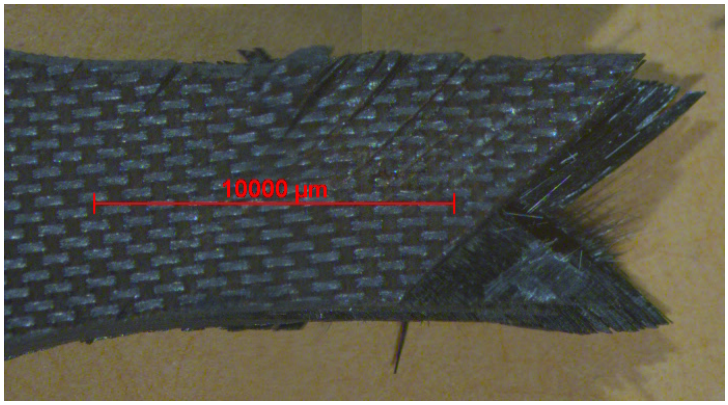

(a)

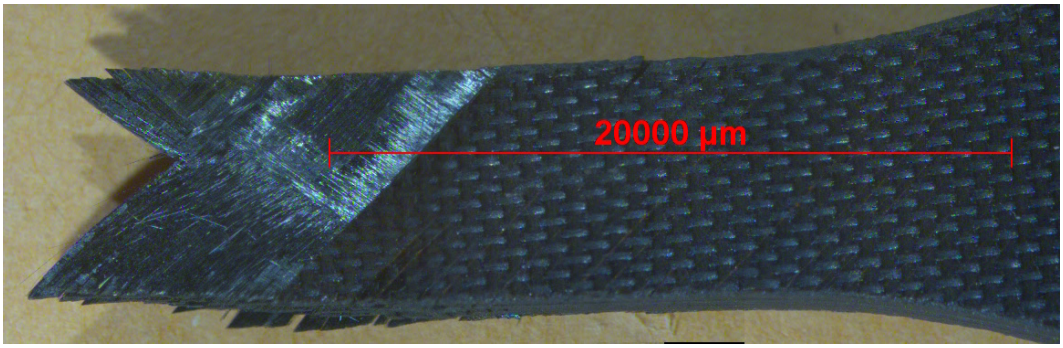

(b)

Figure 25. Micrograph picture of [±45] unaged specimen after undergoing tensile to failure

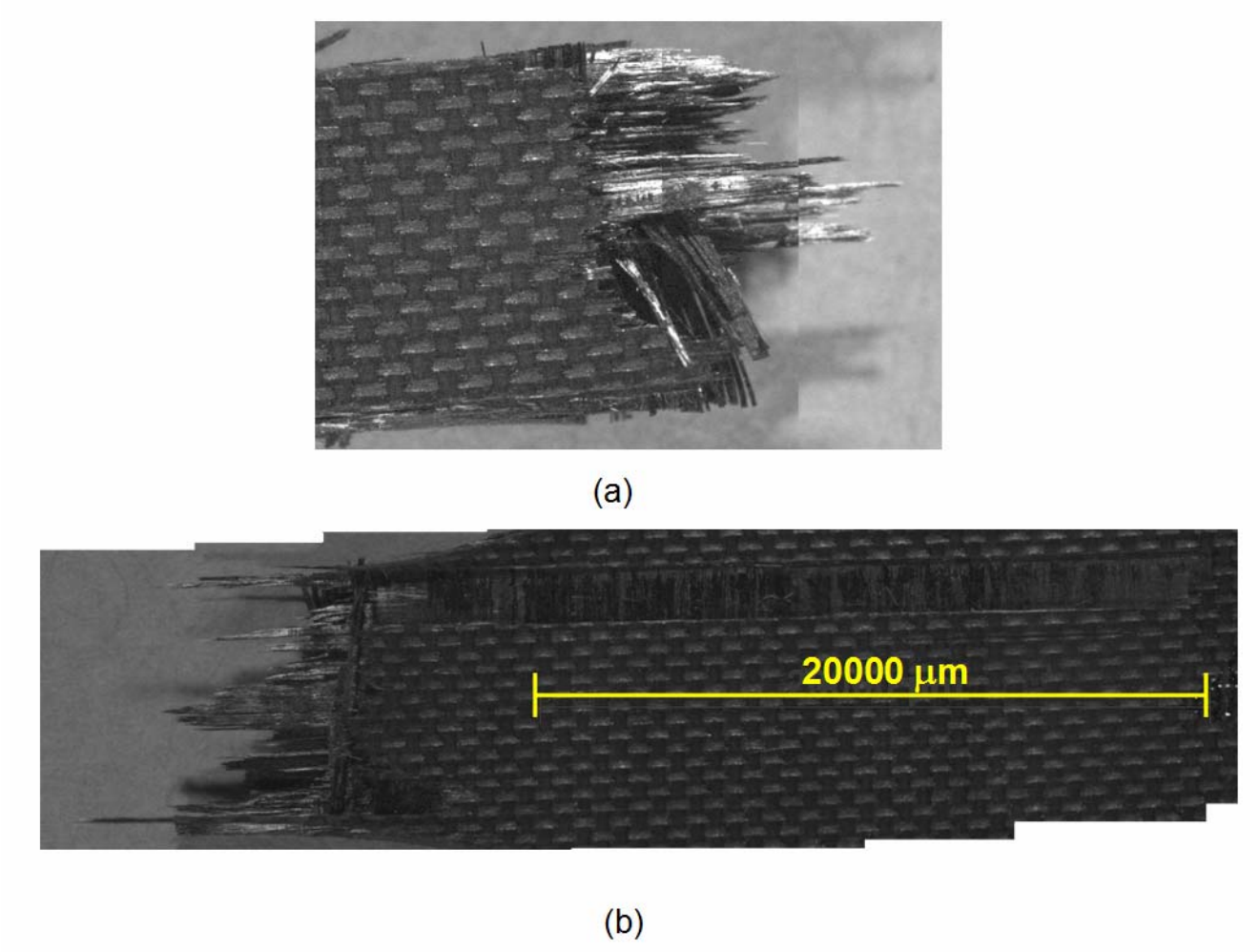

Figure 26. Micrograph picture of [0/90] unaged specimen after undergoing tensile to failure

The [0/90] specimens underwent much more dramatic failures that the [±45] specimens. These specimens actually achieved fiber fracture and pullout as well as regions of ply failures as see in Figure 26(b). These are thought to come from either imperfections introduced into the specimen during fabrication of the laminate or from the degradation of the matrix due to prior aging or simply from the 191°C testing temperature.

Effect of Aging on Specimens

Figure 27 illustrates that there was a steady decrease in weight over the 1000 hours of aging which was similarly experienced by both fiber orientations. Figure 28 provided a percentage form of the weight loss for all the specimens in both fiber orientations. This plot shows that there is actually a difference between the weight losses of the two fiber orientations. From this figure, it can be seen that the percent weight loss during the first 250 hours of aging were similar. For the hours following this, the [±45] specimens lost much more of their weight as compared to the [0/90] specimens. This is thought to stem from the fact more fiber ends were exposed on the edge of the [±45] specimens causing more matrix degradation at these points where oxygen could enter into composite. The oxidation within the composites causes the degradation of the matrix. The weight loss (in grams) of the four specimens aged for 1000 hours for each fiber orientation is presented in Table 6 with respect to the number of hours of aging. It also shows that the average weight of the [0/90] specimens was higher than the [±45] specimens.

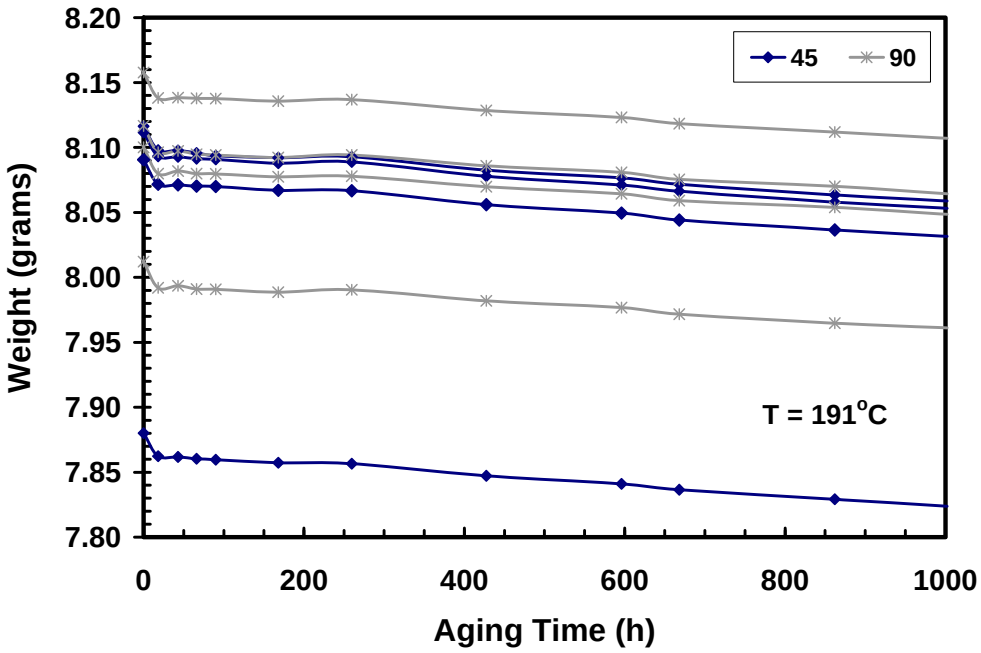

Figure 27. Plot of aging time versus the weight of the 1000 hour specimen for both fiber orientations

Table 6. Weights (in grams) of specimens aged for 1000 hours

	45				90			
Aging Time (h)	**#1**	**#14**	**#16**	**#19**	**#7**	**#8**	**#10**	**#16**
virgin	7.9011	8.113	8.1395	8.1343	8.1408	8.1230	8.0347	8.1817
0	7.8801	8.0906	8.1163	8.1116	8.1167	8.1002	8.0122	8.1577
18	7.8623	8.0716	8.0979	8.0932	8.0963	8.0799	7.9919	8.1381
43	7.8618	8.0712	8.0978	8.0928	8.0973	8.0818	7.9935	8.1384
66	7.8604	8.0702	8.0958	8.0914	8.0948	8.0799	7.9910	8.1378
90	7.8597	8.0699	8.0936	8.0909	8.0942	8.0797	7.9908	8.1376
168	7.8572	8.067	8.0921	8.0879	8.0922	8.0774	7.9886	8.1357
259.5	7.8566	8.0667	8.0928	8.0888	8.0942	8.0778	7.9904	8.1368
427.5	7.8472	8.056	8.0825	8.0778	8.0859	8.0698	7.9820	8.1285
596	7.841	8.0495	8.0766	8.0711	8.0808	8.0643	7.9767	8.1231
668	7.8366	8.0442	8.0716	8.0663	8.0755	8.0591	7.9717	8.1183
862	7.8292	8.0365	8.0635	8.0579	8.0701	8.0539	7.9647	8.1118
1002	7.8238	8.0316	8.0588	8.0532	8.0643	8.0485	7.9611	8.1071

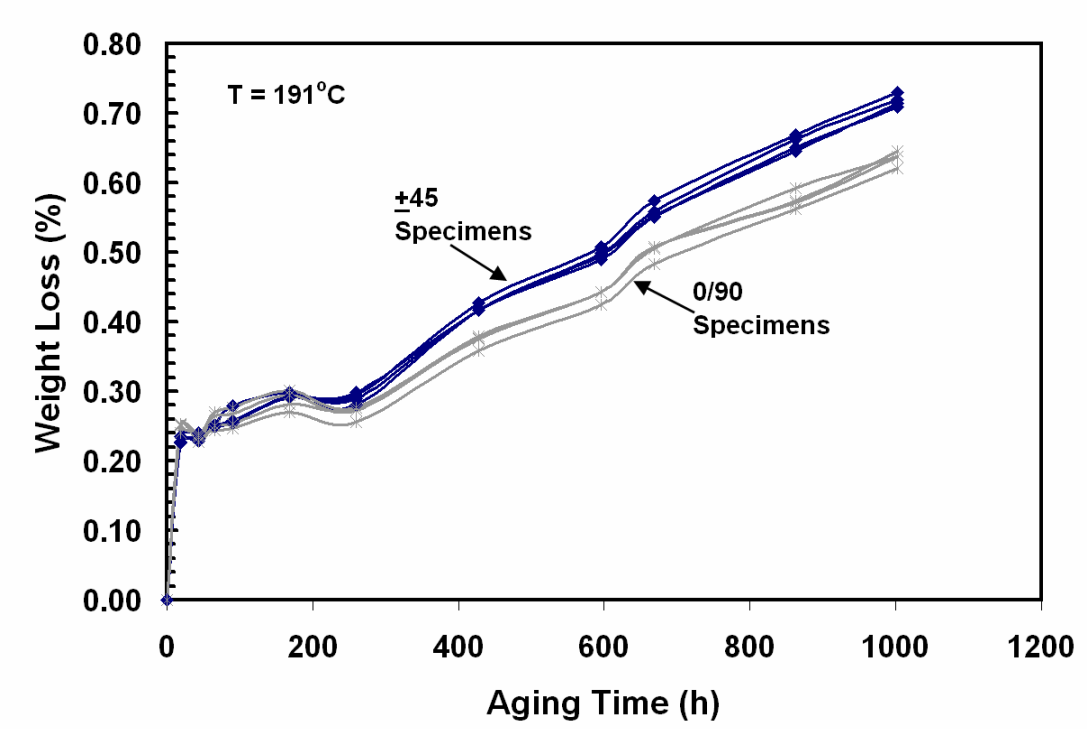

Figure 28. Weight loss (in percentage) of [±45] specimens aged for 1000 hours

Figure 27 and 28 are plots that take into account only the weights from placement into the aging oven. As discussed in Chapter III, the specimens were placed in a vacuum oven prior to being placed in the aging oven to remove any extra moisture it may have contained. The percent weight loss of all the specimens from the vacuum oven resulted in about 0.3%. Much of this weight loss is thought to be attributed by the release of moisture from the specimen that was collected after fabrication in the autoclave as well as during machining and transportation of the materials through ambient air as well as from the people handling them without wearing gloves.

Fatigue Test Results

Using the UTS and modulus from the tension to failure tests, the specimens were tested at varying ranges of fatigue at 191°C. The unaged (as received) specimens were tested at 80%, 70%, 60%, and 40% of the UTS. Figures 29 through 32 show the evolution of hysteresis loops for each of these tests. The evolution of hysteresis loop is a plot of the stress versus the strain during the tension-tension cyclic load fatigue test. Each "loop" in these plots represents a cycle during testing. From these figures it can be seen that the specimen accumulate strain as the number of cycles increased. For the unaged specimen loaded at 80% UTS, the specimen failed after 120 cycles of loading. The plots are presented with similar axes ranges for ease of comparison. It appears that as the percent of UTS decreases, the stress as well as the strain accumulation decreases as well.

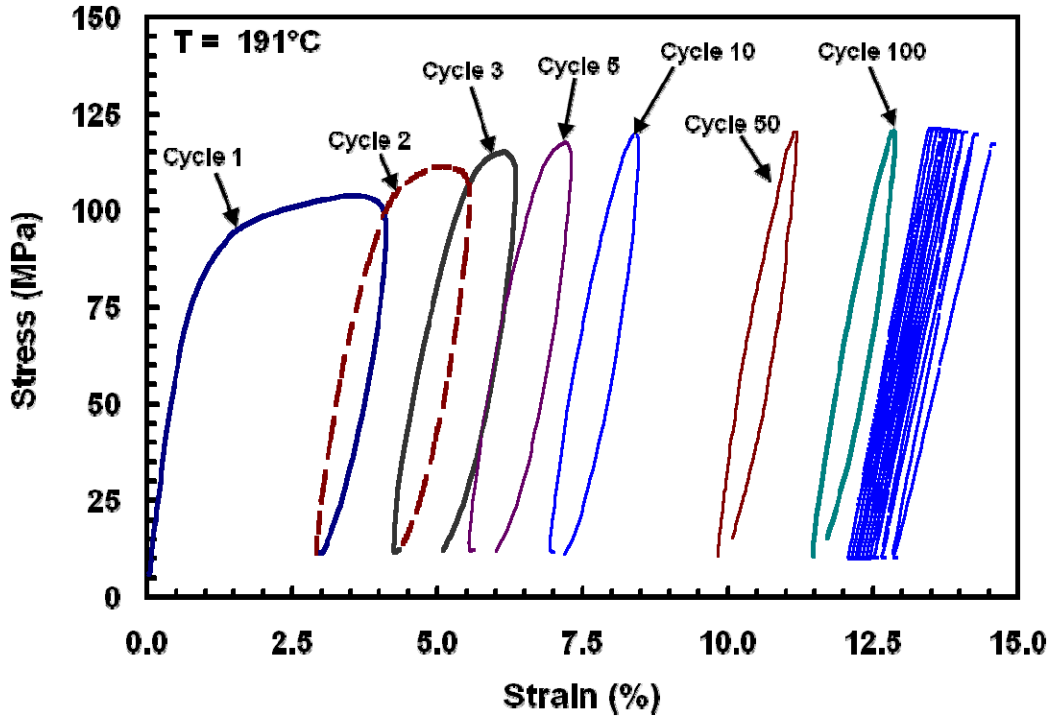

Figure 29. Hysteresis of an unaged [±45] specimen loaded at 132 MPa (80% UTS)

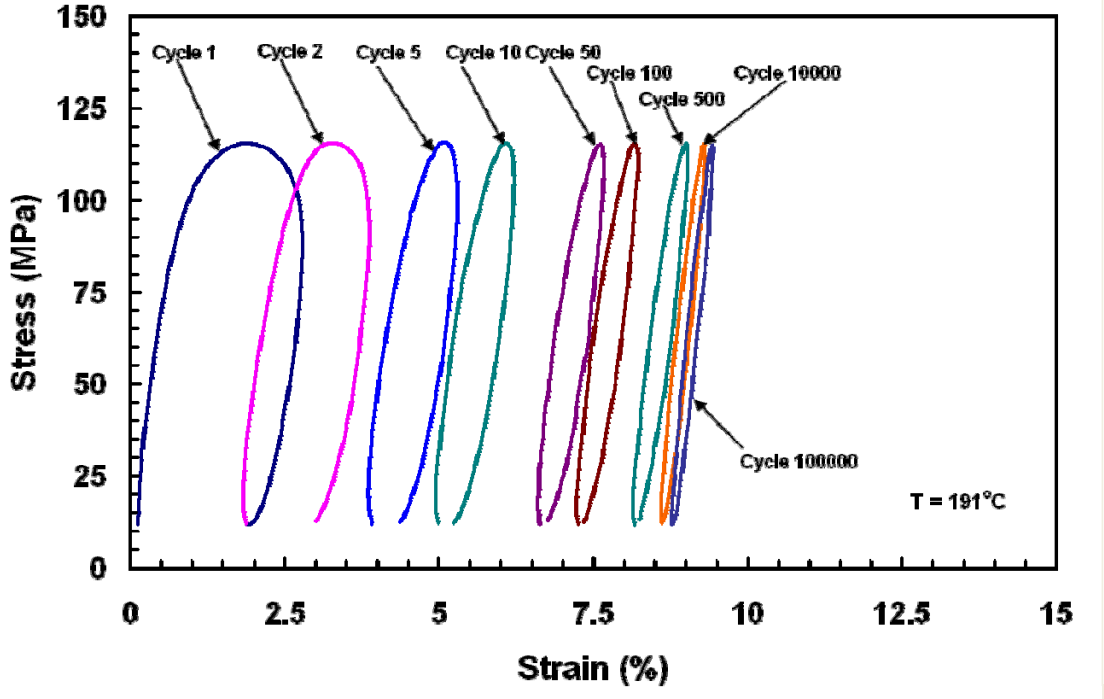

Figure 30. Hysteresis of an unaged [±45] specimen loaded at 115.5 MPa (70% UTS)

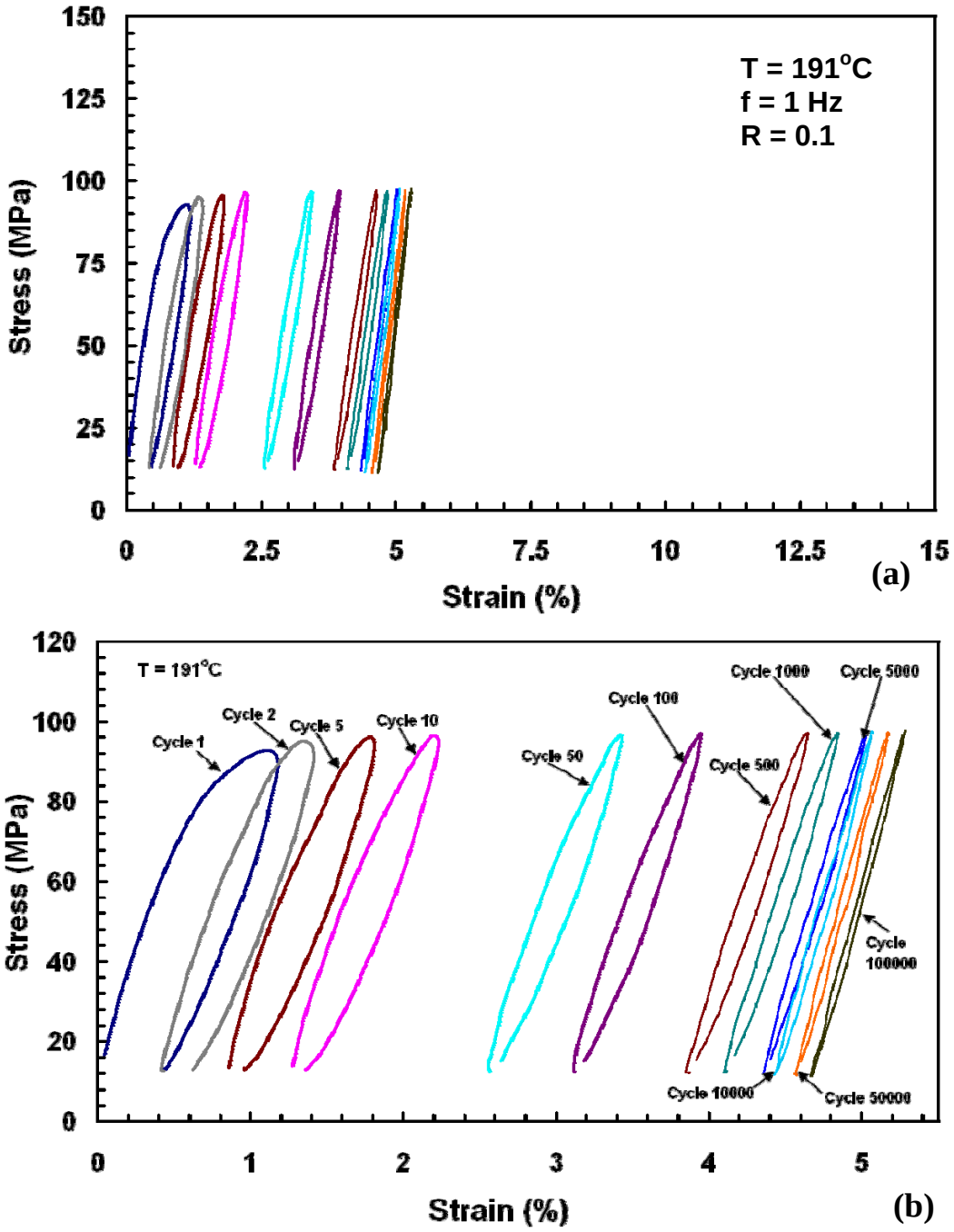

Figure 31. Typical evolution of hysteresis for an unaged [±45] specimen loaded at 99 MPa (60% UTS) (a) for comparison with other hysteresis plots (b) shows more detail

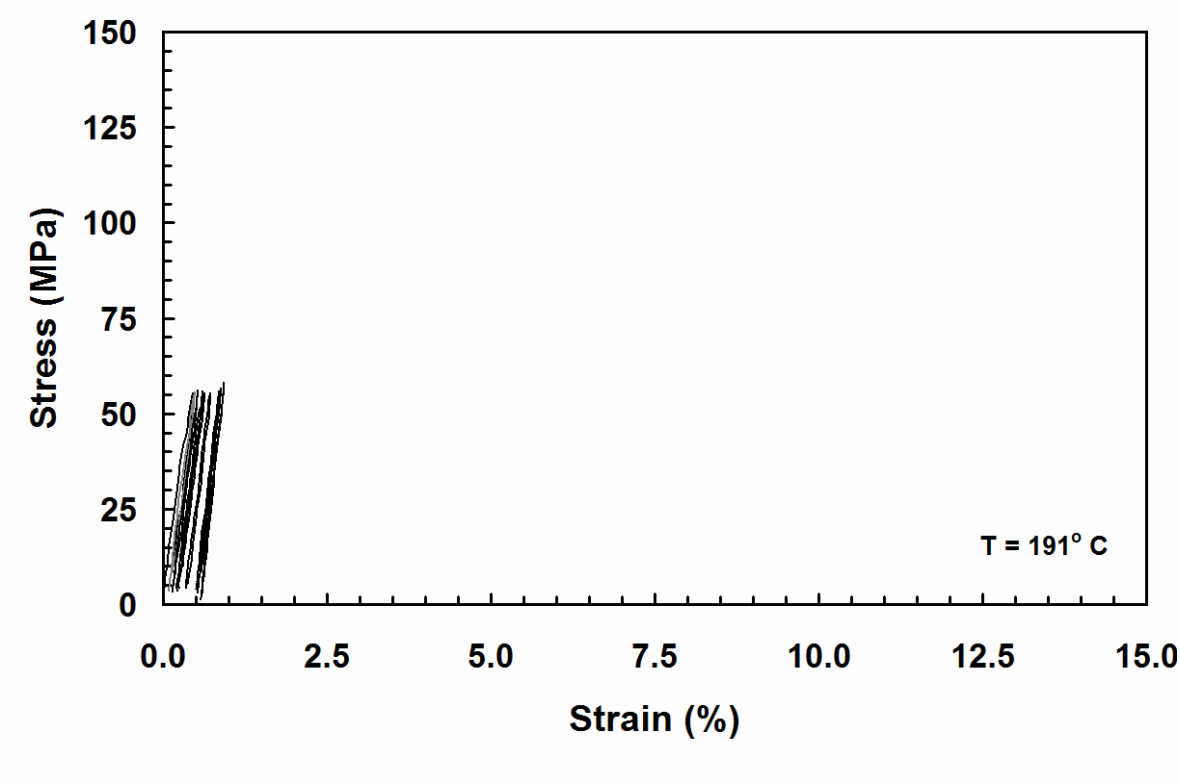

Figure 32. Evolution of hysteresis of an unaged [±45] specimen loaded at 66 MPa (40% UTS)

Figure 33 shows a plot of the maximum and minimum strains as a function of cycle number. From this it can be seen that the specimen seemed to accumulate strain rapidly towards the end of its fatigue life cycle. At the lower UTS levels (≤ 70%) the specimen reached run-out. The fatigue test at the 40% UTS level was stopped early in the interest of time as well as because it was known that it would reach run-out.

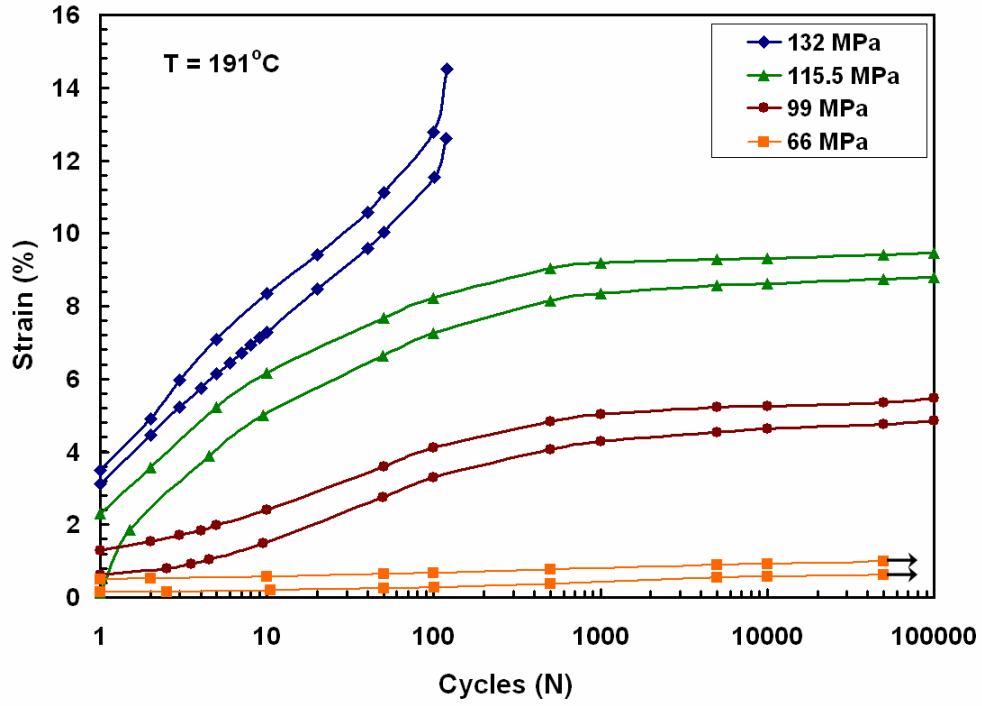

Figure 33. Maximum and minimum strains as functions of cycle number for unaged [±45] specimens

Figure 34 is a plot of how much strain was accumulated at the end of each cycle and is plotted as a function of cycle number for each of the four fatigue load levels. From this plot, it shows that the strain increased drastically prior to failing in the 80% UTS fatigue test. The reason for this could stem from the fact that matrix fracture had already occurred and the final stages of strain accumulation were from the "scissoring" of the fibers.

Figure 35 is a plot of the amount of stress applied to the specimen as a function of the corresponding number of cycles it survived. In addition, the UTS of the virgin specimen is plotted on this graph for comparison.

The normalized modulus as a function of cycle number is plotted in Figure 36. These plots were created by taking the modulus from the initial linear portion of the cycle "loop". For consistency, a range of 10 to 40 MPa was selected to obtain the modulus at each cycle that the material survived. This plot shows that the modulus decreases at the beginning of loading and then at some point starts to increase. This means that through cyclic fatigue loading the composite gets stiffer. This is probably caused by the realigning of the fibers in the load direction. In addition the point at which the specimen starts to increase becomes later in the number of cycles as the load level is decreased. There are some relatively high peaks in these plots that are attributed to noise in the data acquisition.

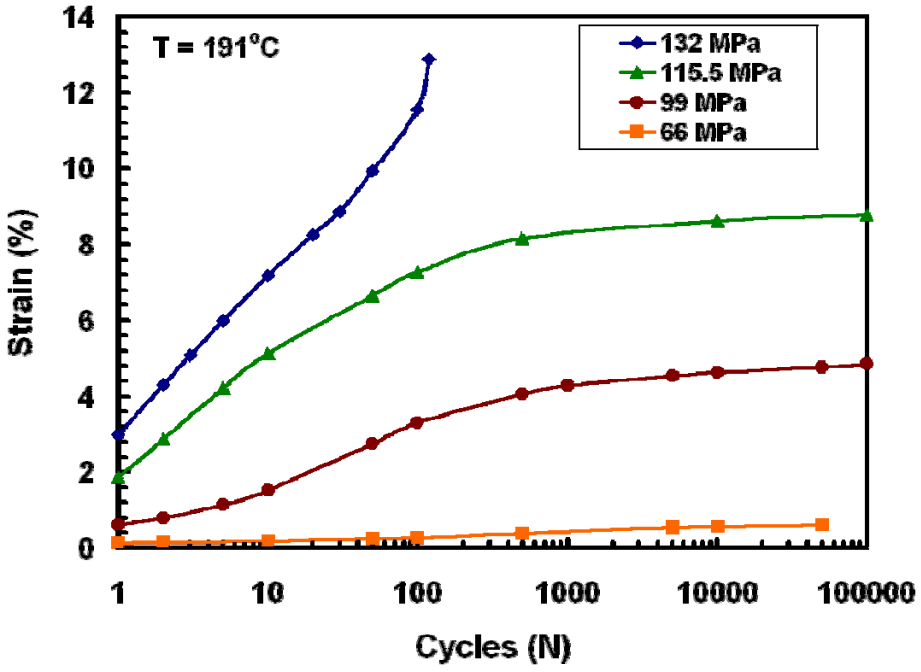

Figure 34. Ratchetting of the unaged [±45] specimen for all of the stress levels

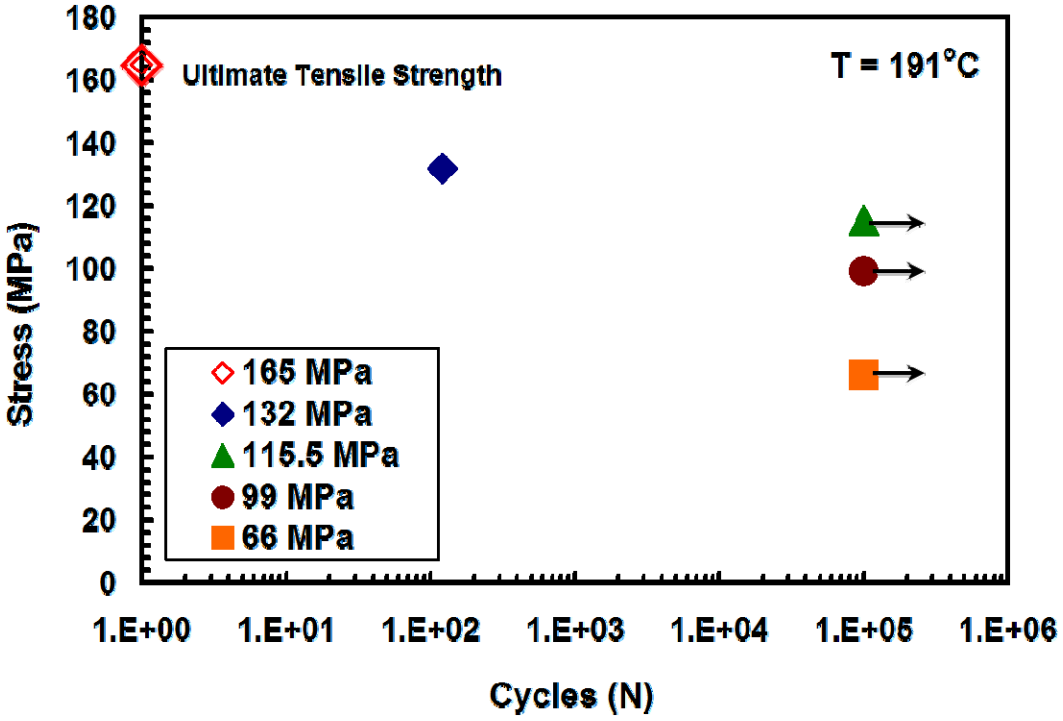

Figure 35. Fatigue S-N Curve for [±45] unaged specimens

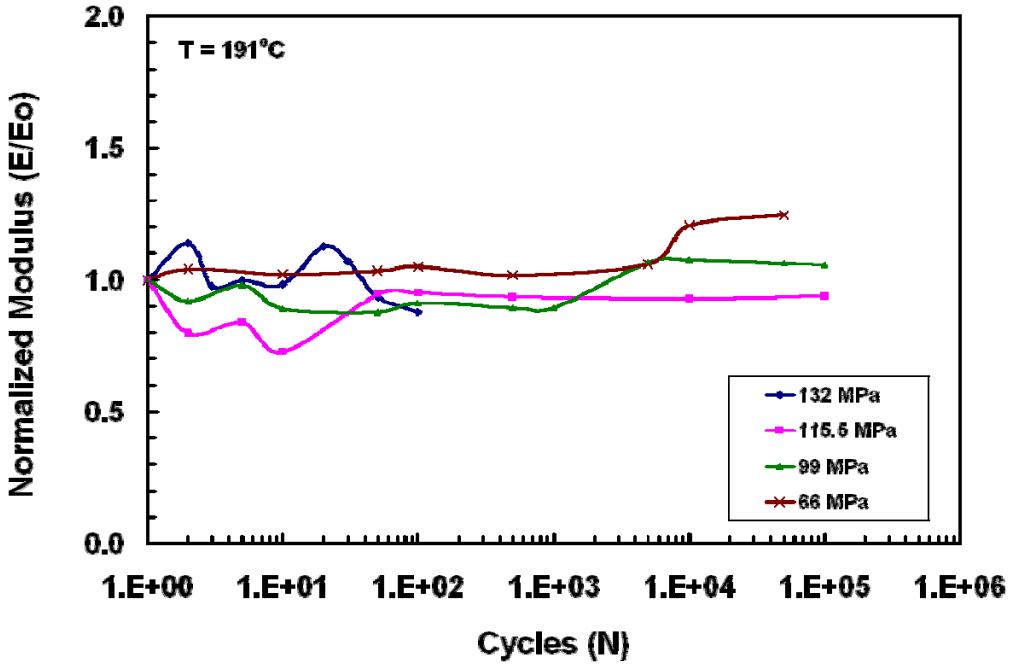

Figure 36. Normalized modulus vs fatigue cycles of [±45] unaged specimen

The following plots show the results for the aged [±45] specimens which were tested under tension-tension fatigue at 70% UTS. It can be seen that as the number of hours of aging time increased, the number of fatigue cycles that the specimen survived, decreased as well. The exact values at which these specimens failed are expressed in Table 7.

Table 7. Number of cycles to failure of each [±45] specimen

Fiber angle	Aging Time (h)	Max Stress (MPa)	% UTS	Cycles to failure
[+/- 45]	0.0	132	80	120
[+/- 45]	0.0	99	60	Run out
[+/- 45]	0.0	66	40	Run out
[+/- 45]	0.0	115.5	70	Run out
[+/- 45]	10.0	115.5	70	Run out
[+/- 45]	50.0	115.5	70	67738.0
[+/- 45]	100.0	115.5	70	49130.0
[+/- 45]	250.0	115.5	70	51927.0
[+/- 45]	500.0	115.5	70	51762.0
[+/- 45]	1000.0	115.5	70	19277.0

Figures 37 through 42 are evolution of hysteresis loops for the specimens aged at 10, 50, 100, 250, 500, and 1000 hours at stress and temperature levels of 70% UTS and 191°C. The same or similar axis ranges have been used on these plots for ease of comparison. It is interesting to see from these graphs at which strain percentage the cycle falls. These results show that tension-tension fatigue life cycle decreases with increasing prior aging time.

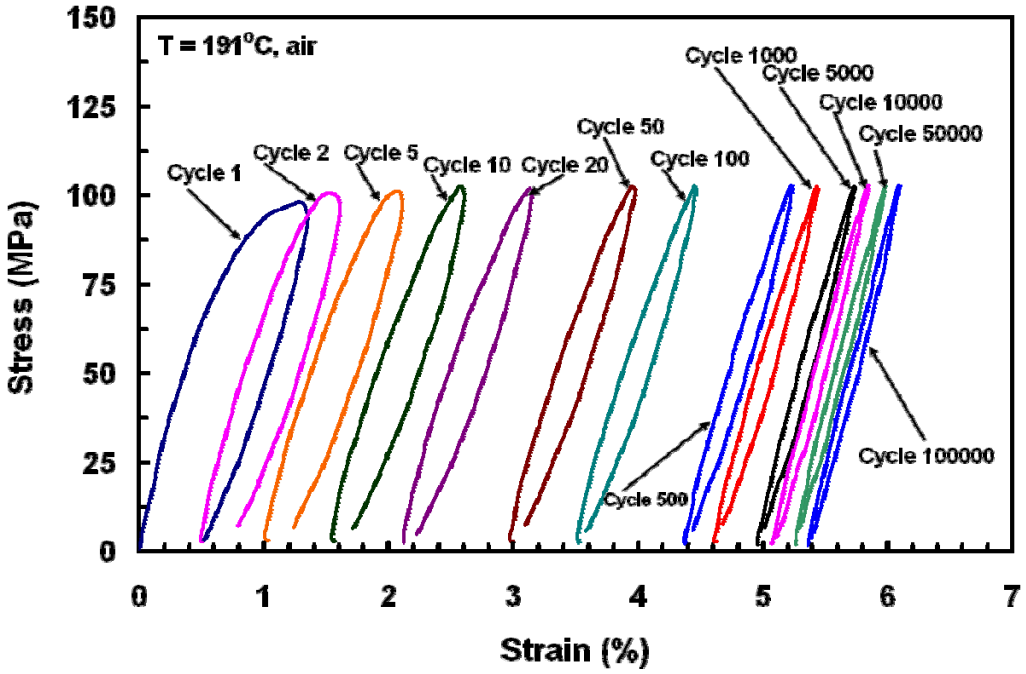

Figure 37. Hysteresis loop for [±45] specimen aged for 10 h

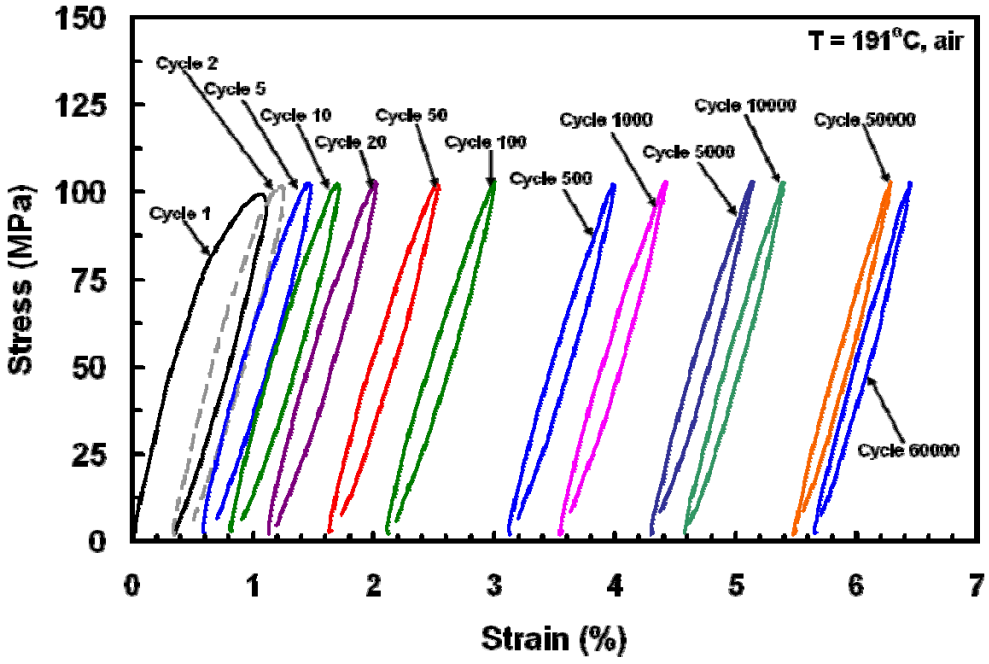

Figure 38. Hysteresis loop for [±45] specimen aged for 50 h

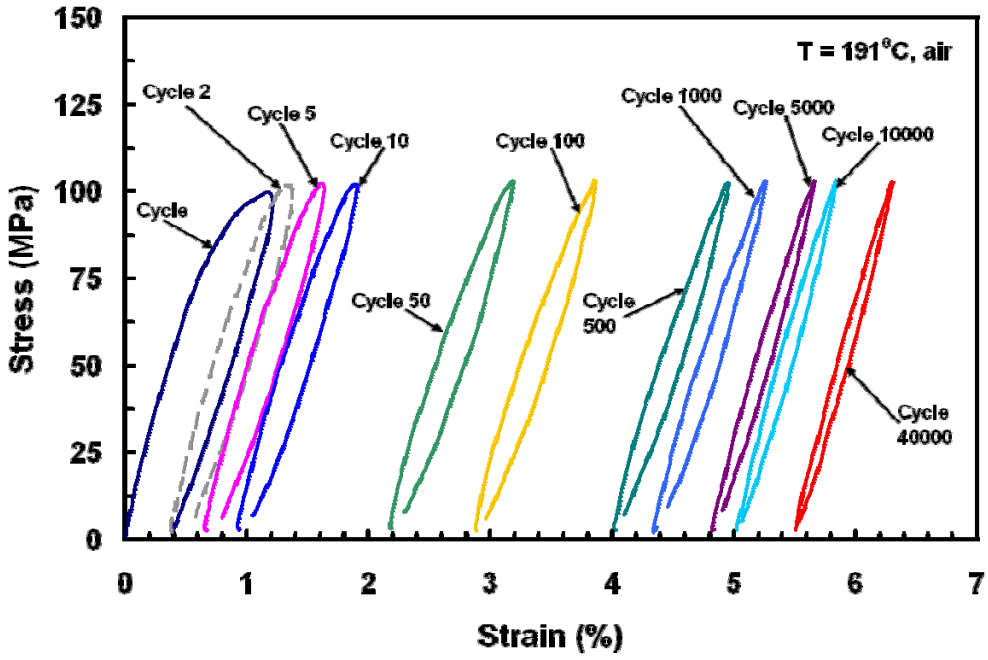

Figure 39. Hysteresis loop for [±45] specimen aged for 100 h

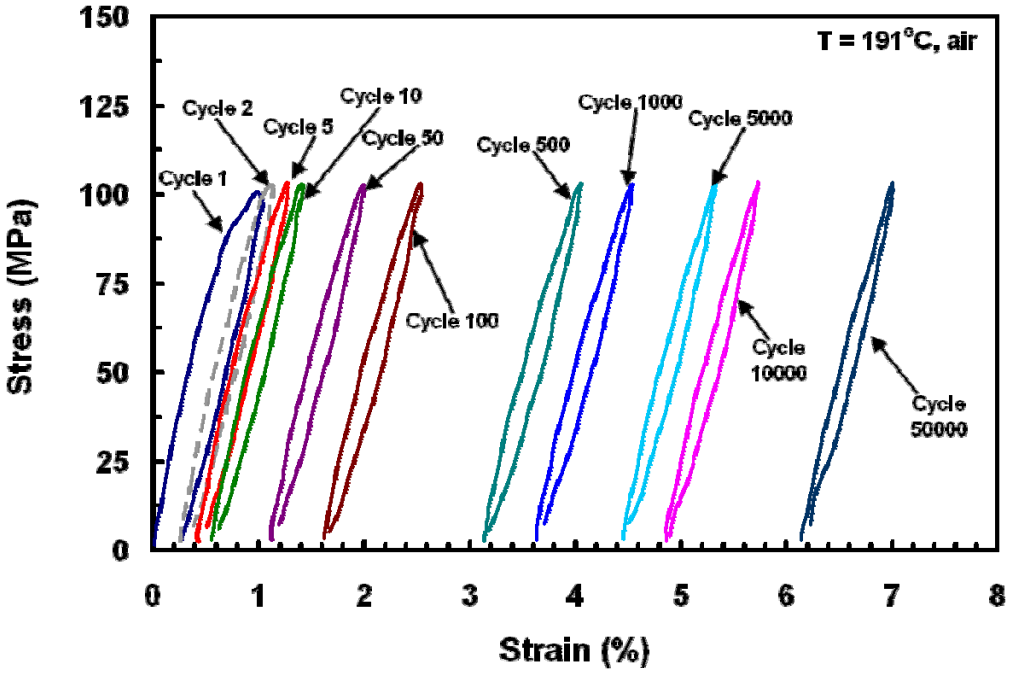

Figure 40. Hysteresis loop for [±45] specimen aged for 250 h

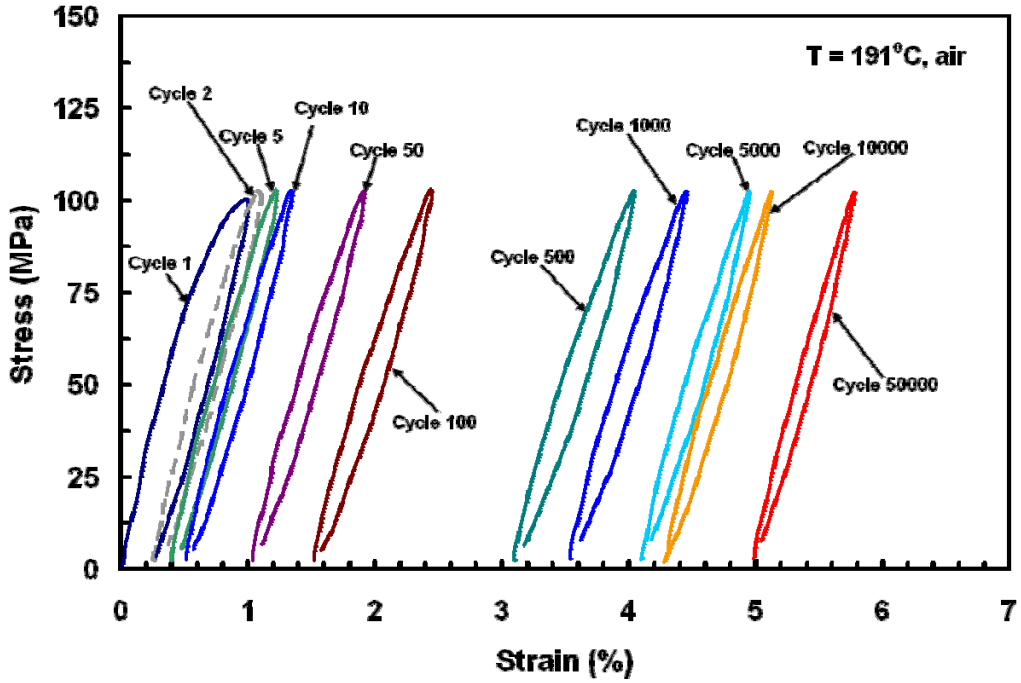

Figure 41. Hystresis loop for [±45] specimen aged for 500 h

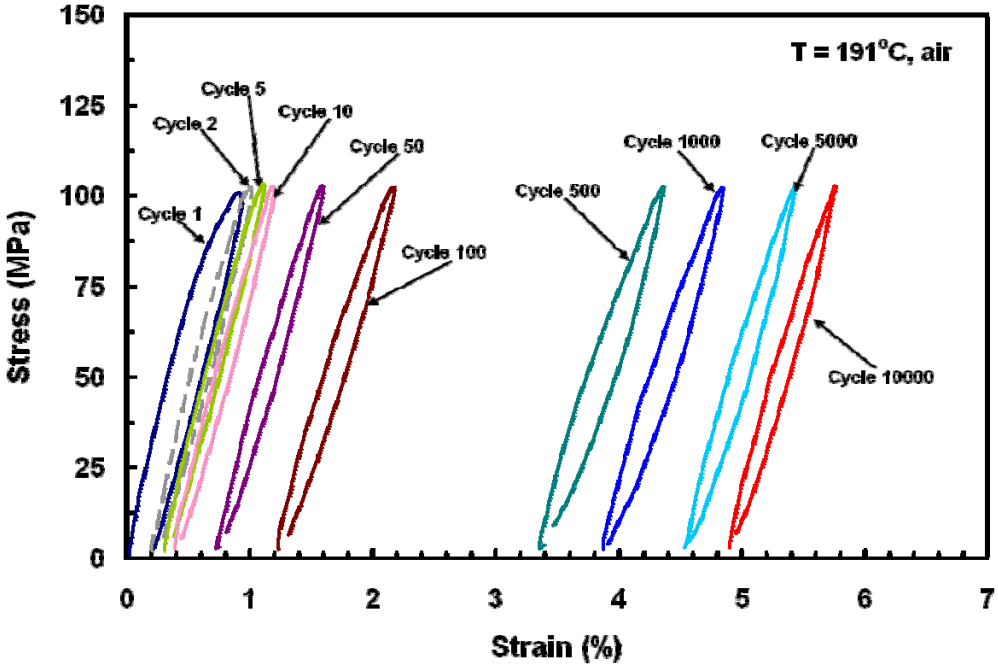

Figure 42. Hystresis loop for [±45] specimen aged for 1000 h

Figure 43 shows the maximum and minimum strain curves as a function of aging time for the aged [±45] specimens. It shows that the specimens followed a similar rate of increase without too much variation among the different aging times. The rapid increase in the 1000 h specimen prior to failure could be attributed to the fact that there was already a crack in the matrix prior to complete separation of the specimen into two pieces.

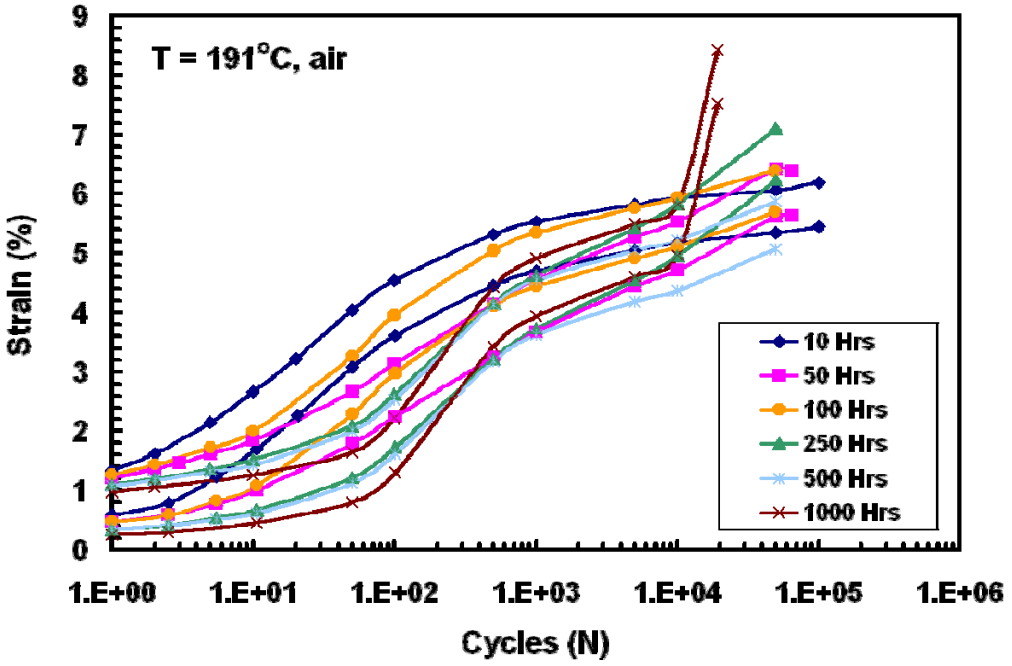

Figure 43. Maximum and minimum strains as functions of cycle number for aged [±45] specimen

Figure 44 shows the maximum amount of strain accumulated after each cycle as a function of cycle number. By examining this plot, it can be seen that the only specimen that survived all 10^5 was the only one that had a more flat slope as the number of cycles increased. Generally, the cyclic strain accumulation increases with increasing stress levels.

Figure 45 shows that as the fatigue cycling increases, the normalized modulus decreases with increasing cycles. For most of the aging times, the modulus decreases between 3 to 13%, but for the 500 and 1000 h specimens, the final decrease reaches up to almost 20%.

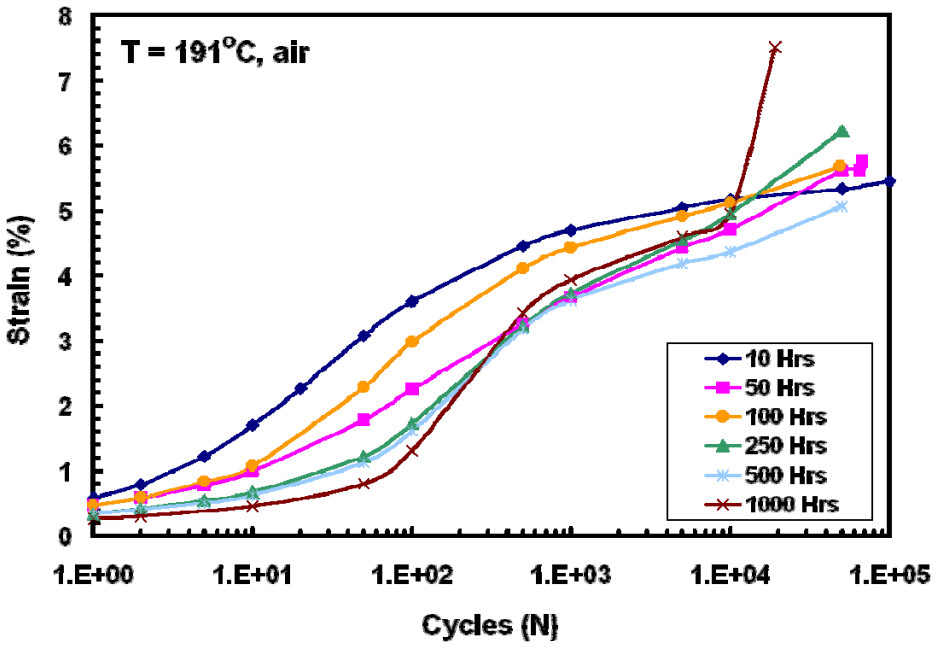

Figure 44. Ratchetting of the aged [±45] specimen for all of the stress levels

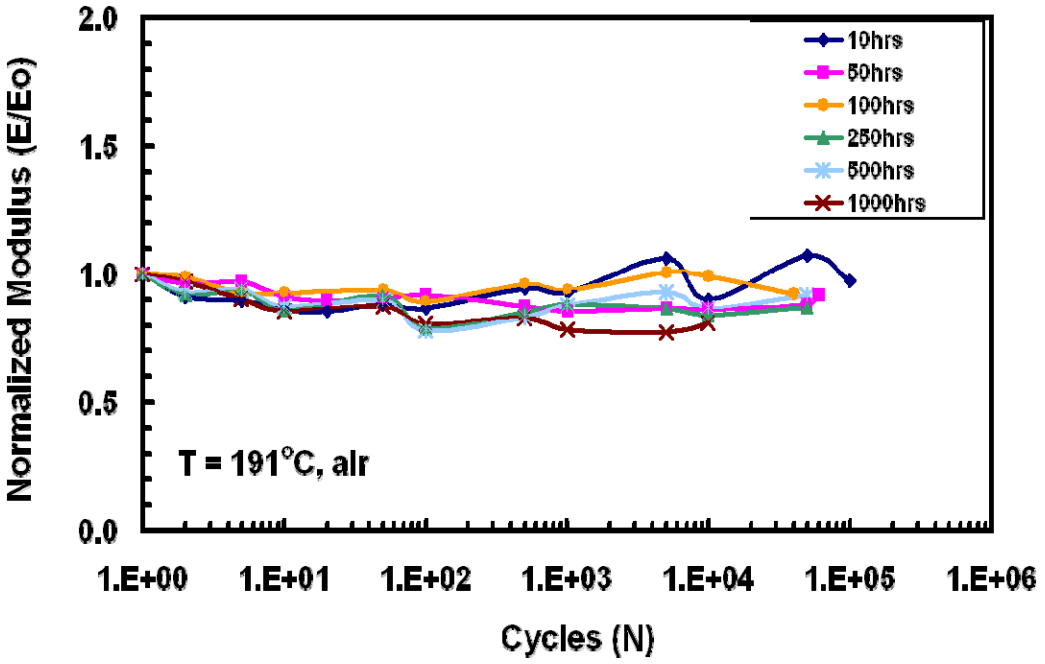

Figure 45. Normalized modulus vs fatigue cycles of [±45] aged specimens

Retained Strength Test Results

The following results were to show how much strength the specimens retained after undergoing fatigue at 191°C. As can be seen from Table 7, the only aged specimen that reached run-out was the specimen that was aged for 10 h. After cyclic loading fatigue was done, this specimen was tested to see how much of the strength was retained. From this test, it was found that the UTS of the specimen was 152.396 MPa, the Young's modulus was 15.5 GPa and the maximum amount of strain accumulated was about 3.1%.

Figure 46 shows a comparison between the stress-strain curves of the unaged and 10 h aged [±45] specimens that underwent 70% UTS cyclic fatigue loading at 191°C.

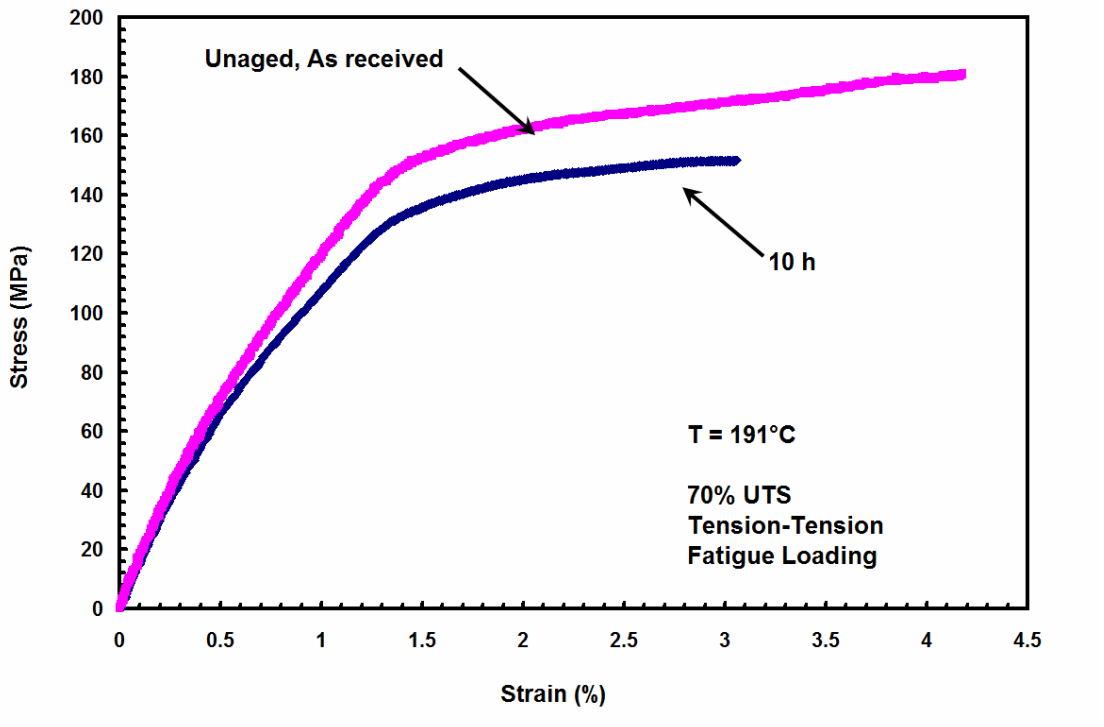

Figure 46. Retained stress-strain curve of the 10 h specimen compared to the unaged specimen at the same load level

Summary

All of the [±45] procedures were conducted without any problems. The data presented in this chapter were presented from evaluating the data received from the MTS machine output. The stress and strain data were initialized to zero so that the results for each test could be compared. This allows for comparison of all the different specimens tested. Data collected for the [0/90] fiber orientation showed no significant effect of prior aging to the fatigue behavior of the material. This is primarily due to the fact that this laminate is fiber dominated and carbon fiber typically degrades at temperatures up to 800°C which were not reached for this study.

V. Conclusions and Recommendations

Chapter Overview

This chapter will take the data presented in the previous chapter and explain the reasons for the behavior of the IM7/BMI 5250-4 composite material. Recommendations for future studies will be presented following this discussion.

Conclusions of Research

From the unaged, as received tension to failure tests, it can be concluded that the IM7/BMI 5250-4 with [±45] carbon fiber orientations have a stress-strain response that becomes non-linear at about 80 MPa. Whereas, the [0/90] specimens sustained a linear stress-strain response until failure. The reason for this is because the [0/90] specimens were relatively more fiber dominated and upon initial matrix fracture the composite was assumed to have reached failure. The [±45] specimens experienced more of the "scissoring" effect. As tension increased, the fibers would detach from the edge of the specimen and realigned in the direction of the load axis. The realigning allowed the specimen to experience more strain than the [0/90] specimens. The damage within the gage sections of the [±45] specimens showed that little to no fiber fracture occurred, whereas on the [0/90] specimens a significant amount of fiber fracture and pullout occurred. This was evident on the aged tension to failure specimens as well.

The results of the tension to failure tests with prior aging on the [±45] specimens showed that the modulus of the composite is not affected by prior aging. The linear elastic region increases as the length of prior aging time increases. For the [0/90] specimens, the modulus of the composite is not influenced by prior aging as well. The

stress limit the material can sustain decreases with increasing prior aging time. A comparison of both fiber orientations showed that the [±45] experienced 0.2% more weight loss than the [0/90] specimens. This is due to the fact that the [±45] specimens had more fibers exposed at the edge of the specimens. At these points, the oxygen would enter into the composite causing oxidation. This oxidation led to the degradation of the matrix. The more "pathways" that the oxidation could enter on the [±45] specimens was the reason these specimens underwent more weight loss after aging. Degradation of the matrix causes the life of the composite to decrease.

The results of the tension-tension cyclic fatigue tests showed that the [±45] specimens fatigue lifetime decreases with increasing prior aging time. The cyclic strain accumulation increases as the stress levels increase, but were not influenced by prior aging. The fatigue limit for the [±45] specimens falls between 115.5 MPa (70% UTS) and 132 MPa (80% UTS). Normalized modulus decreases as fatigue cycling increases. For the [0/90] specimens, there was no significant difference between the aged and unaged specimens. The reason for this is that prior aging in 191°C for up to 1000 hours caused degradation in the matrix, but did not affect the carbon fibers. Since the [0/90] specimens are fiber dominated and the carbon fibers were not affected significantly from aging, the strength of the aged [0/90] specimens remained similar to the unaged specimens.

The only aged [±45] specimen that reached run out was the specimen that was aged for 10 hours. A comparison of this specimen with the unaged specimen tested at the same load level (115.5 MPa, 70% UTS), showed that the retained strength decreased with prior aging and the retained modulus was similar for both unaged and aged specimens.

Recommendations for Future Research

It would be interesting to examine the effects on mechanical behavior at longer aging times, lower temperatures, or aging in argon. Aging in argon eliminates the oxidation effect. Some examination as to the oxidation affects of aging along the fiber orientation would prove to be interesting and possibly allow some prediction as to how oxygen travels through the interphase of the graphite/bismaleimide composite material.

Existing documentation states that unidirectional composites will preferentially oxidize along the fiber direction [32]. An interesting study using a Scanning Electron Microscope (SEM) or Transmission Electron Microscope (TEM) would be interesting to examine whether or not this is a common theme for this a BMI matrix composite as well.

In order to completely determine what applications this specific composite can be used for, it would be beneficial to perform other forms of cycle fatigue load testing such as compression-compression or compression-tension.

In addition to these, further testing of the composite with varying ply or laminate thicknesses or fiber orientations could lead to an ideal stacking sequence or thickness that supports higher stress levels or aging times. From these tests, an optimal composite configuration could be determined for specific load levels or other applications.

Summary

The affects of prior aging essentially show that the fatigue life cycle of the material will decrease. This causes the amount of fatigue that the specimen can undergo to decrease as the aging time increases. In addition, the effects of prior aging do not have

any influence of strain accumulation. Strain accumulation for this material is strongly influenced by stress and not by prior aging.

Appendix

MTS Tension-Tension Fatigue Procedure

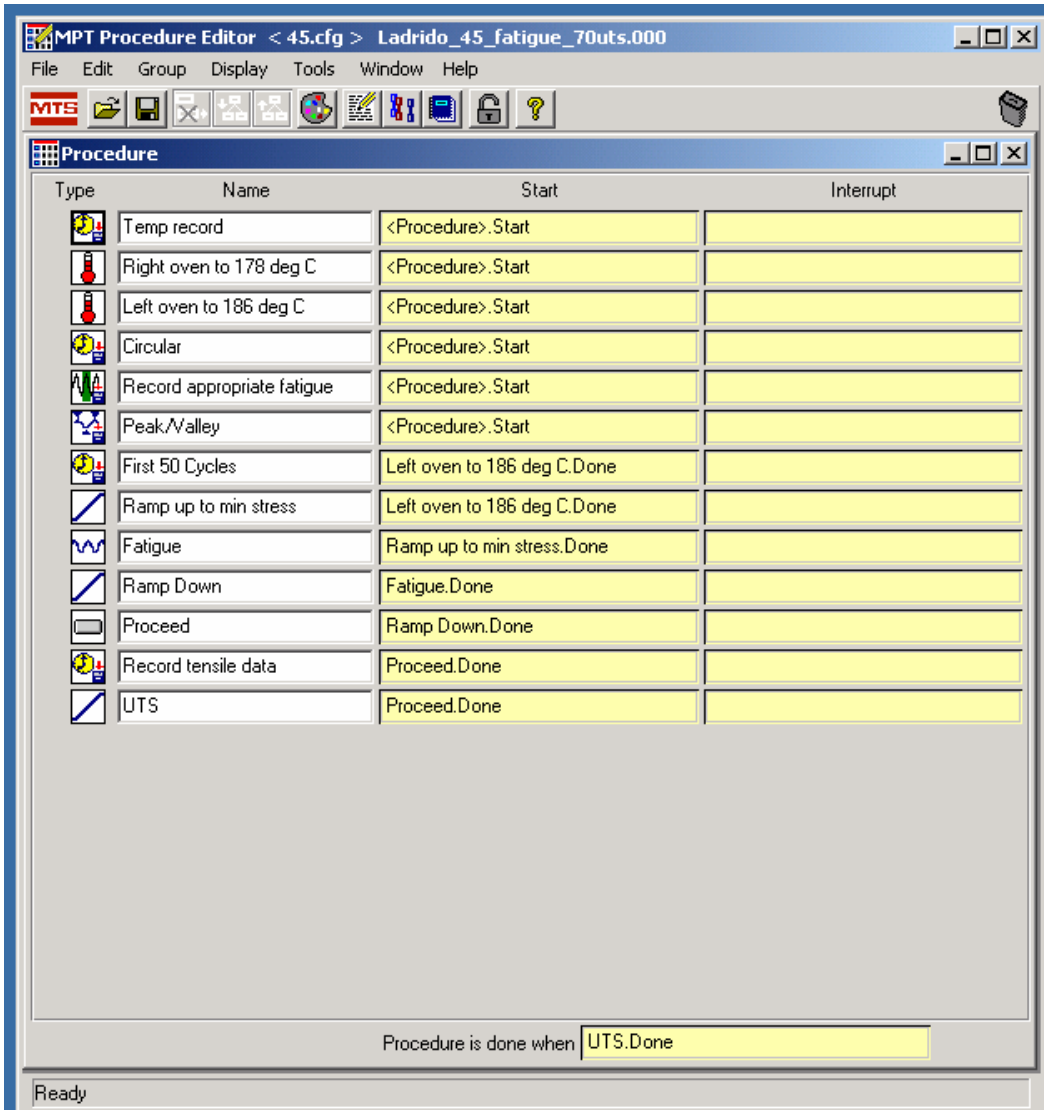

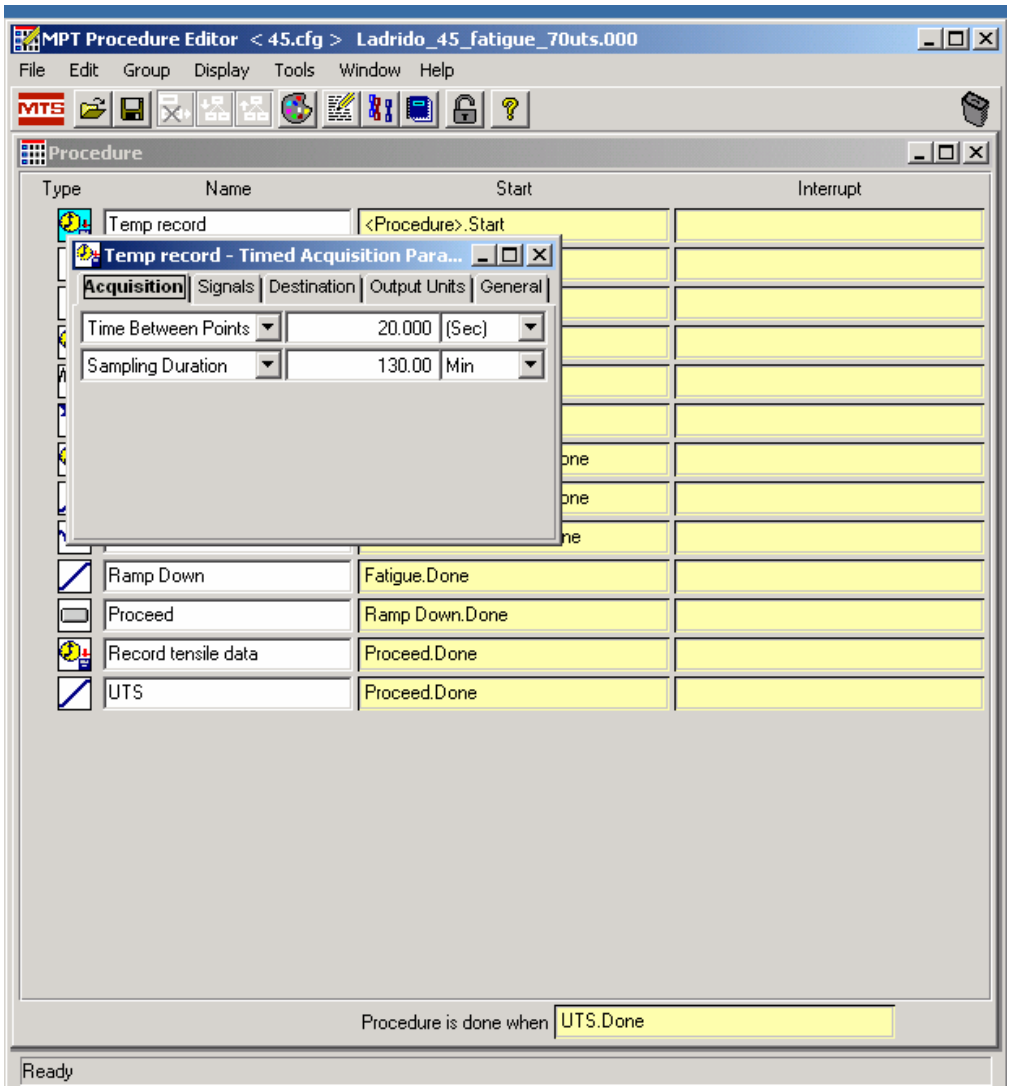
MPT Procedure Editor < 45.cfg > Ladrido_45_fatigue_70uts.000
File Edit Group Display Tools Window Help
Procedure
Type Name Start Interrupt
Temp record
<Procedure>.Start
Temp record - Timed Acquisition Para...
Acquisition Signals Destination Output Units General
Time Between Points 20.000 (Sec)
Sampling Duration 130.00 Min
Ramp Down
Fatigue.Done
Proceed
Ramp Down.Done
Record tensile data
Proceed.Done
UTS
Proceed.Done
Procedure is done when UTS.Done
Ready

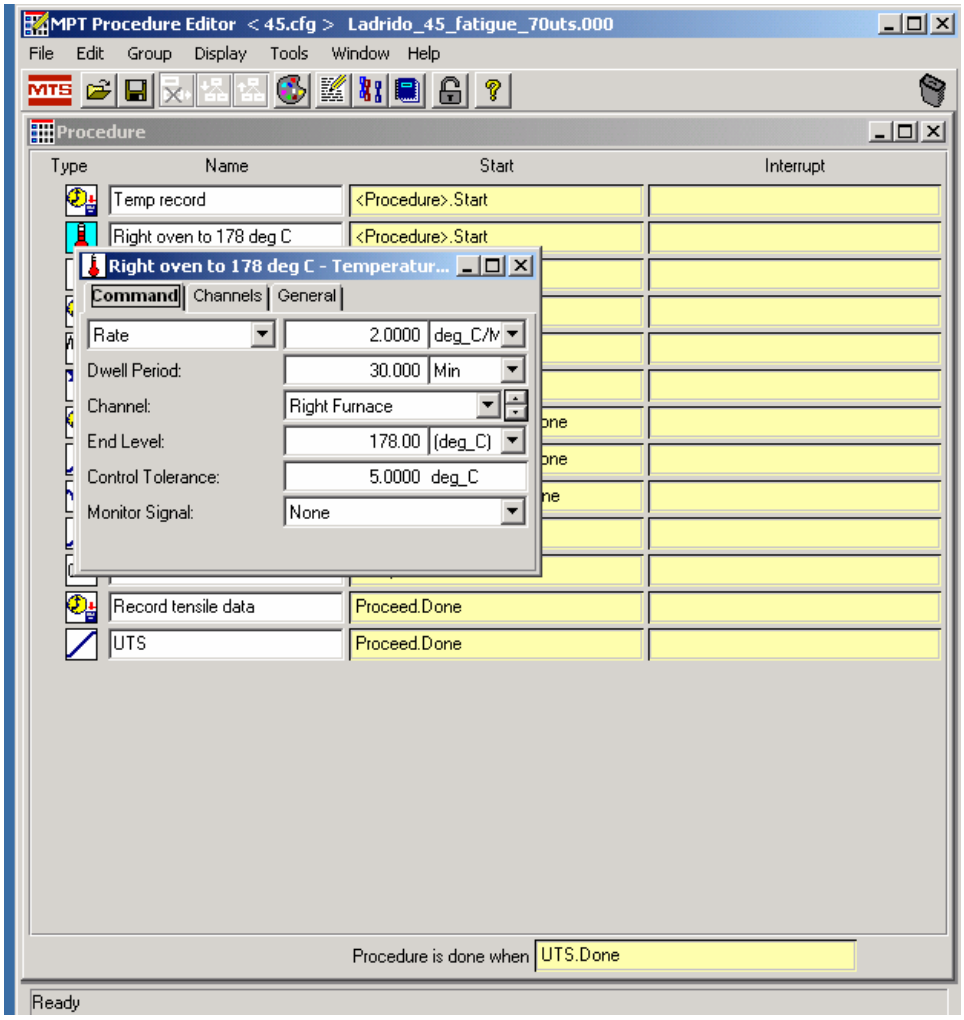
MPT Procedure Editor < 45.cfg > Ladrido_45_fatigue_70uts.000
File Edit Group Display Tools Window Help
Procedure
Type Name Start Interrupt
Temp record <Procedure>.Start
Right oven to 178 deg C <Procedure>.Start
Right oven to 178 deg C - Temperatur...
Command Channels General
Rate 2.0000 deg_C/M
Dwell Period: 30.000 Min
Channel: Right Furnace
End Level: 178.00 (deg_C)
Control Tolerance: 5.0000 deg_C
Monitor Signal: None
Record tensile data Proceed.Done
UTS Proceed.Done
Procedure is done when UTS.Done
Ready

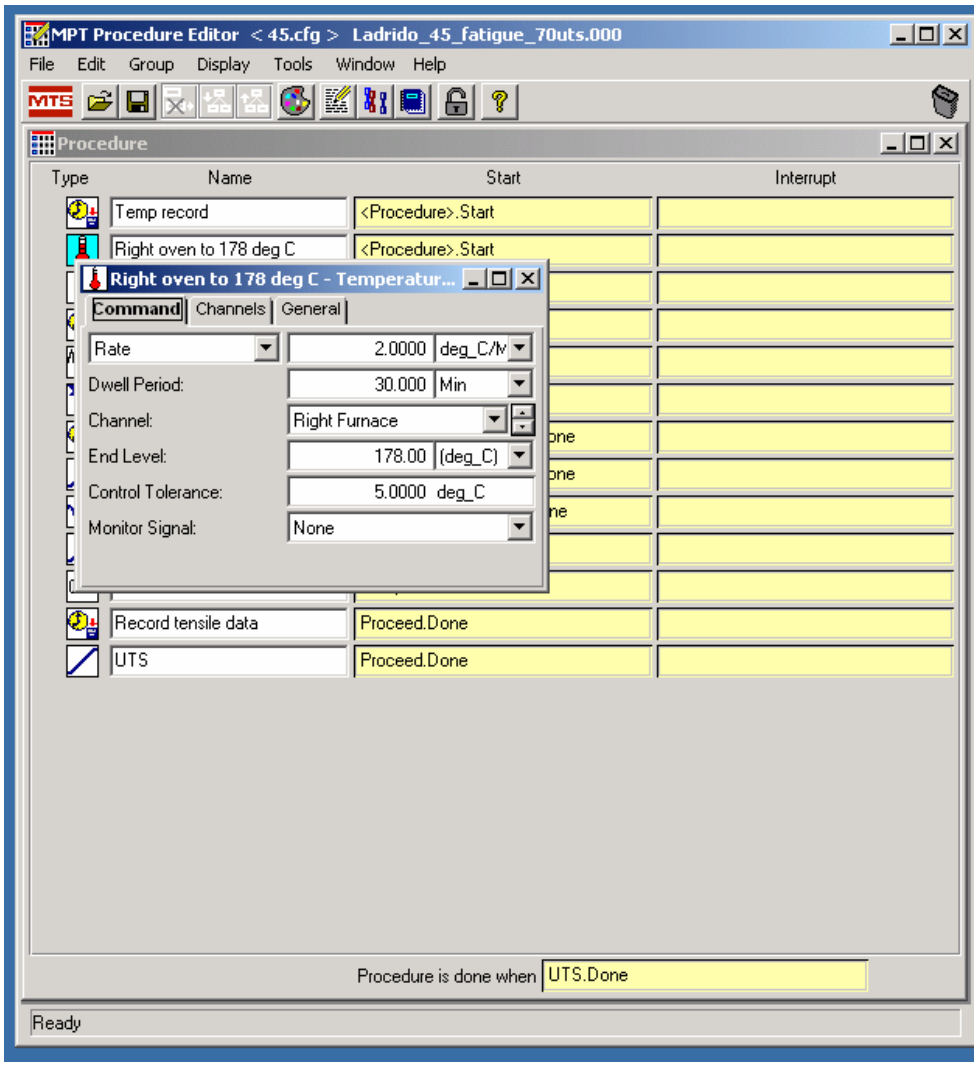
MPT Procedure Editor < 45.cfg > Ladrido_45_fatigue_70uts.000
File Edit Group Display Tools Window Help
Procedure
Type Name Start Interrupt
Temp record <Procedure>.Start
Right oven to 178 deg C <Procedure>.Start
Right oven to 178 deg C - Temperatur...
Command Channels General
Rate 2.0000 deg_C/M
Dwell Period: 30.000 Min
Channel: Right Furnace
End Level: 178.00 (deg_C)
Control Tolerance: 5.0000 deg_C
Monitor Signal: None
Record tensile data Proceed.Done
UTS Proceed.Done
Procedure is done when UTS.Done
Ready

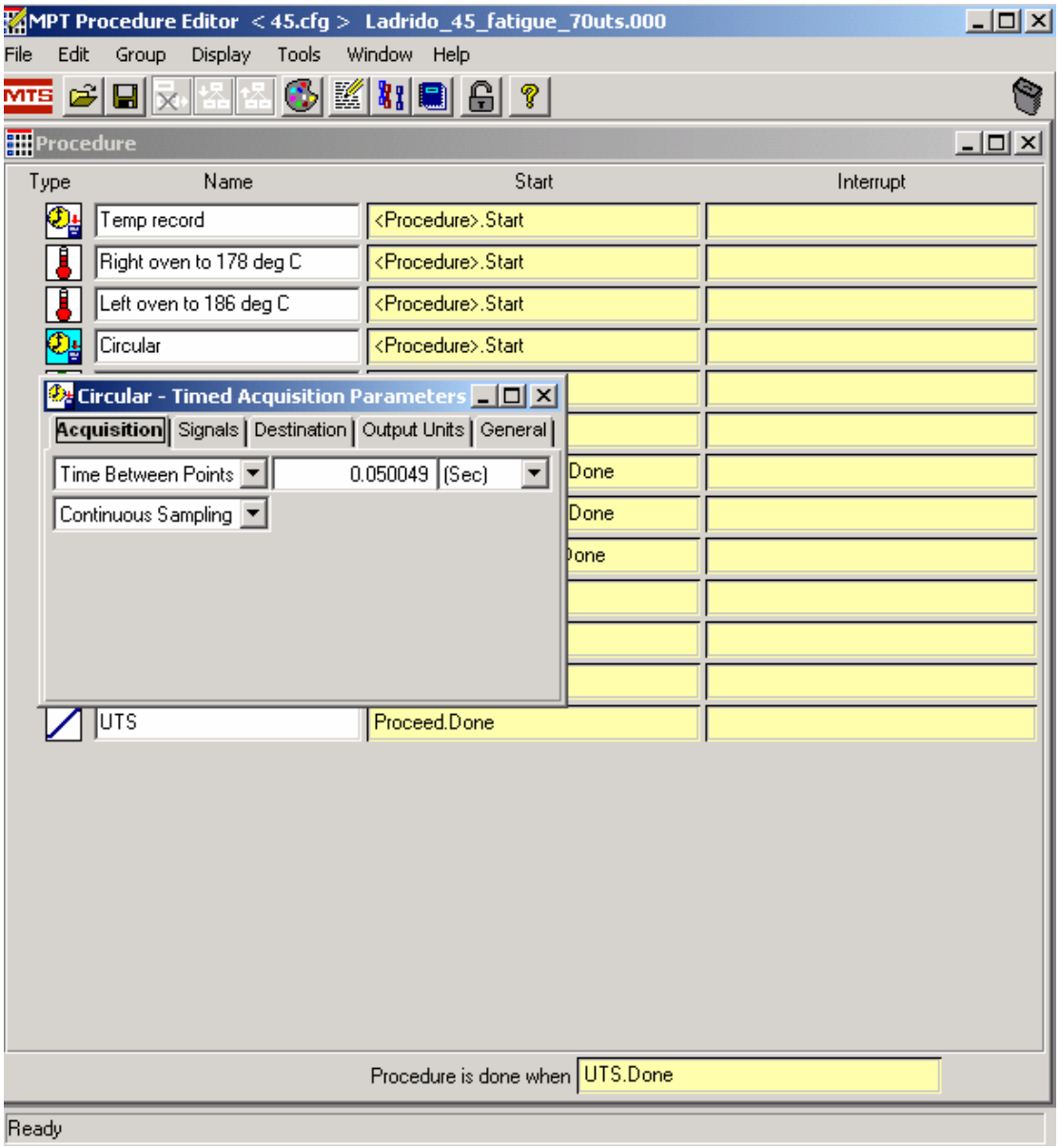
MPT Procedure Editor < 45.cfg > Ladrido_45_fatigue_70uts.000
File Edit Group Display Tools Window Help
Procedure
Type Name Start Interrupt
Temp record <Procedure>.Start
Right oven to 178 deg C <Procedure>.Start
Left oven to 186 deg C <Procedure>.Start
Circular <Procedure>.Start
Circular - Timed Acquisition Parameters
Acquisition Signals Destination Output Units General
Time Between Points 0.050049 (Sec)
Continuous Sampling
Done
Done
Done
UTS Proceed.Done
Procedure is done when UTS.Done
Ready

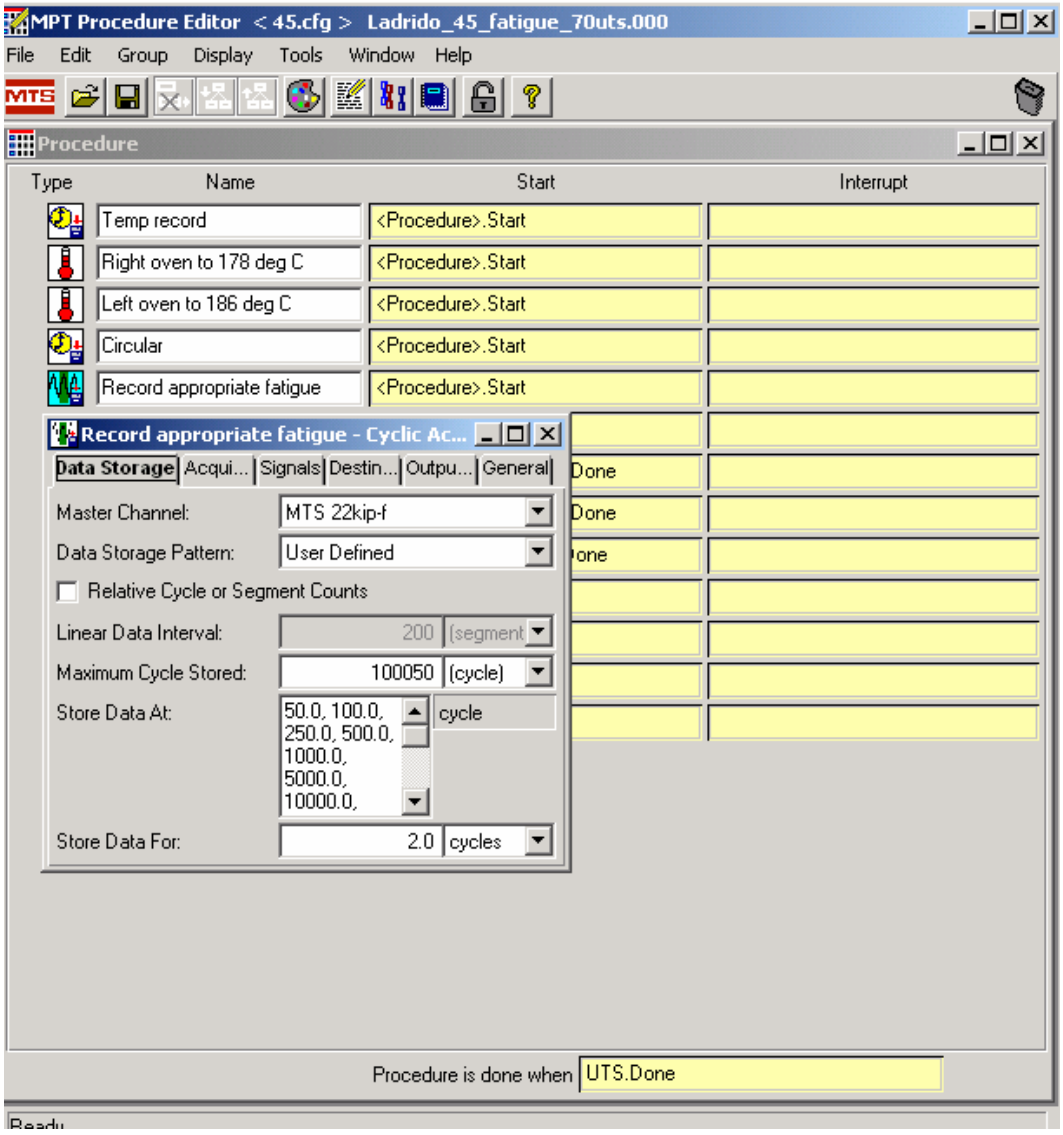
MPT Procedure Editor < 45.cfg > Ladrido_45_fatigue_70uts.000
File Edit Group Display Tools Window Help
Procedure
Type Name Start Interrupt
Temp record <Procedure>.Start
Right oven to 178 deg C <Procedure>.Start
Left oven to 186 deg C <Procedure>.Start
Circular <Procedure>.Start
Record appropriate fatigue <Procedure>.Start
Record appropriate fatigue - Cyclic Ac...
Data Storage Acqui... Signals Destin... Outpu... General
Master Channel: MTS 22kip-f
Data Storage Pattern: User Defined
Relative Cycle or Segment Counts
Linear Data Interval: 200 (segment
Maximum Cycle Stored: 100050 (cycle)
Store Data At: 50.0, 100.0, 250.0, 500.0, 1000.0, 5000.0, 10000.0, cycle
Store Data For: 2.0 cycles
Done
Done
Procedure is done when UTS.Done
Ready

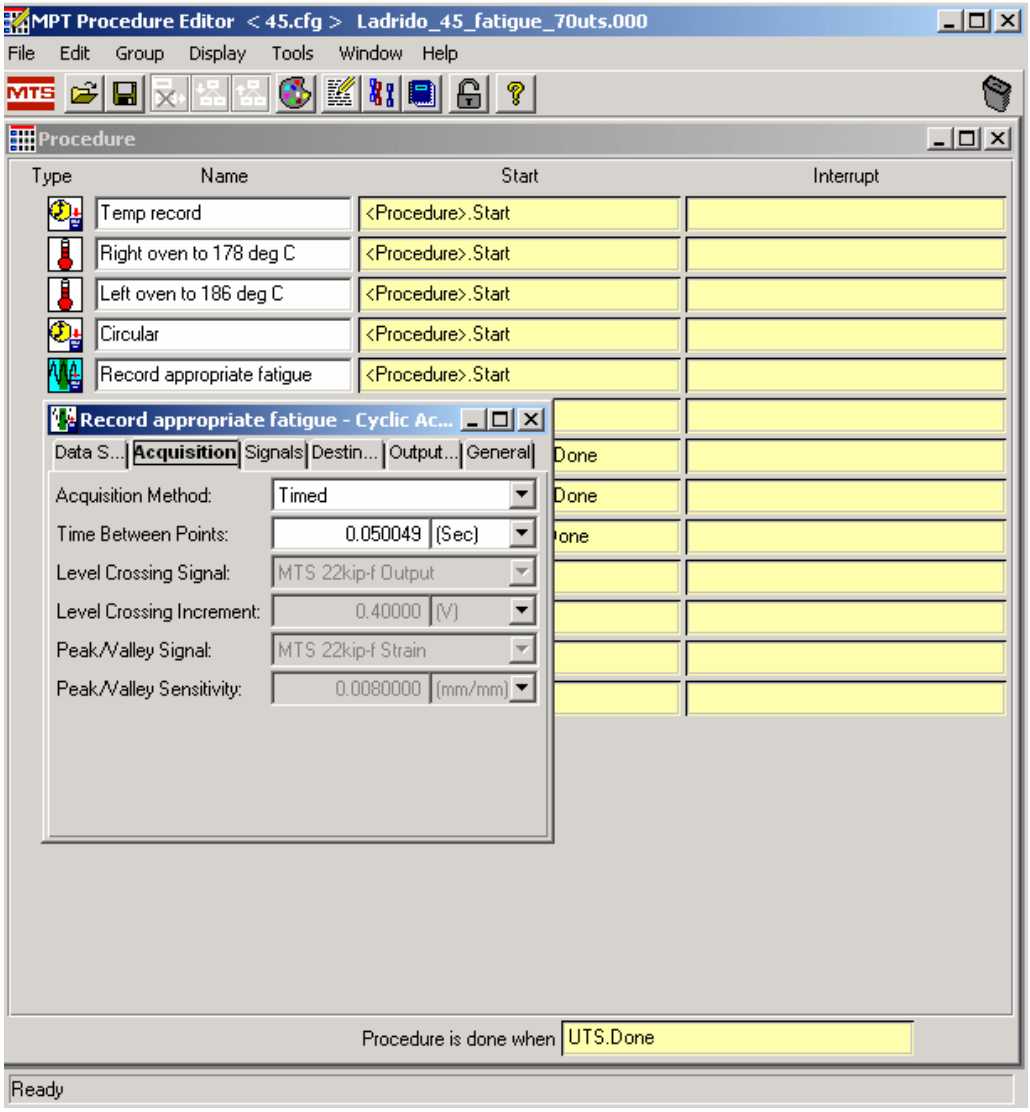
MPT Procedure Editor < 45.cfg > Ladrido_45_fatigue_70uts.000
File Edit Group Display Tools Window Help
Procedure
Type Name Start Interrupt
Temp record <Procedure>.Start
Right oven to 178 deg C <Procedure>.Start
Left oven to 186 deg C <Procedure>.Start
Circular <Procedure>.Start
Record appropriate fatigue <Procedure>.Start
Record appropriate fatigue - Cyclic Ac...
Data S... Acquisition Signals Destin... Output... General
Acquisition Method: Timed
Time Between Points: 0.050049 (Sec)
Level Crossing Signal: MTS 22kip-f Output
Level Crossing Increment: 0.40000 (V)
Peak/Valley Signal: MTS 22kip-f Strain
Peak/Valley Sensitivity: 0.0080000 (mm/mm)
Done
Done
one
Procedure is done when UTS.Done
Ready

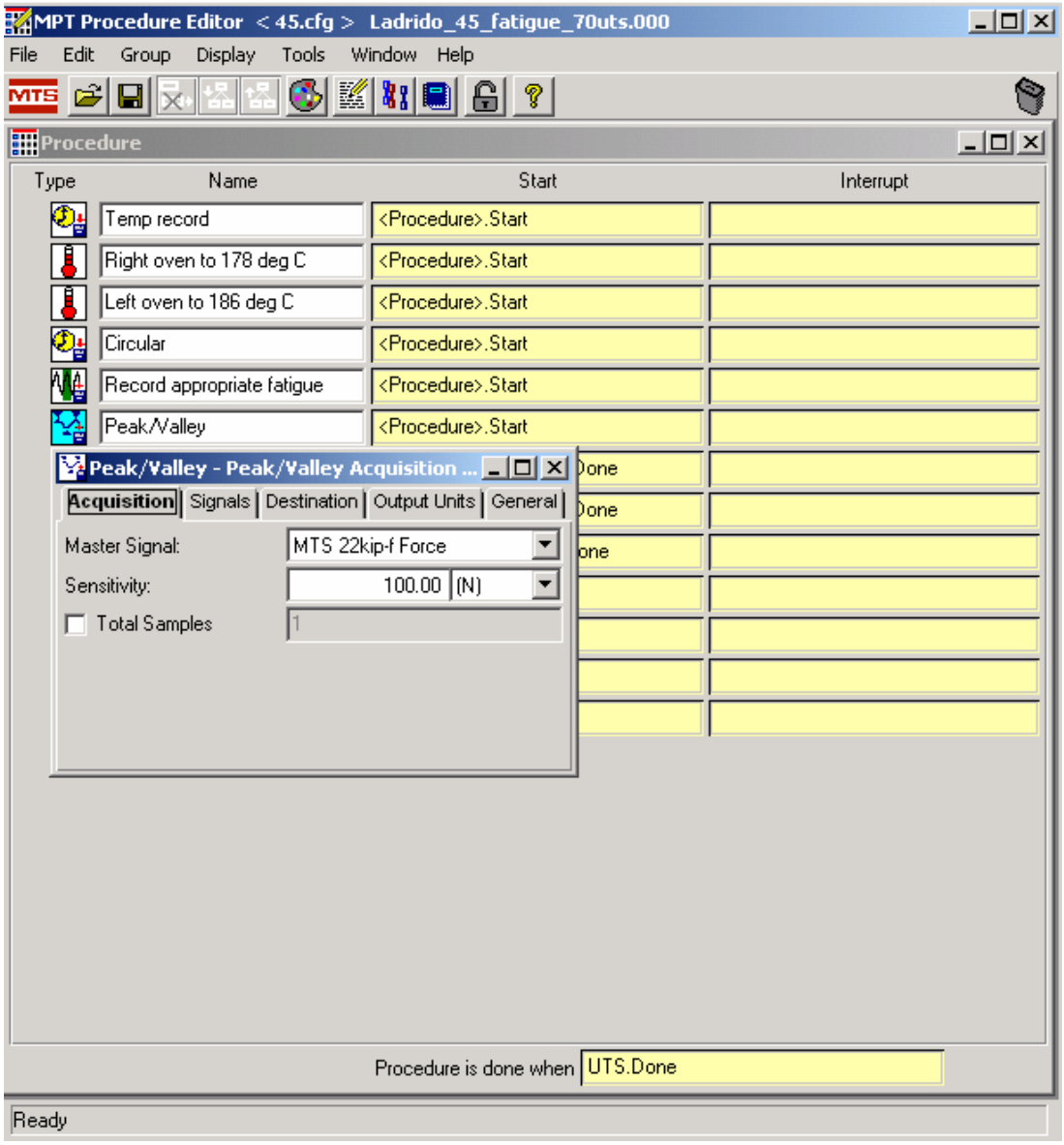
MPT Procedure Editor < 45.cfg > Ladrido_45_fatigue_70uts.000
File Edit Group Display Tools Window Help
Procedure
Type Name Start Interrupt
Temp record <Procedure>.Start
Right oven to 178 deg C <Procedure>.Start
Left oven to 186 deg C <Procedure>.Start
Circular <Procedure>.Start
Record appropriate fatigue <Procedure>.Start
Peak/Valley <Procedure>.Start
Peak/Valley - Peak/Valley Acquisition ...
Acquisition Signals Destination Output Units General
Master Signal: MTS 22kip-f Force
Sensitivity: 100.00 (N)
Total Samples 1
Procedure is done when UTS.Done
Ready

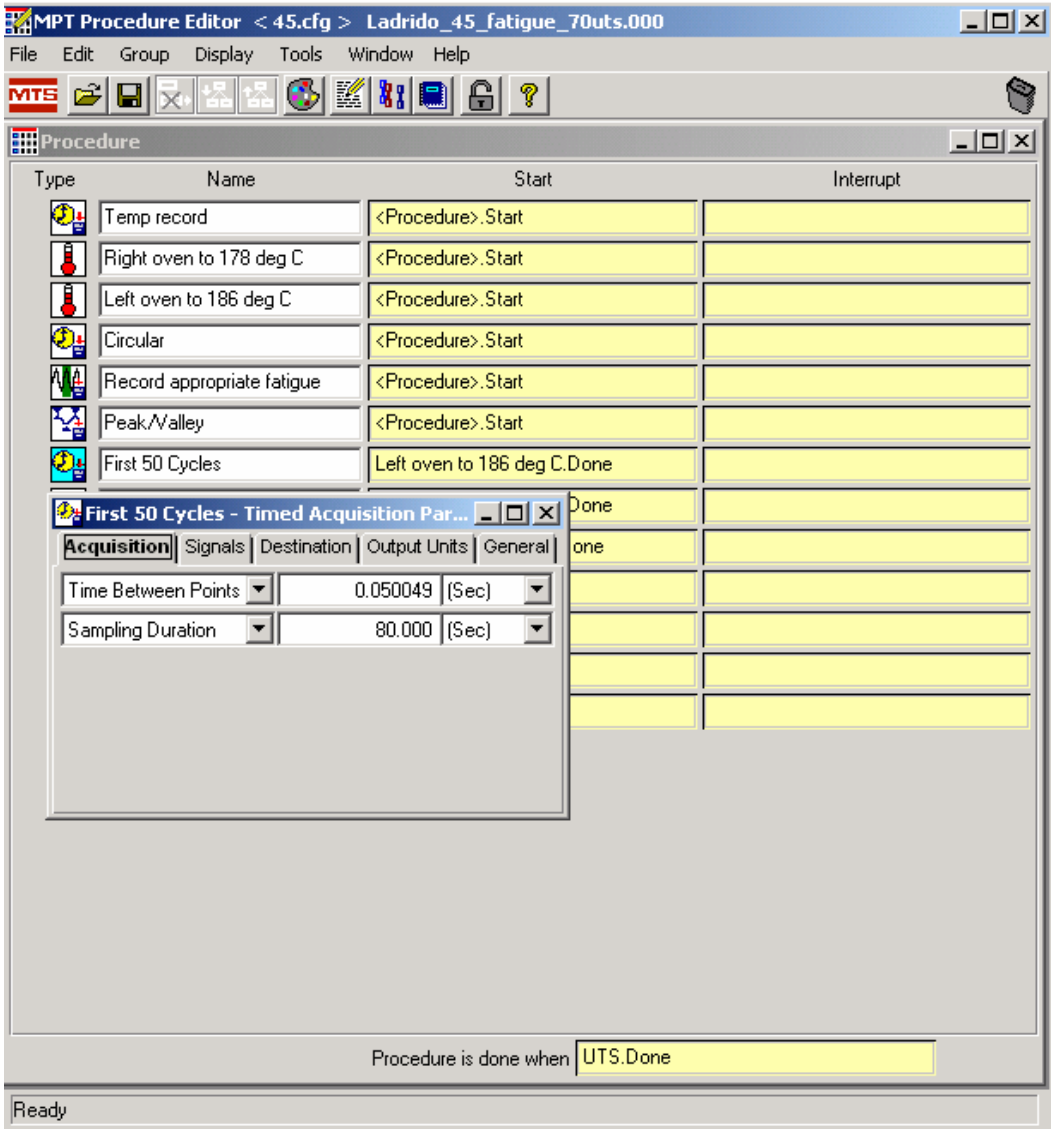
MPT Procedure Editor < 45.cfg > Ladrido_45_fatigue_70uts.000
File Edit Group Display Tools Window Help
Procedure
Type Name Start Interrupt
Temp record <Procedure>.Start
Right oven to 178 deg C <Procedure>.Start
Left oven to 186 deg C <Procedure>.Start
Circular <Procedure>.Start
Record appropriate fatigue <Procedure>.Start
Peak/Valley <Procedure>.Start
First 50 Cycles Left oven to 186 deg C.Done
First 50 Cycles - Timed Acquisition Par...
Acquisition Signals Destination Output Units General
Time Between Points 0.050049 (Sec)
Sampling Duration 80.000 (Sec)
Procedure is done when UTS.Done
Ready

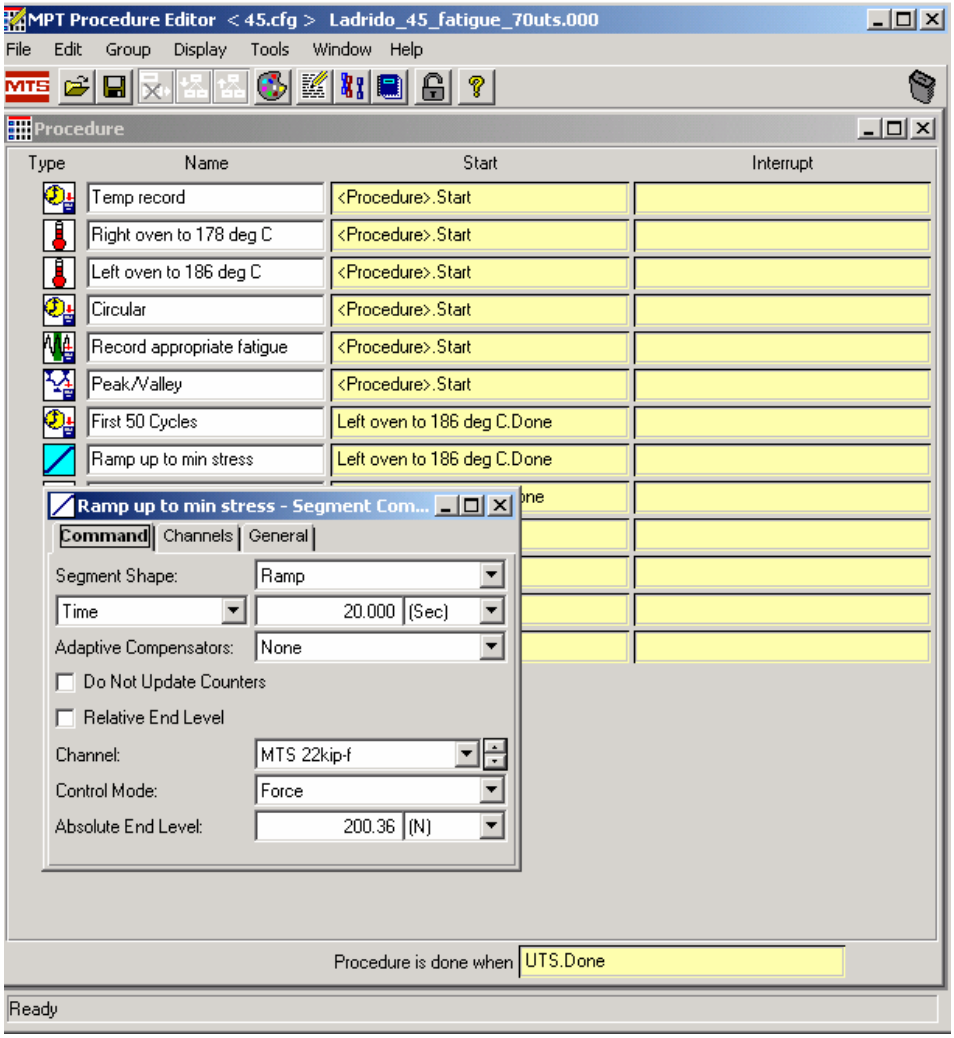
MPT Procedure Editor < 45.cfg > Ladrido_45_fatigue_70uts.000
File Edit Group Display Tools Window Help
Procedure
Type Name Start Interrupt
Temp record <Procedure>.Start
Right oven to 178 deg C <Procedure>.Start
Left oven to 186 deg C <Procedure>.Start
Circular <Procedure>.Start
Record appropriate fatigue <Procedure>.Start
Peak/Valley <Procedure>.Start
First 50 Cycles Left oven to 186 deg C.Done
Ramp up to min stress Left oven to 186 deg C.Done
Ramp up to min stress - Segment Com...
Command Channels General
Segment Shape: Ramp
Time 20.000 (Sec)
Adaptive Compensators: None
Do Not Update Counters
Relative End Level
Channel: MTS 22kip-f
Control Mode: Force
Absolute End Level: 200.36 (N)
Procedure is done when UTS.Done
Ready

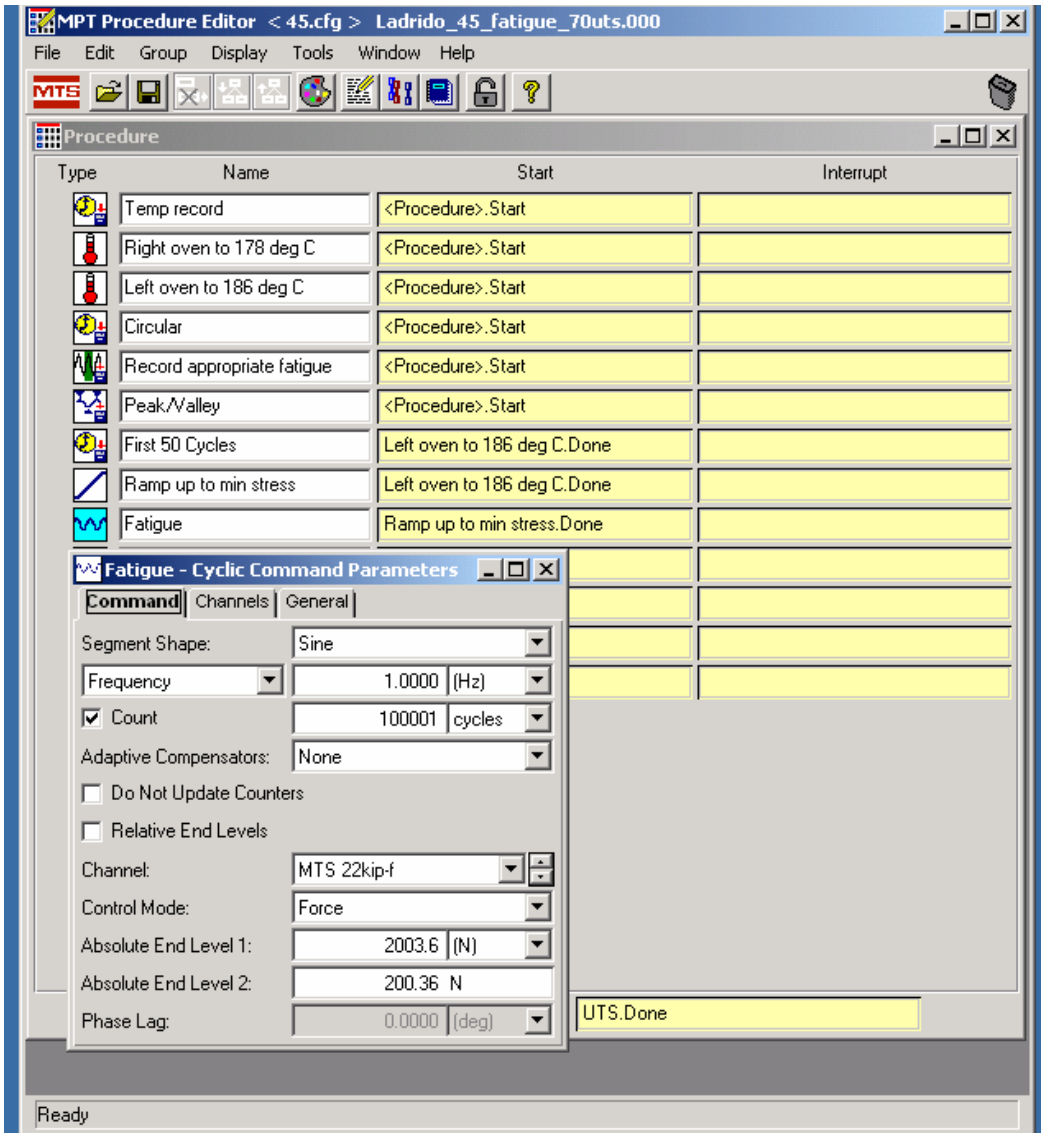
MPT Procedure Editor < 45.cfg > Ladrido_45_fatigue_70uts.000
File Edit Group Display Tools Window Help
Procedure
Type Name Start Interrupt
Temp record <Procedure>.Start
Right oven to 178 deg C <Procedure>.Start
Left oven to 186 deg C <Procedure>.Start
Circular <Procedure>.Start
Record appropriate fatigue <Procedure>.Start
Peak/Valley <Procedure>.Start
First 50 Cycles Left oven to 186 deg C.Done
Ramp up to min stress Left oven to 186 deg C.Done
Fatigue Ramp up to min stress.Done
Fatigue - Cyclic Command Parameters
Command Channels General
Segment Shape: Sine
Frequency 1.0000 (Hz)
Count 100001 cycles
Adaptive Compensators: None
Do Not Update Counters
Relative End Levels
Channel: MTS 22kip-f
Control Mode: Force
Absolute End Level 1: 2003.6 (N)
Absolute End Level 2: 200.36 N
Phase Lag: 0.0000 (deg)
UTS.Done
Ready

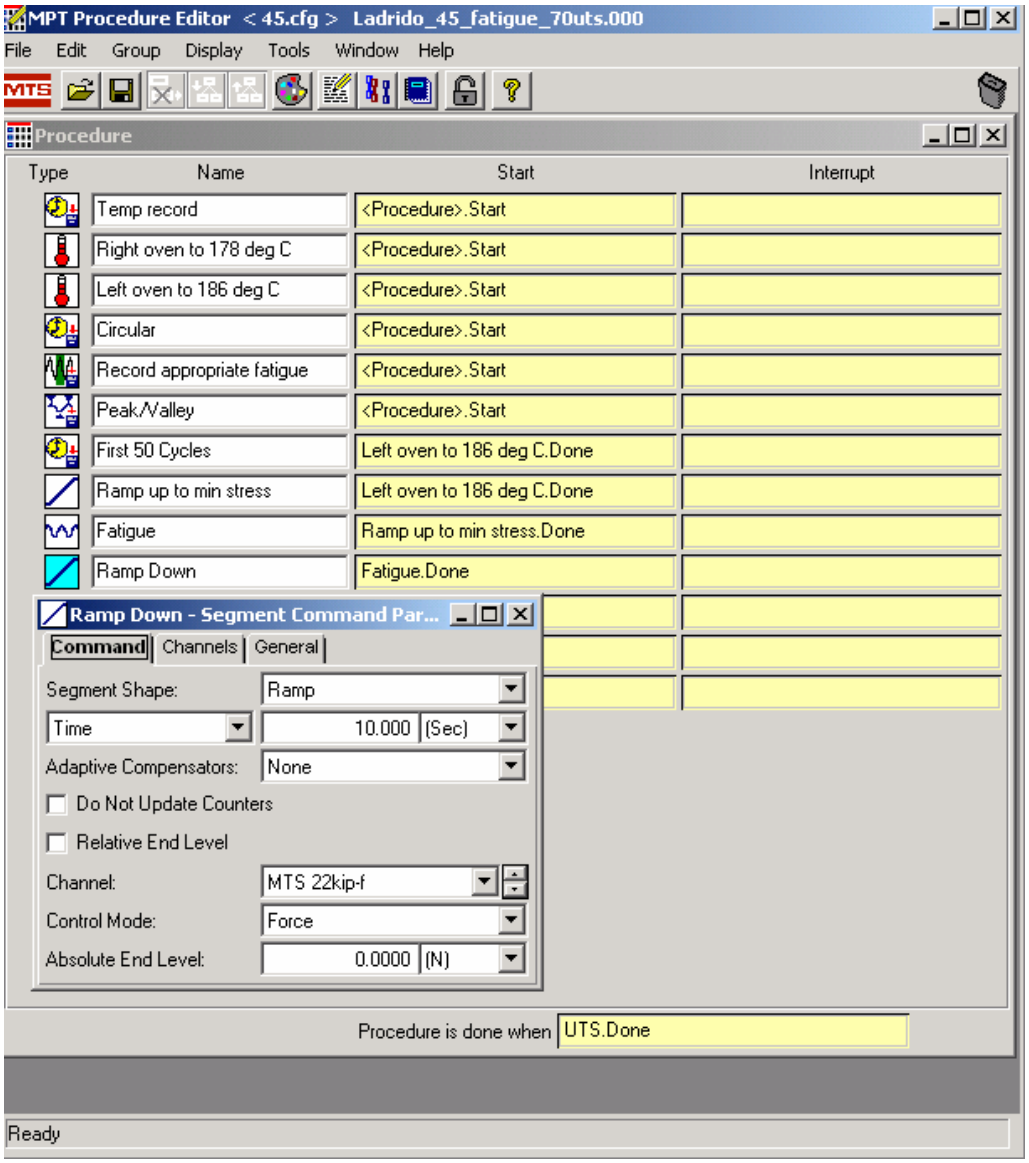
MPT Procedure Editor < 45.cfg > Ladrido_45_fatigue_70uts.000
File Edit Group Display Tools Window Help
Procedure
Type Name Start Interrupt
Temp record <Procedure>.Start
Right oven to 178 deg C <Procedure>.Start
Left oven to 186 deg C <Procedure>.Start
Circular <Procedure>.Start
Record appropriate fatigue <Procedure>.Start
Peak/Valley <Procedure>.Start
First 50 Cycles Left oven to 186 deg C.Done
Ramp up to min stress Left oven to 186 deg C.Done
Fatigue Ramp up to min stress.Done
Ramp Down Fatigue.Done
Ramp Down - Segment Command Par...
Command Channels General
Segment Shape: Ramp
Time 10.000 (Sec)
Adaptive Compensators: None
Do Not Update Counters
Relative End Level
Channel: MTS 22kip-f
Control Mode: Force
Absolute End Level: 0.0000 (N)
Procedure is done when UTS.Done
Ready

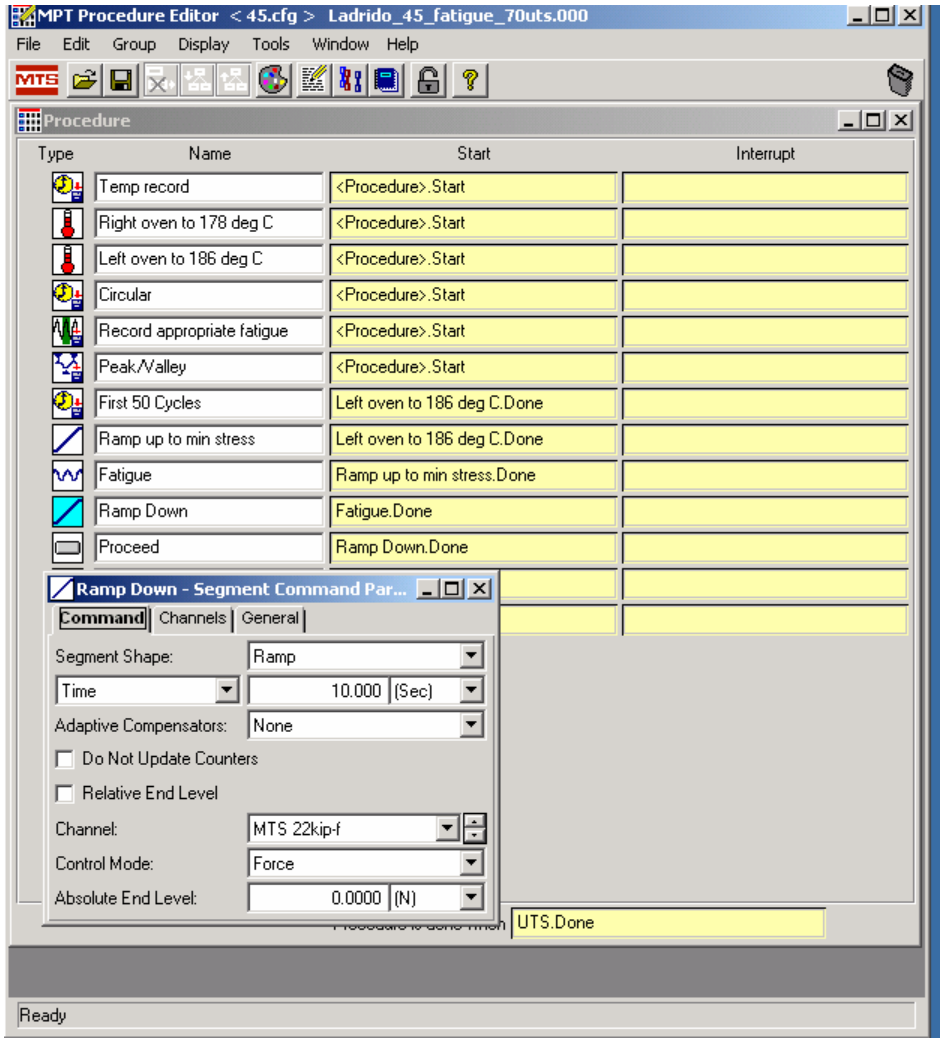
MPT Procedure Editor < 45.cfg > Ladrido_45_fatigue_70uts.000
File Edit Group Display Tools Window Help
Procedure
Type Name Start Interrupt
Temp record <Procedure>.Start
Right oven to 178 deg C <Procedure>.Start
Left oven to 186 deg C <Procedure>.Start
Circular <Procedure>.Start
Record appropriate fatigue <Procedure>.Start
Peak/Valley <Procedure>.Start
First 50 Cycles Left oven to 186 deg C.Done
Ramp up to min stress Left oven to 186 deg C.Done
Fatigue Ramp up to min stress.Done
Ramp Down Fatigue.Done
Proceed Ramp Down.Done
Ramp Down - Segment Command Par...
Command Channels General
Segment Shape: Ramp
Time 10.000 (Sec)
Adaptive Compensators: None
Do Not Update Counters
Relative End Level
Channel: MTS 22kip-f
Control Mode: Force
Absolute End Level: 0.0000 (N)
UTS.Done
Ready

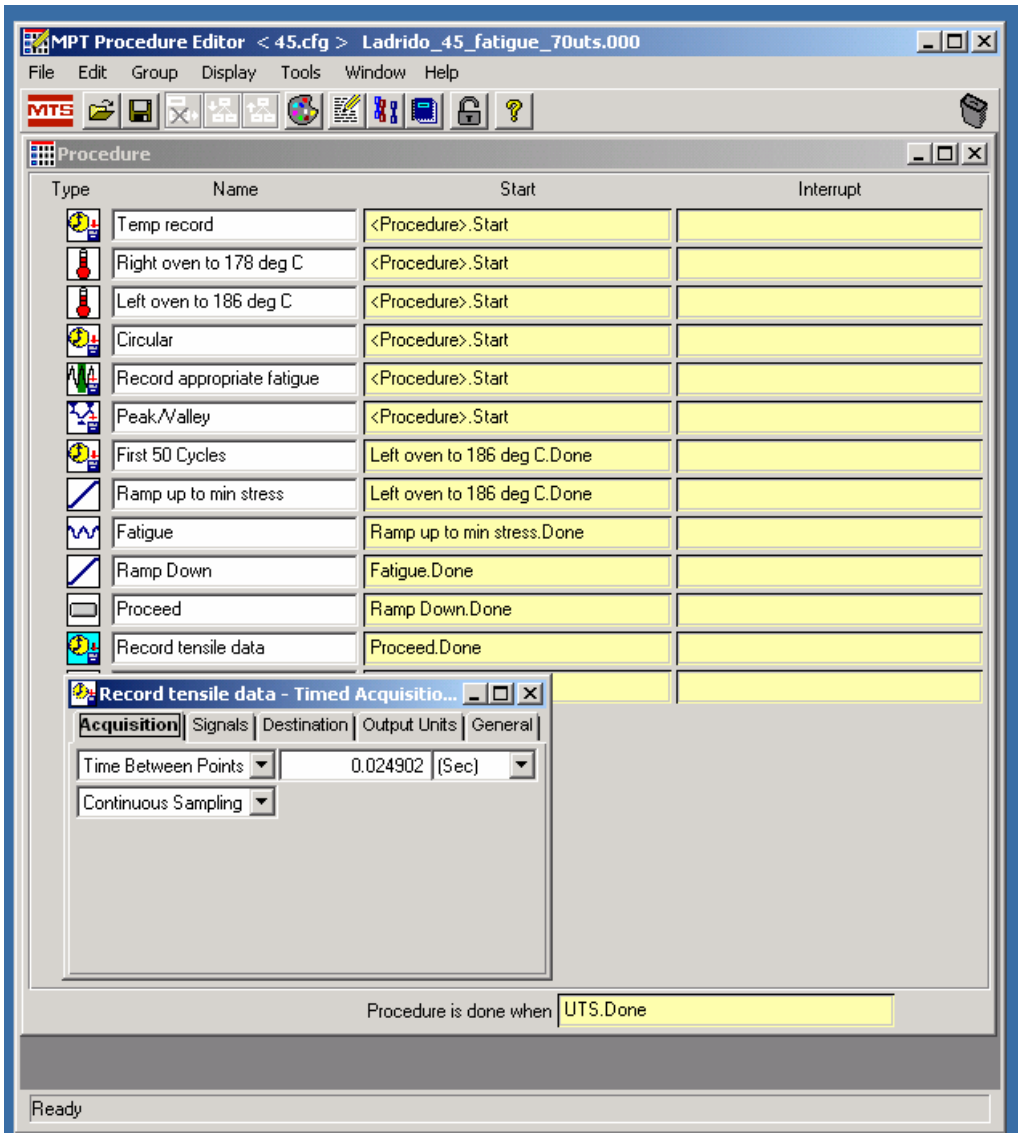
MPT Procedure Editor < 45.cfg > Ladrido_45_fatigue_70uts.000
File Edit Group Display Tools Window Help
Procedure
Type Name Start Interrupt
Temp record <Procedure>.Start
Right oven to 178 deg C <Procedure>.Start
Left oven to 186 deg C <Procedure>.Start
Circular <Procedure>.Start
Record appropriate fatigue <Procedure>.Start
Peak/Valley <Procedure>.Start
First 50 Cycles Left oven to 186 deg C.Done
Ramp up to min stress Left oven to 186 deg C.Done
Fatigue Ramp up to min stress.Done
Ramp Down Fatigue.Done
Proceed Ramp Down.Done
Record tensile data Proceed.Done
Record tensile data - Timed Acquisitio...
Acquisition Signals Destination Output Units General
Time Between Points 0.024902 (Sec)
Continuous Sampling
Procedure is done when UTS.Done
Ready

Bibliography

1. Adams, D.F., Carlsson, L.A., and Pipes, R.B., "Experimental characterization of advanced composite materials," CRC Press, Boca Raton, 2003, pp. 238.

2. Alston, William B.; Scheiman, Daniel A. “Shelf Life of PMR Polyimide Monomer Solutions and Prepregs Extended.” http://www.grc.nasa.gov/WWW/RT1999/5000/5150alston.html, 1999.

3. Balaconis, John G. *Some Aspects of the Mechanical Response of BMI 5250-4 Neat Resin at 191ºC: Experiment and Modeling*. MS thesis, AFIT/GA/ENY/06-M03. School of Engineering and Management, Air Force Institute of Technology (AU), Wright-Patterson AFB, OH March 2003.

4. Bechel, Vernon. “Constituent Level Examination of an E-Beam Cured Graphite/Epoxy” Composite.http://www.sampe.org/store/paper.aspx?pid=755, 2001.

5. Bechel, Vernon T. “Effect of stacking sequence on micro-cracking in a cryogenically cycled carbon/bismaleimide composite”. http://www.sciencedirect.com, 2003.

6. Black, Sara. “Are high-temperature thermoset resins ready to go commerical?” http://www.compositesworld.com/hpc/issues/2004/November/637/1, 2004.

7. Bowles, Kenneth J.; Papadopoulos, Demetrios; Inghram, Linda; McCorkle, Linda; Klan, Ojars. “Longtime Durability of PMR-15 Matrix Polymer at 204, 260, 288, 316 degrees Celsius”. http://gltrs.grc.nasa.gov/GLTRS, 2001.

8. Burke, J.J., Reed, N.L., Weiss, V., "Fatigue--an interdisciplinary approach, proceedings held at Sagamore Conference Center, Raquette Lake, New York, August 13-16, 1963," *Sagamore Army Materials Research Conference proceedings,* Vol. 10, Syracuse University Press, Syracuse, N.Y., 1964, pp. 404.

9. Cytec Engineered Materials. “CYCOM 5250-4 RTM Resin System.” http://www.cytec.com/business/EngineeredMaterials/Datasheets/CYCOM%20RTM%205250-4.pdf.

10. Daniel, I.M., and Ishai, O., "Engineering mechanics of composite materials," Oxford University Press, New York, 2006, pp. 411.

11. *Fatigue of Metals: Part One*. http://www.key-to-steel.com/Articles/Art142.htm. Last accessed 7 May 2007.

12. Gay, D., *Composite materials: design and applications*, CRC Press, Boca Raton, FL, 2003, pp. 531.

13. Gentz, M.; Armentrout, D.; Rupnowski, P.; Kumosa, L.; Shin, E.; Sutter, J.K.; Kumosa, M. "In-plane shear testing of medium and high modulus woven graphite fiber reinforced/polyimide composites". *Composites Science and Technology*. 64 (2), p203-220 (2004).

14. Goodman, S.H., *Handbook of thermoset plastics*, Noyes Publications, Park Ridge, N.J., U.S.A., 1986, pp. 421.

15. Hertzberg, R.W., "Deformation and fracture mechanics of engineering materials," Wiley, New York, 1976, pp. 605.

16. Khan, F., 2002, "The deformation behavior of solid polymers and modeling with the viscoplasticity theory based overstress". Ph.D. Thesis, Rensselaer Polytechnic Institute, New York.

17. Kobayashi, Satoshi ; Takeda, Nobuo. "Experimental and analytical characterization of transverse cracking". *Composites Part B: Engineering*. 33 (6), p471-478 (2002).

18. MTS Systems Corporation. Model 793.00 System Software: User Information and Software Reference. MTS Systems Corporation, 2001.

19. Margolis, J.M., *Advanced thermoset composites: industrial and commercial applications* Van Nostrand Reinhold, New York, 1986, pp. 282.

20. Martin, Roderick; Campion, Robert. "Ageing of Composites". *Materials World*. 4 (4), p200-202 (2004).

21. Mason, Karen Fisher. "Composites Combat Ready in UAVs". http://www.compositesworld.com/hpc/issues/2004/May/463/3, (2004).

22. McKague, Lee. "Design and Process Integration for Low Cost Manufacturing". *Journal of Advanced Materials*. 1 (1), p2-9, (2002).

23. Merriam-Webster Online. http://www.m-w.com

24. MTS.com http://www.mts.com/en/Material/index.asp

25. Nickerson, Seth. “Thermo-Mechanical Failure Analysis of Cryogenic Composite Materials Using Multicontinuum Theory”. http://people.alfred.edu/~mayesjs/AIAA%20Space%202003.pdf. (2003).

26. Pagano, N.J., Schoeppner, G.A., Kim, R., Abrams, F.L., "Steady-state cracking and edge effects in thermo-mechanical transverse cracking of cross-ply laminates," *Composites Science and Technology*, Vol. 58, No. 11, 1998, pp. 1811.

27. Peebles, L.H., *Carbon fibers: formation, structure, and properties.* CRC Press, Boca Raton, FL, 1995, pp. 203.

28. Petermann, J.; Hinz, S.; Schulte, K. “Degradation Parameters and Two-Stress Block Fatigue of Angle-Ply Carbon Fiber Reinforce Epoxy”. *Journal of ASTM International*. 1 (8), p1-12, (2004)..

29. Pilato, L., and Michno, M.J., *Advanced composite materials*, New York : Springer-Verlag, Berlin, 1994, pp. 208.

30. *Resin Matrices: Thermosets*. Available: http://www.compositesworld.com/sb/sb9. Last accessed 7 May 2007.

31. Ruggles-Wrenn, M.B.; Corum, J.M.; Battiste, R.L. “Short-term static and cyclic behavior of two automotive carbon-fiber composites”. http://www.elsevier.com/locate/compositesa, 2003.

32. Schoeppner, G.A., Tandon, G.P., Ripberger, E.R. “Anisotropic oxidation and weight loss in PMR-15 composites”. *Composites Part A: applied science and manufacturing*. 1 (1), p1-15 (2006).

33. Sheppard, M.; Campbell, G.S.; Stoll, F. “Lightweight, Damage Tolerant Composite Sandwhich Structures for High Temperature Applications in Aircraft Engine Components.” http://www.webcoreonline.com/randd/techpapers/sept2003.pdf., 2003.

34. Talreja, R., Månson, J.E., Kelly, A., "Polymer matrix composites," *A comprehensive composite materials publication.* Elsevier, Amsterdam ; New York, 2001, pp. 1129.

35. Tang, Hai C.; Nguyen, Tinh; Tze-jer Chuang; Chin, Joannie; Wu, H. Felix; Lesko, Jack. “Fatigue Model for Fiber-Reinforced Polymeric Composites.” *Journal of Materials in Civil Engineering*. 12 (2), p97-104 (2000).

36. Vigo, T.L., and Kinzig, B.J., *Composite applications: the role of matrix, fiber, and interface* Vch, New York, N.Y., 1992, pp. 407.

37. Xie, W.; Pan, W.-P.; Chuang, K.C. “Thermal Degradation Study of Polymerization of Monomeric Reactants (PMR) Polyimides.” *Journal of Thermal Analysis and Calorimetry*. 64 (1), p477-485 (2001).

REPORT DOCUMENTATION PAGE

Form Approved
OMB No. 074-0188

1. REPORT DATE *(DD-MM-YYYY)*	**2. REPORT TYPE**	**3. DATES COVERED** *(From – To)*
14-06-2007	Master's Thesis	September 2005 – June 2007

4. TITLE AND SUBTITLE

Effect of prior aging on fatigue behavior of IM7/BMI 5250-4 composite at 191°C

5a. CONTRACT NUMBER

5b. GRANT NUMBER

5c. PROGRAM ELEMENT NUMBER

6. AUTHOR(S)

Ladrido, Christine G., Captain, USAF

5d. PROJECT NUMBER
2005-158, 2005-025

5e. TASK NUMBER

5f. WORK UNIT NUMBER

7. PERFORMING ORGANIZATION NAMES(S) AND ADDRESS(S)
Air Force Institute of Technology
Graduate School of Engineering and Management (AFIT/EN)
2950 Hobson Way, Building 640
WPAFB OH 45433-8865

8. PERFORMING ORGANIZATION REPORT NUMBER
AFIT/GAE/ENY/07-J10

9. SPONSORING/MONITORING AGENCY NAME(S) AND ADDRESS(ES)

AFOSR/NL	AFRL/MLBCM	AFRL/MLBCM
Attn: Dr. Charles Y-C Lee	Attn: Greg Schoeppner	Attn: Richard Hall
875 Randolph St	2941 P Street	2941 P Street
Arlington, VA 22203-1954	WPAFB, OH, 45433,	WPAFB, OH, 45433,
Comm No: (703)696-7779	(937)255-9072	(937)255-9097

10. SPONSOR/MONITOR'S ACRONYM(S)

11. SPONSOR/MONITOR'S REPORT NUMBER(S)

12. DISTRIBUTION/AVAILABILITY STATEMENT
APPROVED FOR PUBLIC RELEASE; DISTRIBUTION UNLIMITED.

13. SUPPLEMENTARY NOTES

14. ABSTRACT

IM7/BMI 5250-4 with carbon fiber orientations [±45] and [0/90] were aged in air at 191°C for up to 1000 hours. The weight loss was analyzed during the aging process.
Tension to failure tests were performed on both the unaged and aged specimens to establish a baseline for the Ultimate Tensile Strengths and Young's Modulus.
Tension-tension cyclic load fatigue testing was conducted on the specimen to determine the effect of prior aging on the fatigue response of the composite.
Cyclic strain accumulation was not influenced by prior aging, but it was influenced by the stress levels applied.
[±45] specimens lost 0.2% more weight than the [0/90] specimens from aging in air.

15. SUBJECT TERMS
Composite, IM7/BMI 5250-4, tension, fatigue, prior aging history

16. SECURITY CLASSIFICATION OF:			**17. LIMITATION OF ABSTRACT**	**18. NUMBER OF PAGES**	**19a. NAME OF RESPONSIBLE PERSON**
a. REPORT	**b. ABSTRACT**	**c. THIS PAGE**			Dr. Marina B. Ruggles-Wrenn
U	**U**	**U**	**UU**	97	**19b. TELEPHONE NUMBER** *(Include area code)* 785-3636, ext 4641; e-mail: marina.ruggles-wrenn@afit.edu

Standard Form 298 (Rev. 8-98)
Prescribed by ANSI Std. Z39-18